

# UC San Diego

## UC San Diego Electronic Theses and Dissertations

### Title

High-content array based screening technology for the identification of factors that regulate cell fate

### Permalink

<https://escholarship.org/uc/item/3qw8w75m>

### Author

Brafman, David Adam

### Publication Date

2009

Peer reviewed|Thesis/dissertation

UNIVERSITY OF CALIFORNIA, SAN DIEGO

**HIGH-CONTENT ARRAY BASED SCREENING TECHNOLOGY  
FOR THE IDENTIFICATION OF FACTORS THAT REGULATE  
CELL FATE**

A dissertation submitted in partial satisfaction of the  
requirements for the degree Doctor of Philosophy

in

Bioengineering

by

David Adam Brafman

Committee in Charge:

Professor Shu Chien, chair  
Professor Karl Willert, co-chair  
Professor Lawrence Goldstein  
Professor Shyni Varghese  
Professor Kun Zhang

2009

Copyright

David Adam Brafman, 2009

All rights reserved

The Dissertation of David Adam Brafman is approved and it is acceptable in quality and form for publication on microfilm and electronically:

---

---

---

---

**Co-Chair**

---

**Chair**

University of California, San Diego

2009

## **DEDICATION**

To my parents, Judy and Marvin, for teaching me how to plan for the worst and hope for  
the best

# TABLE OF CONTENTS

<b>Signature Page</b> .....	iii
<b>Dedication Page</b> .....	iv
<b>Table of Contents</b> .....	v
<b>List of Figures</b> .....	xii
<b>List of Tables</b> .....	xiv
<b>Acknowledgements</b> .....	xv
<b>Vita</b> .....	xvii
<b>Abstract of the Dissertation</b> .....	xix
<b>CHAPTER 1 INTRODUCTION</b> .....	1
1.1 THE CELL MICROENVIRONMENT.....	1
1.1.1 Crosstalk in the Microenvironment .....	1
1.2 STEM CELL MICROENVIRONMENTS: THE NICHE.....	2
1.3 EMBRYONIC STEM CELLS (ESCs) .....	3
1.3.1 Human Embryonic Stem Cells (hESCs) .....	4
1.3.1.1 “Optimal” hESC culture conditions.....	4
1.3.1.2 Current hESC derivation and culture conditions .....	4
1.3.1.3 Biomaterials as stem cell growth substrates .....	7
1.4. HIGH-THROUGHPUT APPROACHES FOR STUDYING STEM CELL BIOLOGY .....	7
1.4.1 Traditional HTS For Identifying Modulators of Stem Cell Fate .....	8
1.4.2 Cellular Microarray-based Screening in Stem Cell Research .....	9
1.4.2.1 Microfluidic array approaches to study stem biology.....	10
1.4.2.2 Microwell arrays to analyze factors regulating stem cell biology .....	11

1.4.2.3 Combinatorial arrays for studying stem cell microenvironments .....	12
1.5 OUTLINE OF DISSERTATION .....	14
1.6 ACKNOWLEDGEMENTS.....	15
<b>CHAPTER 2 DEVELOPMENT OF ARRAYED CELLULAR MICROENVIRONMENT</b>	
<b>(ACME) TECHNOLOGY.....</b>	<b>19</b>
2.1 ABSTRACT .....	19
2.2 INTRODUCTION .....	19
2.3 MATERIALS AND METHODS .....	21
2.3.1 Arrayed Cellular Microenvironment (ACME) Fabrication .....	21
2.3.2 Cell Culture .....	22
2.3.3 Wnt Reporter Line Construction .....	23
2.3.4 Slide Staining .....	23
2.3.5 Slide Imaging .....	24
2.3.5 Statistical Analysis .....	25
2.4 RESULTS AND DISCUSSION.....	25
2.4.1 Arrayed Cellular Microenvironments (ACME) to Study Cell Fate.....	25
2.4.2 Characterization of ECMP Deposition .....	25
2.4.3 Reproducibility of Protein Printing .....	26
2.4.4 Cell Culture Compatibility .....	26
2.4.5 Incorporation of Growth Factors into Spotted “Microenvironments” .....	27
2.5 CONCLUSION.....	28
2.6 ACKNOWLEDGEMENTS .....	28

**CHAPTER 3 INVESTIGATING THE ROLE OF THE EXTRACELLULAR ENVIRONMENT IN MODULATING HEPATIC STELLATE CELL BIOLOGY WITH ARRAYED COMBINATORIAL MICROENVIRONMENTS.....35**

3.1 ABSTRACT .....35

3.2 INTRODUCTION .....36

3.3 MATERIALS AND METHODS .....38

    3.3.1 Array Fabrication and Characterization .....38

    3.3.2 Cell Isolation, Purification, and Culture.....39

    3.3.3 Slide Imaging, Quantification, and Analysis.....40

    3.3.4 Microarray Analysis.....42

    3.3.5 HSC Culture on Selected ECMP Conditions .....42

    3.3.6 qRT-PCR Analysis .....43

    3.3.7 Data Analysis.....43

3.4 RESULTS .....44

    3.4.1 Using Arrayed Microenvironments to Study HSC Biology.....44

    3.4.2 HSC Proliferation and Activation Are Modulated By ECMPs.....45

    3.4.3 The Role of Wnt Proteins in HSC Proliferation and Activation Is Context Dependent .....48

3.5 DISCUSSION .....51

    3.5.1 Arrayed Combinatorial Microenvironments As a High-throughput Technology for Understanding HSC Biology .....51

    3.5.2 ECMPs Control HSC Proliferation and Activation.....53



3.5.3 Wnt Proteins Interact with ECMPs to Influence HSC Biology .....	55
3.5.4 Implications for Culture Activation of HSCs .....	56
3.6 CONCLUSION.....	57
3.7 ACKNOWLEDGEMENTS .....	57
 <b>CHAPTER 4 DEFINING LONG-TERM MAINTENANCE CONDITIONS OF HUMAN</b>	
<b>EMBRYONIC STEM CELLS WITH ARRAYED CELLULAR</b>	
<b>MICROENVIRONMENT TECHNOLOGY .....</b>	
<b>MICROENVIRONMENT TECHNOLOGY .....</b>	<b>65</b>
4.1. ABSTRACT .....	65
4.2 INTRODUCTION .....	66
4.3 MATERIALS AND METHODS .....	68
4.3.1 Array Fabrication.....	68
4.3.2 Cell Culture .....	69
4.3.3 Slide Staining, Imaging, and Quantification .....	71
4.3.4 Long Term hESC Culture on Defined Conditions .....	72
4.3.5 Karyotype Analysis.....	73
4.3.6 Embryoid Body Formation.....	73
4.3.7 RT-PCR Analysis .....	73
4.3.8 Data Analysis .....	74
4.4 RESULTS .....	74
4.4.1 Arrayed Cellular Microenvironments to Study hESC Fate .....	74
4.4.2 Individual ECMPs Differentially Support hESC Proliferation In a Concentration-dependent Manner.....	75

4.4.3 Effect of ECMP Composition on hESC Proliferation and Maintenance of Pluripotency .....	76
4.4.4 Effect of GFs and Small Molecules on hESC Proliferation and Maintenance of Pluripotency .....	79
4.4.5 Long-term Culture of hESCs in Completely Defined Conditions .....	81
4.5 DISCUSSION .....	83
4.5.1 Defined Matrix for the Long-term Proliferation of hESCs .....	83
4.5.2 High-throughput Platform for Screening Signaling Molecules to Direct hESC Fate .....	84
4.5.3 Investigation with Arrayed Based High-throughput Approaches .....	84
4.6 CONCLUSION.....	87
4.7 ACKNOWLEDGEMENTS .....	87
<b>CHAPTER 5 SYNTHETIC POLYMERS SUPPORT LONG-TERM HUMAN</b>	
<b>EMBRYONIC SELF RENEWAL.....</b>	<b>98</b>
5.1 ABSTRACT .....	98
5.2 INTRODUCTION .....	99
5.3 MATERIALS AND METHODS .....	100
5.3.1 Polymer Array Fabrication.....	100
5.3.2 Cell Culture .....	101
5.3.3 Slide Staining, Imaging and Quantification .....	102
5.3.4 Oct4-GFP Reporter Line .....	103
5.3.5 Polymer Hydrogel Fabrication .....	103

5.3.6 Polymer Coated Slide Fabrication .....	104
5.3.7 Polymer Coated Slide Fabrication .....	104
5.3.8 Data Analysis .....	104
5.4 RESULTS .....	105
5.4.1 Polymer Microarrays to Study Cell Fate .....	105
5.4.2 Polymer Microarray Screens with hESCs .....	105
5.4.3 Subset of Polymers Support hESC Proliferation and Maintenance of Pluripotency .....	107
5.4.4 Long-term Culture of hESCs on Defined Polymers.....	108
5.5 DISCUSSION .....	110
5.5.1 Biomaterial Based Expansion of hESCs.....	110
5.5.2 PMVE-alt-MA Promotes hESC Proliferation in the Absence of Exogenous ECMPs .....	111
5.5.3 Polymer Microarrays to Modulate hESC Fate.....	112
5.6 CONCLUSIONS .....	113
5.7 ACKNOWLEDGEMENTS .....	114
 <b>CHAPTER 6 FUTURE PROSPECTIVES</b>	
6.1 ABSTRACT .....	123
6.2 CREATING “COMPREHENSIV” MICROENVIRONMENTS .....	123
6.3 “OFF CHIP” ANALYSIS .....	124
6.4 ARRAY BASED RNA INTERFERENCE TO STUDY GENE FUNCTION.....	125
6.5 CELLULAR MICROARRAYS IN DRUG DISCOVERY .....	126

6.6 CONCLUSION.....	127
<b>REFERENCES.....</b>	<b>13</b>

## LIST OF FIGURES

FIGURE 1-1: Cellular Microenvironment.....	16
FIGURE 1-2: Organization of Stem Cell Niches.....	17
FIGURE 1-3: Derivation and Culture of Human Embryonic Stem Cells.....	18
FIGURE 2-1: Arrayed Cellular Microenvironment (ACME) Technology.....	30
FIGURE 2-2: Characterization of ECMP Deposition .....	31
FIGURE 2-3: Reproducibility of Printed Proteins .....	32
FIGURE 2-4: Cell Culture Compatibility—Human Embryonic Kidney (HEK) Cells on ACME .....	33
FIGURE 2-5: Spotted Signaling Molecules Remain Localized and Retain Their Signaling Ability .....	34
FIGURE 3-1: High Throughput Combinatorial Array Technology .....	38
FIGURE 3-2: Effect of ECMPs on HSC Proliferation and Activation .....	39
FIGURE 3-3: Identification of ECMPs Having Prominent Effect on HSC Proliferation and Activation .....	40
FIGURE 3-4: Characterization of Array-based Data .....	41
FIGURE 3-5: Effect of Wnt Proteins on HSC Proliferation and Activation .....	42
FIGURE 4-1: Cellular Microarray Technology Platform.....	89
FIGURE 4-2: HESC Proliferation As a Function of ECMP Substrate Concentration .....	90
FIGURE 4-3: Effect of ECMP Composition on HESC Proliferation .....	91
FIGURE 4-4: Effect of ECMP Composition on HESC Proliferation and Maintenance of Pluripotency.....	92
FIGURE 4-5: Principle Component Analysis of ECMP Effect on Proliferation and Maintenance of Pluripotency of HESCs .....	93
FIGURE 4-6: Spotted Signaling Molecule Modulate HESC Fate.....	94

FIGURE 4-7: Identification of Optimum ECMP Condition for Long-term Culture of HESCs.....	95
FIGURE 4-8: An Optimized ECMP Composition (C1 + C4 + Fn + Ln) Supports Long-term Culture of HESCS in Defined Conditions .....	96
FIGURE 4-9: Differentiation Potential of HESC Grown on Defined Matrix .....	97
FIGURE 5-1: Schematic Representation of Polymer Array Assay .....	115
FIGURE 5-2: Validation of GFP Detection .....	116
FIGURE 5-3: Sample of H1299 “Hits” on Polymer Arrays.....	117
FIGURE 5-4: Synthetic Polymers Supporting HESC Proliferation and Maintenance of Pluripotency.....	118
FIGURE 5-5: Influence of Molecular Weight on Cell Proliferation is Specific to HESCs.....	119
FIGURE 5-6: Short Term Propagation of HESCs on Polymer Hydrogels.....	120
FIGURE 5-7: Long Term Culture of HESCs on Defined Substrates.....	121
FIGURE 6-1: Diagram of Set to Apply Mechanical Stimuli to ACME.....	128
FIGURE 6-2: Diagram of “Off Chip” Analysis.....	127

## LIST OF TABLES

TABLE 3-1: Reproducibility Between Biological Repeats.....	63
TABLE 3-2: Groupings of ECMP Microenvironments.....	64
TABLE 5-1: Polymer Microarray Design .....	113

## AKNOWLEDGEMENTS

I would like to acknowledge the many people who made it possible for me to complete my thesis. First and foremost, I would like to thank my advisors Dr. Shu Chien and Dr. Karl Willert for providing me the freedom to pursue the research that interested me. Without their mentorship I would not have achieved the level of success that I have. I would also like to thank Dr. Shyni Varghese for her advisement and for treating me like one of her own graduate students. I am also grateful towards Dr. Thomas Fellner, Zoe Vomberg, and Megan Robinson of UCSD Human Embryonic Stem Cell Core for their assistance in my research. I am also grateful toward Kevan Shah for his assistance towards the end of my dissertation. As always, I am grateful to the many friends and family that provided encouragement and support over the years. In particular, I am grateful for my wife, Jayna, who provided much love, support, and tolerance.

The text and figures in Chapter 1 are in part reproductions from: Brafman DA and Chien S. High-throughput systems for stem cell engineering. 2009. *In preparation*. The text and figures in Chapter 2 and Chapter 4 are in part reproductions from: Brafman DA, Shah KD, Fellner T, Chien S, Willert K. Defining long-term maintenance conditions of human embryonic stem cells with arrayed cellular microenvironment technology. *Stem Cell Dev.* 2009. 18(8). The text and figures in Chapter 3 are in part reproductions from: Brafman DA, De Minicis S, Seki E, Brenner DA, Willert K, Chien S. Investigating the role of the extracellular environment in modulating hepatic stellate cell biology with arrayed combinatorial microenvironments. 2009. *Integ Bio.* *In review*. The text and figures in Chapter 5 are in part reproductions from: Brafman DA, Chang J, Shah KD, Varghese S, Willert K, Chien S. Synthetic polymers support long term human embryonic stem cell self-renewal. 2009. *In preparation*. In all cases, the dissertation author was the primary researcher and author pertaining to this work.



## VITA

### EDUCATION

**Doctor of Philosophy, Bioengineering**, September 2009  
University of California-San Diego, La Jolla, CA

**Masters of Science, Bioengineering**, June 2007  
University of California-San Diego, La Jolla, CA

**Bachelor of Science, Bioengineering**, Minor: Chemistry, May 2005  
University of California-Berkeley, Berkeley, CA

### PUBLICATIONS

1. **Brafman DA**, Chien S. High-throughput systems for stem cell engineering. 2009. *In preparation.*
2. **Brafman DA**, Chang J, Shah KD, Varghese S, Willert K, Chien S. Synthetic polymers support long term human embryonic stem cell self-renewal. 2009. *In preparation.*
3. **Brafman DA**, De Minicis S, Seki E, Brenner DA, Willert K, Chien S. Investigating the role of the extracellular environment in modulating hepatic stellate cell biology with arrayed combinatorial microenvironments. 2009. *Integ Bio. In review*
4. Sary CM, Walsh BJ, Knapp AE, **Brafman D**, Hogan MC. Calcium transients contribute to the contraction-induced elevation of heat shock protein 72 mRNA in isolated single skeletal muscle fibers. *Am J Physiol: Regul Integr Comp Physiol.* 2009. *In review.*
5. Story M.F, Winters JM, Lemke, M, Barr A, Omiattek E, Janowitz I, **Brafman D**, Rempel DM. A method for evaluating accessibility of medical equipment for patients with disabilities. *Appl Ergon.* 2009. *In review.*
6. **Brafman DA**, Shah KD, Fellner T, Chien S, Willert K. Defining long-term maintenance conditions of human embryonic stem cells with arrayed cellular microenvironment technology. *Stem Cell Dev.* 2009. 18(8)
7. Sary CM, Walsh BJ, Knapp AE, **Brafman D**, Hogan MC. Elevation in heat shock protein 72 mRNA following contractions in isolated single skeletal muscle fibers. *Am J Physiol: Regul Integr Comp Physiol.* 2008. 295(2):p.R643-8.
8. DeMinicis S, **Brafman DA**, Marizoni M, Seki E, Willert K, Chien S, Brenner DA. Extracellular matrix combinations differentially modulate hepatic stellate cell biology. *Dig Liv Dis.* 40(10):pA132-A133.
9. Sary CM, Walsh BJ, Knapp AE, **Brafman D**, Hogan MC. Elevation of heat shock

protein 72 mRNA in contracting single *Xenopus* muscle fibers is fiber type and not fatigue dependent. *Med Sci Sports Exerc.* 2007. 39(5):p.S222.

10. Rempel D, Barr A, **Brafman D**, Young E. The effect of six keyboard designs on wrist and forearm postures. *Appl Ergon.* 2007. 38(3):p.293-8.

## **PATENTS**

1. **Brafman DA**, Willert K, Chien S. (2009) Defined Matrix for the Culture of Human Embryonic Stem Cells (U.S. Provisional Application Serial No. 61/164,823 filed on March 30, 2009)
2. **Brafman DA**, Willert K, Chien S. (2009) Array-based High Throughput Screening Technology for the Identification of Factors that Modulate Stem Cell Fate (SD2009-182, pending)

## **HONORS/AFFILIATIONS**

National Science Foundation Graduate Research Fellowship, 2006-present

University of California BREP GREAT Fellowship, 2006-present

National Institutes of Health Pre-doctoral Fellowship, 2005-2006

Guidant Research Fellowship, 2004

Tau Beta Pi Engineering Society

ABSTRACT OF THE DISSERTATION

HIGH-CONTENT ARRAY BASED SCREENING TECHNOLOGY FOR THE  
IDENTIFICATION OF FACTORS THAT REGULATE CELL FATE

by

David Adam Brafman

Doctor of Philosophy in Bioengineering

University of California, San Diego, 2009

Professor Shu Chien, Chair

Professor Karl Willert, Co-Chair

High throughput screens (HTS) of biological and synthetic molecules has become a useful tool in drug discovery and basic biology. However, traditional HTS can

be cost-prohibitive given the costs of purified biological molecules and the rarity of certain cell types. Additionally, these approaches employ a candidate based strategy ignoring the complex crosstalk that occurs between combinations of biological molecules. To that end, we have developed a technology platform, called arrayed cellular microenvironments (ACME), which allows for the real-time simultaneous screening of thousands of biological and synthetic physiochemical parameters on cell attachment, proliferation, differentiation and gene expressions. We demonstrate that our platform provides data comparable to that obtained from traditional multi-well based assays while using 1,000-10,000 times fewer cells and reagents. As proof of principle, we applied this technology to identify combinations of microenvironment components that differentially modulate the phenotype of hepatic stellate cells (HSCs), a progenitor cell population of the liver that are involved in liver homeostasis. Next, we modified the ACME technology to screen the full complement of factors that may regulate human embryonic stem cell (hESC) proliferation and maintenance of pluripotency. Through the systematic screening of extracellular matrix proteins (ECMPs) and other signaling molecules, we developed and characterized a completely defined culture system for the long-term self-renewal of three independent hESC lines. Finally, we extended the ACME technology to screen synthetic polymers and peptides to identify artificial matrices that support self-renewal of hESCs. This system will be useful for future stem cell research, including the elucidation of differentiation protocols, as well as the identification of culture conditions of rare and recalcitrant primary cell populations, such as progenitor, adult stem, and cancer stem cells.

# CHAPTER 1

## INTRODUCTION

### 1.1 THE CELL MICROENVIRONMENT

The *in vivo* cellular microenvironment can be thought of as a complex mixture consisting of four distinct “compartments”: (1) Immobilized protein factors such as extracellular matrix proteins (ECMPs) interact with their environment through integrin binding. (2) Soluble protein factors (such as growth factors, small molecules, and hormones) influence cell signaling pathways via their appropriate extracellular receptors. (3) Mechanical forcers (such as stretch or shear stress) can influence intracellular signaling processes by activating mechanoreceptors. (4) Neighboring cell types communicate with each other by cadherin mediated signaling (Figure 1-1) [1, 2]. Each of these compartments include tens to thousands of “members” that influence numerous signaling pathways, which perturb gene and protein function, and ultimately affect cell fate and cell function.

#### 1.1.1 Crosstalk in the Microenvironment

Members of each of these compartments interact in complex manner to influence each other’s signaling ability, a phenomenon known as crosstalk. For example, endothelial cell attachment to fibronectin via  $\alpha 5\beta 1$  integrin potentiates  $\alpha v\beta 3$  mediated migration on vitronectin [3]. Along similar lines, growth factors and ECMPs often have a reciprocal relationship—cell adhesion to ECMPs is required for activation of growth

factor receptors, and growth factors are necessary to stimulate cell adhesion, migration and the resulting integrin-dependent response. These interactions, which can be synergistic or antagonistic, have been well documented in numerous biological systems [4, 5]. For example,  $\alpha\beta3$  integrin associates with activated insulin and platelet derived growth factor (PDGF) receptors and potentiates the biological activity of PDGF [6]. Likewise, in human blood mononuclear cells, collagen-induced release of interleukin 1 (IL-1) through binding integrin  $\alpha7\beta1$  is potentiated by fibronectin binding to  $\alpha5\beta1$  [7]. These few examples demonstrate the importance in crosstalk in regulating cell fate. Given that these interactions are often unpredictable, a systematic approach to study crosstalk is needed.

## **1.2 STEM CELL MICROENVIRONMENTS: THE NICHE**

Stem cells have the unique ability to grow indefinitely (proliferation) or adopt new cellular fates (differentiation). As a result, stem cells hold great potential for cell based therapies. Experimental manipulation of these cells to affect proliferation and differentiation is central to developing strategies for the production of defined cell types, which can be potentially used to treat a variety of degenerative disorders such as Alzheimer's and heart disease.

*In vivo*, stem cells reside in specialized regions of organs and tissues called niches that regulate self renewal and differentiation [8, 9]. The niche also serves to prevent excessive cell production that could lead to cancer [10]. Thus, the niche must maintain a delicate balance between stem cell proliferation and quiescence.

The first stem cell niche identified in mammals was the hematopoietic stem cell niche. Individual hematopoietic stem cells (HSCs) are multipotent and highly self-renewing yet proliferate quite slowly [11]. However, the manner in which HSCs interact

with their niche to promote self-renewal has not been elucidated. Furthermore, few poorly defined culture systems exist that allow for maintenance and expansion of HSCs *in vitro* [12]. More recently, niches have been identified in a wide range of tissues such as the skin, brain, gut, and liver [13, 14]. Similarly, it has been difficult to expand these stem/progenitor cell populations *in vitro* without the loss of stem cell potential.

The numerous tissue specific stem cell niches are similarly organized (Figure 1-2). The niche cells provide cell-cell contacts and paracrine signaling that regulate the self-renewal of the neighboring stem cells. The extracellular matrix (ECM) provides a scaffold for stem cell growth in the niche and can interact with soluble factors to regulate signal transduction. Additionally, glycoasaminoglycans serve to locally concentration and present soluble cytokines. The physiochemical environment, including oxygen gradients, pH, matrix stiffness, and topography also contribute to the regulation of stem cell proliferation, self-renewal, and differentiation [15].

### **1.3 EMBRYONIC STEM CELLS (ESCs)**

Embryonic stem cells (ESCs), which are derived from the inner cell mass of the pre-implantation embryo, the blastocyst, are able to generate all derivatives of the three primary germ layers—ectoderm, endoderm and mesoderm—a property referred to as pluripotency.

Unlike tissue specific adult stem cells, ESCs are only transiently present during development and do not have a stable niche *in vivo*. Nonetheless the many culture systems exist for ESC proliferation and differentiation exploit the interactions between ECMPs, soluble factors, and the physiochemical environment that may exist during this transient state.

### **1.3.1 Human Embryonic Stem Cells (hESCs)**

Human embryonic stem cells (hESCs) hold great potential in the treatment of many human disorders for which no effective therapies presently exist. However, many challenges remain before such therapies can become a reality: (a) lack of well-defined conditions for derivation and expansion of clinical grade hESCs, (b) insufficient systematic control over conditions that regulate hESC behavior, and (c) inability for large-scale production of hESCs in defined conditions needed for human therapy and drug screening.

#### **1.3.1.1 “Optimal” hESC culture conditions**

There has been much debate about the optimal hESC culture conditions. The ideal culture conditions will allow hESCs to maintain their fundamental characteristics: 1) proliferate extensively *in vitro*, 2) express high levels of pluripotency markers such as Oct4, Nanog, and Sox2, 3) maintain a normal euploidy karyotype, 4) differentiation into derivations of all three germ layers, and 5) show telomerase activity. The culture conditions should also be robust enough to support multiple hESC lines. It is also important for therapeutic applications that the conditions be free from xenogeneic proteins. Thus, the ideal culture conditions will consist of a defined matrix and defined media supplemented with recombinant or purified human proteins. Finally, the optimal conditions should be cost-effective in order to allow for expansion of sufficient quantity of cells.

#### **1.3.1.2 Current hESC derivation and culture conditions**

Since their derivation, hESCs have been derived and culture in numerous ways. Most hESC culture protocols utilize mouse embryonic fibroblast (MEF) feeders that



secrete a combination of many uncharacterized factors, some of which are critical to the maintenance of the pluripotent state [16] while others promote their differentiation. More recently, several protocols for the “feeder-free” culture of hESCs have been described [17]. These methods generally involve the use of extracellular matrices, such as Matrigel™ (BD), to provide a suitable cell adhesion substrate and media that have been conditioned on mouse or human feeder layers [18]. Both of these methods of derivation and culture are outlined in Figure 1-3. Matrigel is a soluble basement membrane extract of the Engelbreth-Holm-Swarm (EHS) mouse tumor, and consisting of an undefined composition of laminin, collagen IV, entactin and heparan sulfate proteoglycan, as well as various growth factors such as basic fibroblast growth factor ( $\beta$ FGF), epidermal growth factor (EGF), insulin-like growth factor-1 (IGF-1), platelet-derived growth factor (PDGF), nerve growth factor (NGF) and transforming growth factor  $\beta$ 1 (TGF $\beta$ 1) [16]. Both Matrigel and conditioned media (CM) contain undefined components of non-human origin, making the cells cultured in these conditions unsuitable for any future therapeutic applications. Specifically, hESC cultured in the presence MEF feeders or mouse CM incorporated a murine sialic acid, Neu5Gc [19]. The sialic acid was shown to result in binding of antibodies specific for Neu5Gc which would lead to rejection of any transplanted cells.

A number of studies have explored the role of a subset of signaling pathways on the proliferation, maintenance of pluripotency, and differentiation of hESCs. Many signaling pathways regulating hESC proliferation and maintenance have been identified. Fibroblast growth factor (FGF) signaling (specifically FGF2) is essential for proliferation and maintenance of pluripotency [17, 20]. Modulation of other pathways, such as activation of Activin (a member of the transforming growth factor (TGF) superfamily) or

inhibition of BMP (another member of the TGF superfamily) signaling, has affected the regulation of hESC proliferation and maintenance of pluripotency [17, 21, 22].

Recent studies investigating the composition of MEF-CM has provided clues about the specific factors required for supporting hESC pluripotency. These studies have demonstrated the use of several factors to enhance hESC culture, such as hyaluronic acid [23], glycogen synthase kinase 3 (GSK3 inhibitor) [24], Activin A [25], platelet derived growth factor (PDGF) [26], spingosine-1-phosphate [26], and Noggin [27]. However, individually these factors were unable to support the long-term maintenance of hESCs in the absence of CM. Recently, several groups have reported the successful use of combinations of factors to replace the need for CM [20-24, 28-30]. Ludwig *et al.* developed a defined media in which basic fibroblast growth factor ( $\beta$ FGF), lithium chloride (LiCl),  $\gamma$ -aminobutyric acid (GABA), peipecolic acid, and transforming growth factor could replace the need for CM in hESC cultures. Along similar lines, Wang *et al.* developed a defined medium containing an insulin growth factor 1 (IGF1 analog), heregulin-1 $\beta$ ,  $\beta$ FGF, and Activin A that supported long-term growth of multiple hESC lines.

Despite these advances in replacing CM with combinations of defined components, only a few studies have been performed to replace Matrigel with extracellular matrix proteins (ECMPs) such as fibronectin, laminin, or vitronectin [31-34]. These previous attempts to define the optimal culture conditions for hESCs, however, were made with random variations of a few ECMPs and other signaling molecules without systematically assessing the optimal conditions required for the long-term culture of hESCs. While ECMPs interact in a complex manner to regulate ESC proliferation, maintenance of pluripotency, and differentiation [35, 36], these interactions have not been studied systematically in hESCs.

### 1.3.1.3 Biomaterials as stem cell growth substrates

Approaches in which hESCs are grown on recombinant or human purified ECMPs will eliminate the risk of contamination with components of non-human origin. However, most of these proteins are expensive, difficult to isolate and subject to batch-to batch variation and thus are not a viable option for large scale expansion of hESCs. On the other hand, biomaterials are an inexpensive, easily produced, and reliable alternative for *in vitro* hESC expansion.

Biomaterials have been used for the expansion of many human adult stem cell and progenitor populations. Mesenchymal stem cells (MSCs), for example, have been maintained and differentiated on several different classes of synthetic and natural biomaterials [37-41]. Curran *et al.* used unmodified and methyl modified silane surfaces to enhance MSC proliferation. Likewise, neural stem cells (NSCs) have been maintained and expanded on 3D scaffolds composed of amino polymers such as poly(D-lysine) [42]. There has been some progress in the application of polymers for expansion and maintenance of ESCs. For example Harrison *et al.* used aliphatic poly( $\alpha$ -hydroxy esters) such as poly(D,L-lactide) and poly(glycolide) to propagate murine ESCs [43]. Biomaterial based expansion of hESCs, however, has not been met with the same success [43, 44]. This is not surprising because of the limited diversity of polymers that were tested in these studies and given that there is no established set of principles or properties that can assist in prediction of which polymers would be satisfactory for supporting hESC expansion.

## 1.4 HIGH-THROUGHPUT APPROACHES FOR STUDYING STEM CELL BIOLOGY

The traditional reductionist biological approaches have elucidated the importance and roles of individual members that compromise the cellular microenvironment. However, cells respond to combinations of these factors rather than any single molecule. Additionally, conventional cell culture methods, such as multi-well cell culture dishes, are limited in their ability to screen the vast number of possible combinations of factors that may influence cell behavior. The establishment of high-throughput screening (HTS) approaches will be important for a broad range of applications including basic understanding of the role of certain signaling networks in regulating stem cell fate decisions.

#### **1.4.1 Traditional HTS For Identifying Modulators of Stem Cell Fate**

Traditional HTS uses microtiter plates along with robotics, liquid handling devices, and automated imagers to quickly conduct thousands to millions of simultaneous experiments. These screens have become a useful tool to address questions in basic stem cell biology and chemistry. Many groups have used HTS of chemical libraries to identify small molecules that regulate murine ESC self-renewal [45]. For example, Chen *et al.* used a high-throughput iterative screening approach to identify a small molecule that promoted the self-renewal of mouse embryonic stem cells in the absence of leukemia inhibitory factor (LIF) and feeder cells. Furthermore, HTS has been used to identify various small molecules that promote murine ESC differentiation into multiple lineages. Ding *et al.* used a high-throughput phenotypic cell base screen of kinase directed libraries to identify a synthetic small molecule, TWS119, that induces neurogenesis in murine ESCs [46]. Using a combinatorial library of peroxisome proliferator-activated receptor (PPAR) ligands, Wei *et al.* designed novel molecules to promote mesodermal differentiation of murine ESCs into beating cardiomyocytes [47].

Along similar lines, Wu *et al.* utilized a phenotypic cell-based screen of a large combinatorial chemical library to discover a class of diaminopyrimidine compounds that efficiently induce murine ESCs to differentiate into cardiomyocytes [48].

The development of HTS for hESCs has been difficult because of challenges involved in establishing suitable and growth conditions. More recently, though, HTS has been adapted to identify compounds that regulate self-renewal and differentiation in hESCs [49]. For example, Zhu *et al.* used HTS to identify a small molecule, stauprimide, that down regulates c-Myc and thus increases the efficiency of the directed differentiation of hESCs [50].

Although HTS have greatly advanced modern biology and drug discovery, it is not practical for all purposes given the cost and large number of cells and reagents required. For example, typical HTS require 25-50 X 10<sup>4</sup> cell per molecule screened [49]. Thus, HTS is not feasible for screens involving primary and other progenitor cells which are rare and difficult to isolate. Along similar lines, HTS using conventional multi-well plates can be cost prohibitive and often do not provide adequate quantitative information on cell function. Additionally, most HTS approaches only have the capacity to investigate the effects of one factor at time, often ignoring the complex crosstalk that typically occurs in biological settings between combinations of molecules.

#### **1.4.2 Cellular Microarray-based Screening in Stem Cell Research**

Cellular microarrays have become a useful tool for the screening of large numbers of biological molecules [51]. Typical cellular microarrays consist of a chip (e.g. glass microscope slide) where minute volumes ( $\mu\text{L}$  to nL) of various molecules (e.g. ECMPs, small molecules, cytokines, biopolymers) can be distributed in defined locations and can be analyzed for their effect on cellular processes (e.g. changes in gene and

protein expression levels). These arrays can be fabricated using robotic spotting, photo-assisted, and soft-lithography approaches.

The major challenge hindering the progress of stem cell based therapies is identifying the multitude of conditions that regulate and influence their fate. Being able to identify components that mimic the stem cell niche will aid in the expansion and differentiation of stem cells *in vitro*. Considering the complexity of the microenvironments in which stem cells reside, it is impractical to test proliferation and differentiation conditions using current established HTS methods. Cellular microarrays are advantageous to traditional well-based HTS as they provide more information from smaller sample volumes in a rapid, efficient, and cost effective manner.

#### **1.4.2.1 Microfluidic array approaches to study stem biology**

Microfluidic devices are powerful tools that have the ability to control the soluble and mechanical properties of the cell culture environment. Microfluidic devices are fabricated by the casting poly-dimethylsiloxane (PDMS) over a prefabricated mold. The advantages of microfluidics include 1) decreased reaction rates and analysis times, 2) reduced consumption of reagents, 3) reduced production of harmful by-products, and 4) ability to run multiple experiments on a single chip [52].

Recently, microfluidic approaches have been used for the analysis of signals that affect stem cell fate. Kim *et al.* developed a microfluidic device for analyzing 16 unique murine ESC cultures in parallel [53]. Using this platform, the authors identified an optimal flow rate that enhanced murine ESC colony formation, proliferation, and maintenance of pluripotency. Along similar lines, Figallo *et al.* developed a micro-bioreactor array that was fabricated using soft lithography and contains twelve independent micro-bioreactors [54]. Each micro-bioreactor can be perfused with independent culture media containing

various biological molecules. Finally, Zhong *et al.* designed an integrated microfluidic platform that allows the screening of individual hESC colonies in real-time using six individual cell culture chambers [55]. Although these microfluidic platforms enable the multiplexing of experiments, they suffer from the following disadvantages: 1) relative low throughput, 2) difficulty of fabrication 3) inability to perform on chip immunocytochemistry and 4) lack of compatibility with conventional, high magnification light and fluorescent microscopy.

#### **1.4.2.2 Microwell arrays to analyze factors regulating stem cell fate**

By using soft lithography methods, microwell arrays with defined dimensions can be fabricated. For example, microfabrication was used to create an array of approximately 10,000 microwells on a glass coverslip for the parallel, quantitative analysis of single ESCs [56]. Furthermore, the well sizes could be adjusted from 10-500  $\mu\text{m}$  in height and 20-500  $\mu\text{m}$  in diameter and the platform was compatible with traditional light and fluorescent microscopy. The microwell platform was used to investigate the effect of cell density on the proliferation dynamics of rat neural stem cells (NSCs).

Microwell arrays have been utilized for the parallel manipulation and quantitative analysis of stem cells at the single cell level. For example, Cordey *et al.* combined biomimetic hydrogel matrix technology with microengineering to fabricate a microwell array which can be used to control NSC fate and neurosphere formation [57]. Using this technology, the authors were able to enhance the viability and control the size of neurospheres formed from a single founding cell. Similarly, clonal microwell arrays have been generated by seeding a population of cells at a clonal density on micropatterned surfaces [58]. Clones then can be selected after being assayed for various cellular properties such as proliferation, signal transduction, and differentiation.

Directed differentiation of ESCs through formation of embryoid bodies (EB) has been enhanced by using microwell array techniques. EBs are typically formed using the hanging drop method [59] or in suspension culture [60]. The resulting EBs are heterogeneous in shape and size. As a result, cell populations obtained from EBs formed by these methods can vary considerably. To provide more uniform microenvironments to EBs and thus more uniformly direct EB differentiation microwell approaches have been implemented. For example, Mohr *et al.* used poly(ethylene glycol) (PEG) microwells to create EBs of homogenous size and shape [61].

Microwell approaches can provide precise control over microenvironment parameters such as shape and size. However, in contrast to most multi-well formats all wells share the same culture media. Thus, it is difficult to vary other parameters of the microenvironment in a high throughput manner.

#### **1.4.2.3 Combinatorial arrays for studying stem cell microenvironments**

Combinatorial arrays consist of immobilization of signaling molecules on a surface onto which cells are seeded. Flaim *et al.* developed a microarray platform to screen ECMPs and their effects on stem cells in a combinatorial fashion [62]. Specifically, with the use of robotic devices different ECMP combinations were spotted and the commitment of mouse ESCs towards an early hepatic fate was evaluated. Several combinations of ECMP components that influenced stem cell differentiation and hepatocyte function were identified. This platform was further developed to probe the interactions between ECMPs and soluble growth factors on stem cell fate [63]. Along similar lines, Soen *et al.* used robotic spotting techniques to print arrays of ECMPs, growth factors, and other signaling molecules to evaluate their effects on the proliferation and differentiation of human adult neural precursor cells [64]. This study revealed



significant effects of certain signaling molecules (such as BMPs, Wnts, and Notch) on the extent and direction of differentiation into neuronal or glial fate. For example, the authors found that Wnt and Notch co-stimulation maintained the cells in an undifferentiated state. Although these platforms have been used to elucidate the role of certain microenvironmental components on stem cell fate, they have some shortcomings. Specifically, the platform developed by Flaim *et al.* relied on the addition of signaling molecules to the surrounding media, thereby limiting the throughput and the complexity of the microenvironments that could be screened. Likewise, the platform developed by Soen *et al.* had the following limitations: (1) Only one ECMP was printed at a time thereby limiting the complexity of the microenvironment. (2) Proteins are covalently attached directly to aldehyde-derivatized slides which may limit the biological activity of certain signaling molecules. (3) The large size of the spotted microenvironments (> 500  $\mu\text{m}$ ) limits the throughput of the system. These platforms also rely on end-point assays thus ignoring the dynamic, time sensitive effects of certain signaling molecules.

Synthetic polymers can also be printed in arrays using robotic patterning techniques. Anderson *et al.* developed a high-throughput, miniaturized array platform that enabled the nanoliter scale synthesis and cell-based screening of biomaterials using stem cells [65]. However, this technique required that materials be synthesized on the array limiting the screening those polymers that could be synthesized via free radical polymerization. Additionally, given the stochastic nature of free radical polymerization the final composition of the screened polymers is undefined. Finally, while this platform was able to characterize many conditions that facilitate cell interactions with these synthetic polymers, these synthetic microenvironments do not contain signaling molecules that are instructive in cell fate choice.

## 1.5 OUTLINE OF DISERTATION

Development and maintenance of multi-cellular life forms involves complex interactions between cells and biomolecules that mediate cell-cell and cell-matrix contact. Due to the vast number of molecules used in biological systems and furthermore the virtually limitless possible combinations of these molecules, it has been extremely difficult to identify sets of conditions that specifically affect in a biologically relevant manner the behavior of any cell type *in vitro*. Conventional cell culture methods, such as multi-well cell culture dishes, are limited in their ability to screen the vast number of possible combinations of factors that may influence hESC behavior. **Chapter 2** describes the development a technology platform, called arrayed cellular microenvironments (ACME), which allows for the real-time simultaneous screening of thousands of biological and synthetic physiochemical parameters on cell attachment, proliferation, differentiation and gene expressions. As proof of principle, we applied this technology to identify combinations of microenvironment components that differentially modulate the phenotype of hepatic stellate cells, a progenitor cell type of the liver that are involved in liver homeostasis (**Chapter 3**).

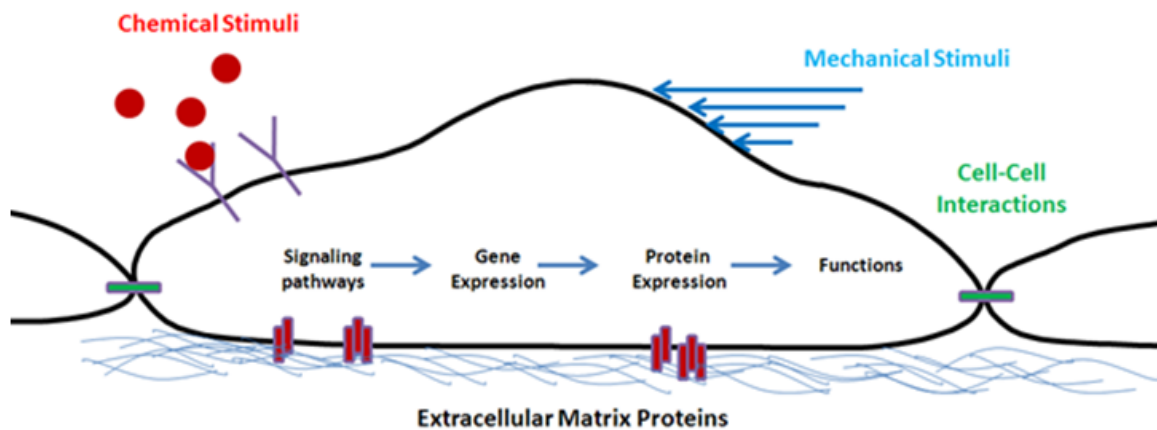
With the derivation of human embryonic stem cells (hESCs) [66], it has for the first time become conceivable to study various aspects of human development at the cellular level in a culture dish. In addition, hESCs represent an infinite supply of cellular “raw-material” for future cell-based therapies, drug testing and disease modeling. However, the *in vitro* culture conditions and the cellular microenvironments that either promote hESC expansion or their specific differentiation have either not been developed or not been defined. Through the systematic screening of extracellular matrix proteins (ECMPs) and other signaling molecules using ACME, we developed and characterized a

completely defined culture system for the long-term self-renewal of three independent hESC lines (**Chapter 4**). We also demonstrate the feasibility of future studies in which ACME is applied towards the directed differentiation of hESCs and maintenance of other stem and progenitor cell populations.

Although, approaches in which hESCs are grown on recombinant or human purified ECMPs will eliminate the risk of contamination with components of non-human origin, most of these proteins are expensive, difficult to isolate and subject to batch-to-batch variation and thus are not a viable option for large scale expansion of hESCs. Biomaterials are an inexpensive, easily produced, and reliable alternative for *in vitro* hESC expansion, but few studies have assessed the efficacy of synthetic polymers in expanding and maintaining ESCs. **Chapter 5** describes the adaptation of ACME to identify synthetic biomaterials that control cell fate. Specifically, this technology was used to identify and optimize artificial matrices that can support growth and maintenance of undifferentiated hESCs. Finally, **Chapter 6** summarizes our research and provides some future directions for the technology.

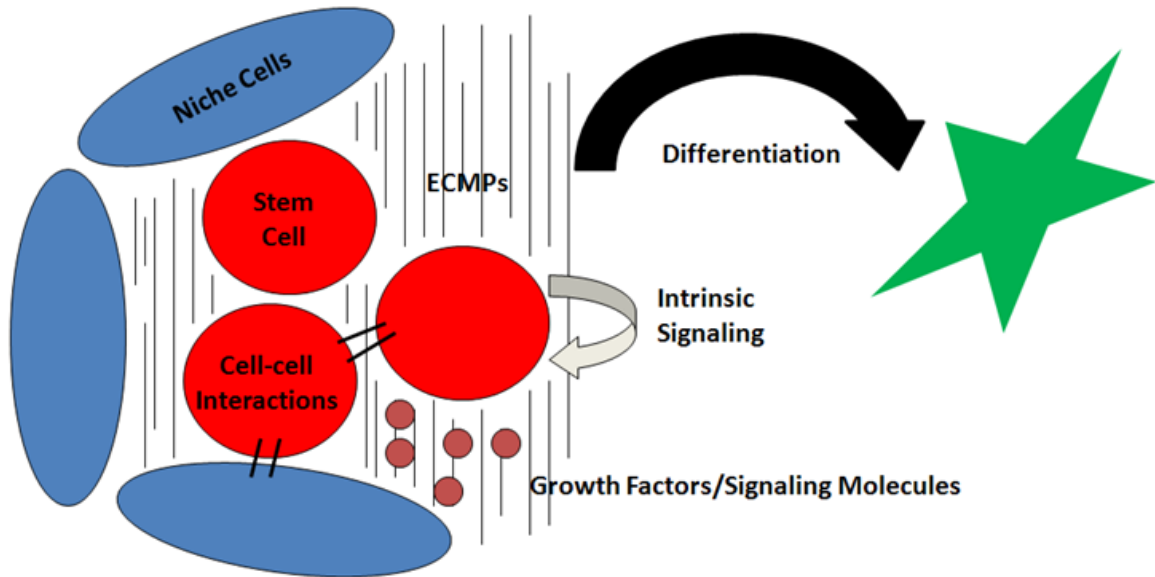
## 1.6 ACKNOWLEDGEMENTS

The text and figures in Chapter 1 are in part reproductions from: Brafman DA and Chien S. High-throughput systems for stem cell engineering. 2009. *In preparation*. The dissertation author was the primary researcher and author pertaining to this work.



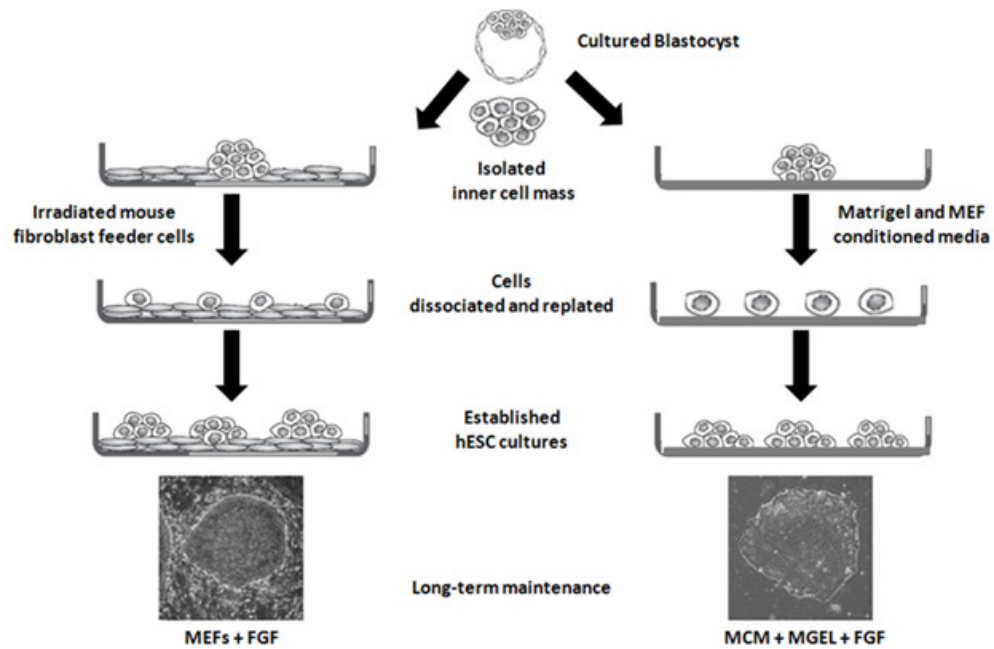
**Figure 1-1: Cellular Microenvironment**

Four distinct compartments of the cellular microenvironment that affect cell fate. (1) Extracellular matrix proteins interact with the cell through most commonly through integrin signaling. (2) Cell to cell interactions are mediated through cadherin signaling. (3) Chemical stimuli such as growth factors and hormones interact with the cell through their respective receptors. (4) Mechanical stimuli such as shear stress or flow signal the cell through mechanoreceptors. These distinct compartments have numerous members that interact in a complex manner, known as crosstalk, to affect a variety of signaling pathways which in turn affect gene and protein expression and ultimately cell fate and function.



**Figure 1-2: Organization of Stem Cell Niches**

Stem cells reside in specialized niches that regulate self renewal and differentiation. The numerous tissue specific stem cell niches are similarly organized : The niche cells provide cell-cell contacts and paracrine signaling that regulate the self-renewal of the neighboring stem cells. Extracellular matrix proteins provide a scaffold for stem cell growth in the niche and can interact with soluble factors to regulate signal transduction. Additionally, glycoaminoglycans serve to locally concentration and present soluble cytokines. The physiochemical environment, including oxygen gradients, pH, matrix stiffness, and topography also contribute to the regulation of stem cell proliferation, self-renewal, and differentiation



**Figure 1-3: Derivation and Culture of Human Embryonic Stem Cells**

Human embryonic stem cells (hESCs) are isolated from the inner cell mass of a cultured blastocyst. The inner cell mass is mechanically isolated and then transferred to either (1) Irradiated mouse embryonic fibroblast (MEF) feeder layer or (2) Tissue culture plate that have been coated with Matrigel and supplemented with media that has been conditioned on MEFs (MEF-CM). The cells are subsequently dissociated and replated until hESC cultures are established. For long-term maintenance hESCs are cultured on MEFs or Matrigel with MEF-CM supplemented with basic fibroblast growth factor (FGF).

## **CHAPTER 2**

# **DEVELOPMENT OF ARRAYED CELLULAR MICROENVIRONMENT (ACME) TECHNOLOGY**

### **2.1 ABSTRACT**

The cellular microenvironment comprised of extracellular matrix proteins (ECMPs), growth factors (GFs), glycans (GCs), and mechanical forces, is crucial in determining the behavior and fate of cells. Current technologies, such as multi-well based assays, are inadequate to screen the vast number of combinations of factors that may influence cell fate. We have developed a technology platform, called arrayed cellular microenvironments (ACME) for the real-time simultaneous screening of thousands of physiochemical parameters on cell attachment, proliferation, differentiation and gene expressions. We demonstrate that these printed biological molecules remain localized within the spotted microenvironment and retain their signaling ability. Furthermore, this system is compatible with dynamic image-based screens and requires 1,000-10,000 fewer cells and reagent than traditional microtiter-based screens. This novel approach allows for the systematic assessment and probing of the complex relationships between various cell types and their microenvironment.

### **2.2 INTRODUCTION**

Microarrays are widely used tools that have been applied in diverse biological studies. The advantage of microarrays over traditional techniques is the ability to generate enormous amounts of data through miniaturization and multiplexing of experiments. For example, DNA microarrays consist of repeating arrays of DNA and can be used to measure changes in gene expression [67]. DNA microarrays have been used for mRNA profiling, diagnostic applications, SNP analysis, and DNA sequencing [68, 69]. More recently, protein microarrays have been used for measuring the biological activity of proteins, protein interactions, and ligand binding to proteins [70-72].

The cellular microenvironment is crucial in determining cellular behavior. This microenvironment, composed mainly of extracellular matrix proteins (ECMPs), growth factors (GFs), glycans (GCs), and mechanical forces, forms complex signaling networks to affect cell behavior. The reductionist biological approach has elucidated the role of individual microenvironment components in modulating cell behavior. However, these “first-order” experiments, such as cellular response to ECMPs or GFs tested individually, cannot predict well a cell’s response to more complex mixtures without knowledge about the underlying signaling network.

Since the number of combinations to be investigated increases exponentially with the number of factors, high-throughput screening (HTS) approaches will be necessary. Traditional HTS uses microtiter plates along with robotics, liquid handling devices, and automated imagers to quickly conduct thousands of simultaneous experiments. These approaches typically require on the order of 1-10  $\mu$ g of protein and 1,000-10,000 cells per experimental condition. However, such experiments can be prohibitive given the cost of certain proteins or the rarity of cells originating from limited sources, such as primary cells.



To investigate the influence of combinatorial signaling, we integrated the use of ECMPs and signaling molecules into a cellular microarray technology platform, thereby creating comprehensive “microenvironments” that closely resemble the *in vivo* environment in which cells reside. Based on previous array technologies [62, 63], we have developed a technology platform, called arrayed cellular microenvironments (ACME), that allows for the real-time simultaneous screening of thousands of physiochemical parameters on cell attachment, proliferation, differentiation and gene expressions. This system requires small amount of proteins (1-10 pg) and cells (10-100) per experimental condition. Additionally, we have addressed several methodological issues: (1) deposition and retention of microenvironment components such as ECMPs and GFs, (2) reproducibility of protein printing (3) cell culture compatibility, and (4) biological activity of printed proteins. The novel approach we present here will allow for the systematic assessment and probing of the complex relationship between various cell types and their microenvironment.

## **2.3 MATERIALS AND METHODS**

### **2.3.1 Arrayed Cellular Microenvironment (ACME) Fabrication**

Glass slides (75mm x 25mm x 1mm) were washed with 100% acetone, 100% methanol, and ten times in Millipore water (MQH<sub>2</sub>O) to remove residual debris and oils. The slides were etched overnight in 0.05 N NaOH, rinsed five times with MQH<sub>2</sub>O, and dried with filtered compressed air and in vacuum oven (65 °C, 20 psi) for 1 hr. The slides were then silanized in a 2% solution of 3-(trimethoxysilyl)propyl methacrylate in anhydrous toluene overnight, rinsed in toluene, dried with compressed air, and baked for 1 hr in a vacuum oven (65 °C, 20 psi).

A stock solution of 10% (w/v) acrylamide, 0.55% (w/v) bis-acrylamide, 10% (w/v) photoinitiator I2959 (200 µg/ml in 100% methanol; Igacure 2959, Ciba Specialty Chemicals) was prepared. Subsequently, 100 µl of this stock solution was placed on a silanized slide and covered with a 75mm x 25 mm coverslip (Bellco Glass). The slide was then exposed to 1.5 mW/cm<sup>2</sup> 365-nm ultraviolet A light for 7 min and immersed in MQH<sub>2</sub>O for 10 min. The coverslip was then removed, leaving a thin (~75 µm) polyacrylamide gel pad. The polyacrylamide slides were soaked in MQH<sub>2</sub>O for 48 hr to remove residual unpolymerized acrylamide and photoinitiator, and then dehydrated on a hot plate (40 °C) for 10 min.

Stock solutions of collagen I, collagen III, collagen IV, collagen V, fibronectin, and laminin (Sigma) were prepared in an ECMP printing buffer (200 mM acetate, 10 mM EDTA, 40% (v/v) glycerol, and 0.5% (v/v) triton X-100 in MQH<sub>2</sub>O, with pH adjusted to 4.9 using glacial acetic acid). We discovered that signaling molecules were largely inactive in the ECMP spotting buffer (data not shown). Hence, stocks of Wnt3a [73] were prepared in a signaling molecule buffer (40% (v/v) glycerol, 1% (w/v) CHAPS in PBS). Signaling molecules printed using this buffer retained their signaling ability. Combinations of ECMPs and signaling molecules were mixed in separate 384-well plates.

SMP 3.0 spotting pins (Telechem) were washed with 90% ethanol. All printings were performed with a SpotArray 24 (Perkin Elmer) at room temperature with 65% relative humidity. ECMP mixtures were printed first, followed by the signaling molecule mixtures. The acrylamide substrate served to retain the printed proteins to the spots. To control for variability, each microenvironment was printed in replicates of 5 spots. Each spot had a diameter of 150 µm and neighboring microenvironments were separated by a center-to-center distance of 450 µm.

### 2.3.2 Cell Culture

The following media were used for HEK-293 (1X high glucose DMEM, 10% fetal bovine serum, 1% (v/v) L-glutamine penicillin/streptomycin); H9/WA09 hESCs (1X DMEM-F12, 20% (v/v) Knockout Serum Replacement, 1% (v/v) non-essential amino acids, 0.5% (v/v) glutamine, 120  $\mu$ M 2-mercaptoethanol [Sigma]); Hues1 and 9 hESCs (1X Knockout DMEM, 10% (v/v) Knockout Serum Replacement, 10% (v/v) human plasmanate (Talecris Biotherapeutics), 1% (v/v) non-essential amino acids, 1% (v/v) penicillin/streptomycin, 1% (v/v) Gluta-MAX, 55  $\mu$ M 2-mercaptoethanol [Sigma]). All media components are from Invitrogen unless indicated otherwise. HEK-293s were passaged ( $2.5 \times 10^5$  cells per slide) directly onto the array slides and allowed to settle on the spots for 18 hr prior to rinsing with HEK-293 medium 3 times to remove residual cells and debris.

### 2.3.3 Wnt Reporter Line Construction

The Super8XTOP-GFP construct used to generate the Wnt reporter line was constructed by replacing the CMV promoter of pEGFP-N2 (Clontech) with the Wnt responsive promoter Super8XTOP (a 227-bp KpnI to HindIII fragment) excised from Super8XTOP-Flash (kindly provided by Dr. R. Moon). HEK-293 cells were stably transfected with Super8XTOP-GFP, and single cell clones were isolated and screened for (i) low basal GFP expression levels, and (ii) strong GFP induction in response to Wnt3a stimulation. GFP expression upon Wnt3a stimulation is detectable within 24 hr after Wnt3a addition (50nM Wnt3a).

### 2.3.4 Slide Staining

For characterization of ECMP and signaling molecule printing, the slides were fixed in 4% (w/v) paraformaldehyde (PFA) for 10 min and blocked with 1% (w/v) BSA (Sigma) and 3% (w/v) milk for 30 min at room temperature. The slides were then stained with Sypro Ruby (Probes) solution overnight, destained with 10% (v/v) methanol and 7% (v/v) acetic acid, and air dried. Additionally, slides were stained with primary antibodies mouse anti-collagen I, mouse anti-collagen III, mouse anti-collagen IV, mouse anti-collagen V, mouse anti-fibronectin, rabbit anti-laminin, rabbit anti-bFGF, or rabbit anti-Wnt3a [73], diluted 1:250 in 1% BSA at 4°C overnight. The slides were subsequently washed 3 times with Tris buffered saline (TBS), incubated with a goat anti-mouse or goat anti-rabbit Alexa 647 (Invitrogen) at 1:400 for 1 hr at 37°C, washed 3 times with TBS, and air dried immediately before imaging.

Because fixing and staining protocols may cause cell detachment and alter the cell counts on each spot, arrays were stained live for DNA with Hoescht 33342 (2 µg/ml; Invitrogen) for 5 min. The arrays were washed 3 times with the medium and then imaged. After live imaging, the arrays were fixed in 4% PFA for 5 min at 4°C, followed by 10 min at room temperature. Nucleic acids were stained using the Cy3 equivalent POPO-3 (Invitrogen) for 5 min at room temperature. The slides were then washed 3 times with TBS and air dried immediately before imaging.

### **2.3.5 Slide Imaging**

Live imaging of slides was performed using an automated confocal microscope (Olympus Fluoview 1000 with motorized stage and incubation chamber). Imaging of fixed slides was performed using a confocal DNA microarray scanner (Scanarray 400) at 5-µm pixel resolution. Sypro Ruby stain was imaged using a Scanarray 4000 (Perkin Elmer) with 546-nm laser excitation and a 617-nm emission filter. The POPO-3 nucleic

acid stain (Cy3 equivalent) was imaged using a 543-nm laser excitation and 570-nm emission filter. Each array was individually imaged using a focus height that gave the maximum signal in the Z-direction for each channel at the center of the array. Images were then quantified using GenePix software (MDS Analytical Technologies).

### **2.3.6 Statistical Analysis**

All values were presented as mean  $\pm$  standard deviation. All statistical analysis was performed using Minitab statistical software. A p-value  $<0.05$  was considered statistically significant.

## **2.4 RESULTS AND DISCUSSION**

### **2.4.1 Arrayed Cellular Microenvironments (ACME) to Study Cell Fate**

A general layout of the arrayed cellular microenvironments (ACME) is described in Figure 2-1. Using a DNA microarray spotting instrument, we deposited protein mixtures onto hydrogel-coated glass microscope slides. In the format shown a single slide carries 1,600 spots arranged in 16 10x10 matrices. Each protein spot, or microenvironment, is 150  $\mu\text{m}$  in diameter and each protein mixture is spotted in replicates of five so that in the format shown one slide carries 320 unique conditions. However, to increase throughput the platform can be modified to contain up to 1,826 unique conditions deposited in 5 replicates for a total of 9,300 spots/slide. In this work we spot multiple extracellular matrix proteins (ECMPs; collagen I, III, IV and V, fibronectin, laminin) and growth factors (GFs; Wnt3a).

### **2.4.2 Characterization of ECMP Deposition**

In order to characterize for ECMP deposition we stained the arrays using SYPRO Ruby protein (Figure 2-2a). Quantitative analysis showed consistent protein deposition between replicate spots within each array (Figure 2-2b). We next characterized the special location of ECM proteins using antigenic recognition (Figure 2-2c). For each ECMP printed, uniform fluorescence corresponded to the expected spatial distribution of the ECMP used. Finally, analysis of serially diluted fibronectin (Fn) spots showed a linear trend ( $R^2 = 0.996$ ) between spotted protein concentration and measured antigenic fluorescence (Figure 2-2d).

### **2.4.3 Reproducibility of Protein Printing**

Another parameter of ACME fabrication that we wanted to characterize was the reproducibility of protein printing. Thus, three replicate array slides were printed each with four subarrays. Each subarray had five replicate sets and each replicate set had five replicate spots (Figure 2-3a). All arrays were printed with fibronectin at a concentration of 250  $\mu\text{g/ml}$ . Quantitative image analysis revealed a high level of consistency between replicate spots and replicate sets. Furthermore, one-way analysis of variance (ANOVA) did not reveal any statistical differences between replicate subarrays within the same slide (slide 1 p-value = 0.385; slide 2 p-value = 0.631; slide 3 p-value = 0.060) or between replicate slides (p-value=0.958).

### **2.4.4 Cell Culture Compatibility**

Next, we seeded human embryonic kidney (HEK) 293 cells on arrays that were printed with fibronectin (250  $\mu\text{g/ml}$ ; Figure 2-4a). Because of the non-fouling nature of the acrylamide, HEK-293 cells only adhered to regions where protein was printed. The ECMP printing and subsequent cell adhesion and growth was highly reproducible over a

large surface area (one subarray = 9 mm X 9 mm). Cells could grow on the spots for up to two weeks or until they reach confluency. Phase contrast and Hoescht stained images showed compact cells with distinct nuclei (Figure 2-4b and 2-4c). To ensure combinations of ECMPs were functional and able to support equal growth HEK-293 cells, we seed the cells on arrays that had all possible combinations of six ECMPs (collagen I, collagen III, collagen IV, collagen V, laminin, and fibronectin). All combinations of ECMPs supported very similar levels of HEK-293 growth (Figure 2-4d).

#### **2.4.5 Incorporation of Growth Factors Into Spotted “Microenvironments”**

To more accurately mimic the *in vivo* interactions between the ECMPs and GFs and to increase the screening capability of the cellular microarray technology, we sought to incorporate GFs into the spotted ECMP microenvironments. As a proof-of-principle whether GFs can be deposited into the spotted microenvironments, we printed purified Wnt3a together with ECMPs and verified its retention and activity. The amount of Wnt3a per spot remained the same after soaking a spotted slide in PBS for 24 hrs, demonstrating that this GF is physically retained to the microenvironment (Figure 2-5a). Spotting Wnt3a alone in the absence of ECMPs was not sufficient for its immobilization (data not shown), suggesting that it interacts directly with one or more of the deposited ECMPs.

In order to characterize the biological activity of the spotted Wnt3a, we developed a genetically modified human embryonic kidney cell (HEK-293) line carrying a stably integrated GFP reporter gene under control of a Wnt-responsive promoter (Super 8X-TOP-GFP; Figure 2-5b). The Wnt-GFP HEK-293 line responds in a linear manner to increasing concentrations of exogenously added Wnt3a (Figure 2-5c). Next, we demonstrated that the spotted Wnt protein retained its activity (Figure 2-5d). GFP

intensity increased in a linear manner with the spotted Wnt3a concentration up to a saturation level at 300  $\mu\text{g/ml}$  (Figure 2-5e). The Wnt activity remained localized since spots in the neighboring subarray, in which no Wnt3a was deposited, exhibited no reporter activity.

## **2.5 CONCLUSION**

In order to study the numerous microenvironmental components that can influence cell fate, a combinatorial and systematic approach is needed. Here we have developed an array based technology, called arrayed cellular microenvironments (ACME), which can be used for the real-time simultaneous screening of thousands of physiochemical parameters on cell attachment, proliferation, differentiation and gene expressions. Qualitative and quantitative characterization revealed: (1) deposition and retention of microenvironment components such as ECMPs and GFs, (2) reproducibility of protein printing (3) cell culture compatibility, and (4) biological activity of printed proteins. In the future, this platform will be aide in dissecting the role of different components of the microenvironment in regulating cell fate.

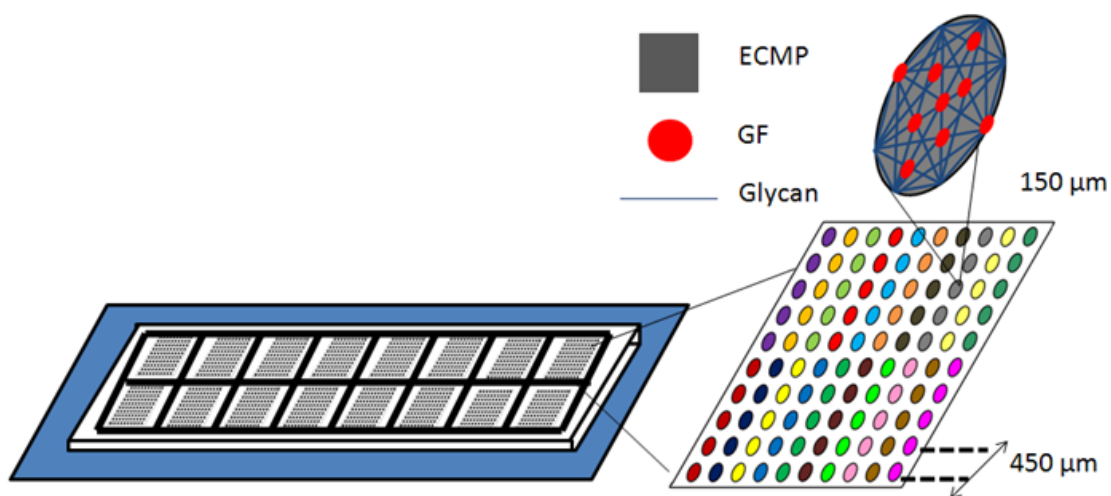
## **2.6 ACKNOWLEDGEMENTS**

D.A.B. was supported by funding from the University of California Biotechnology Research and Education Program (2007-006). This research was supported in part by the California Institute of Regenerative Medicine (RS1-00172-1) to S.C. and K.W., and NHLBI Research Grant HL080518 to S.C.

The text and figures in Chapter 2 are in part reproductions from: Brafman DA, Shah KD, Fellner T, Chien S, Willert K. Defining long-term maintenance conditions of human embryonic stem cells with arrayed cellular microenvironment technology. Stem

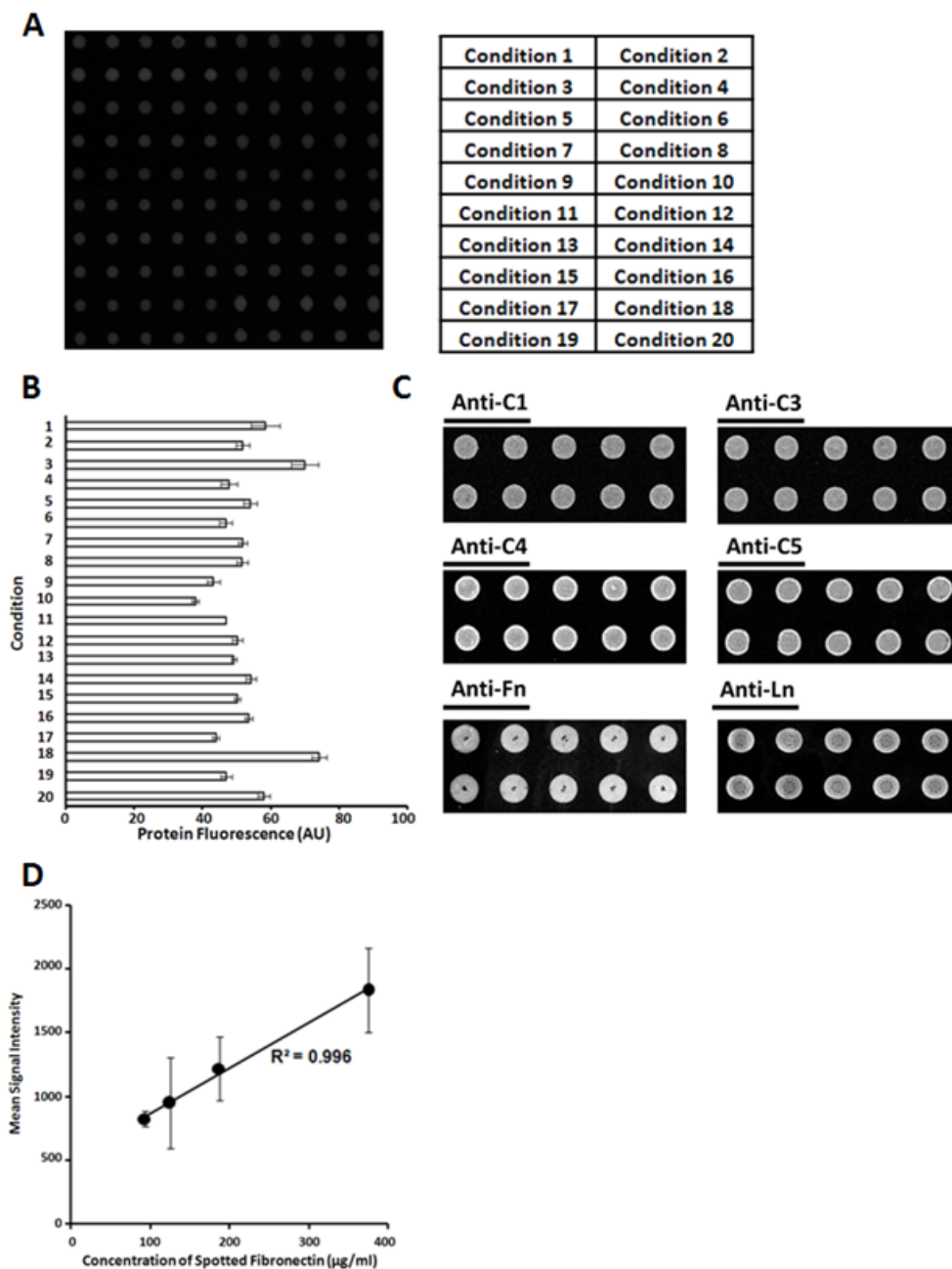


Cell Dev. 2009. 18(8). The dissertation author was the primary researcher and author pertaining to this work.



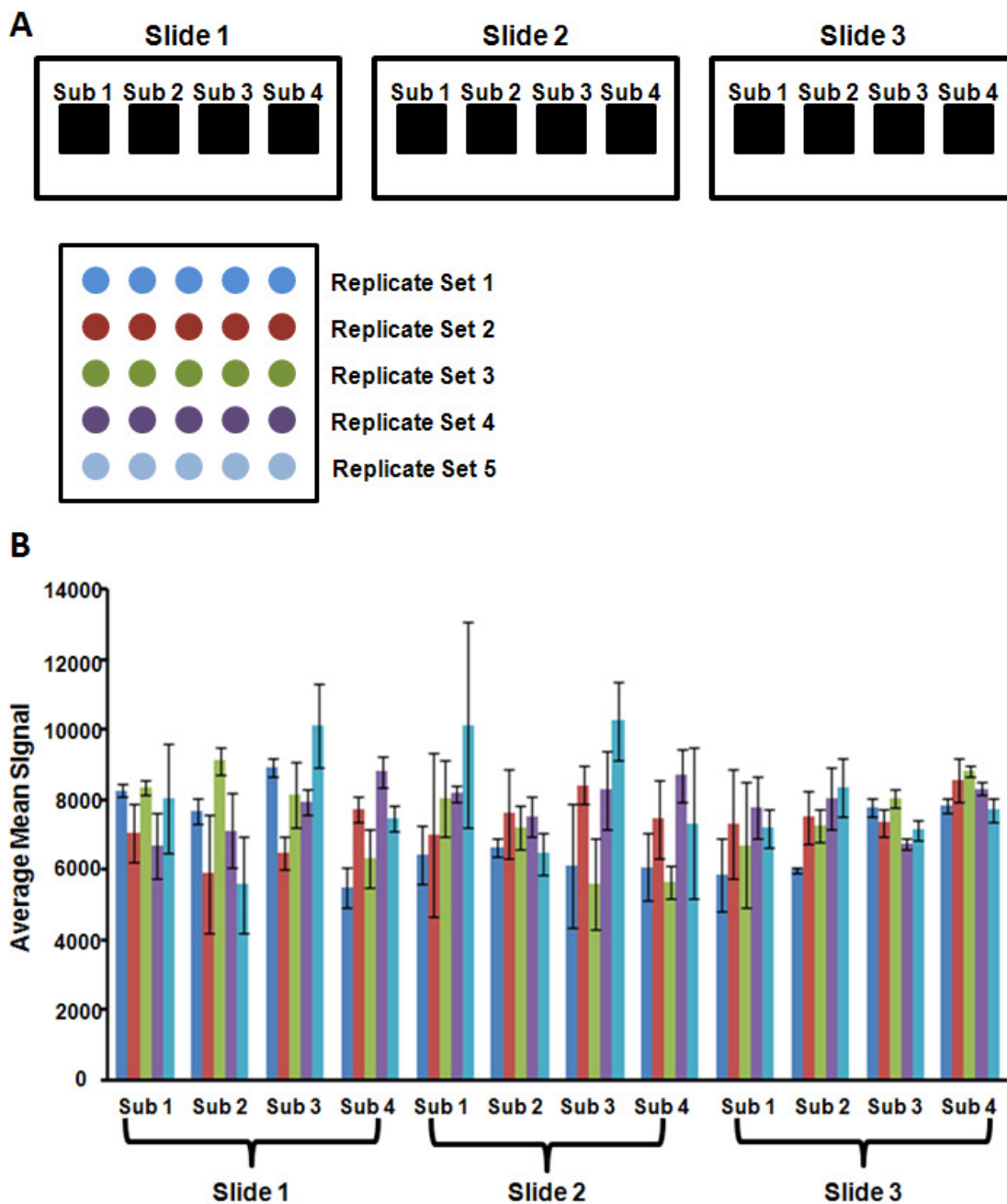
**Figure 2-1: Arrayed Cellular Microenvironment (ACME) Technology**

Typical layout of arrayed cellular microenvironments. Arrays of pre-mixed combinations of extracellular matrix proteins (ECMPs), growth factors (GFs), and glycans are arranged in 16 subarrays consisting of a 10X10 matrix of spots. Each combination was printed in five replicates.



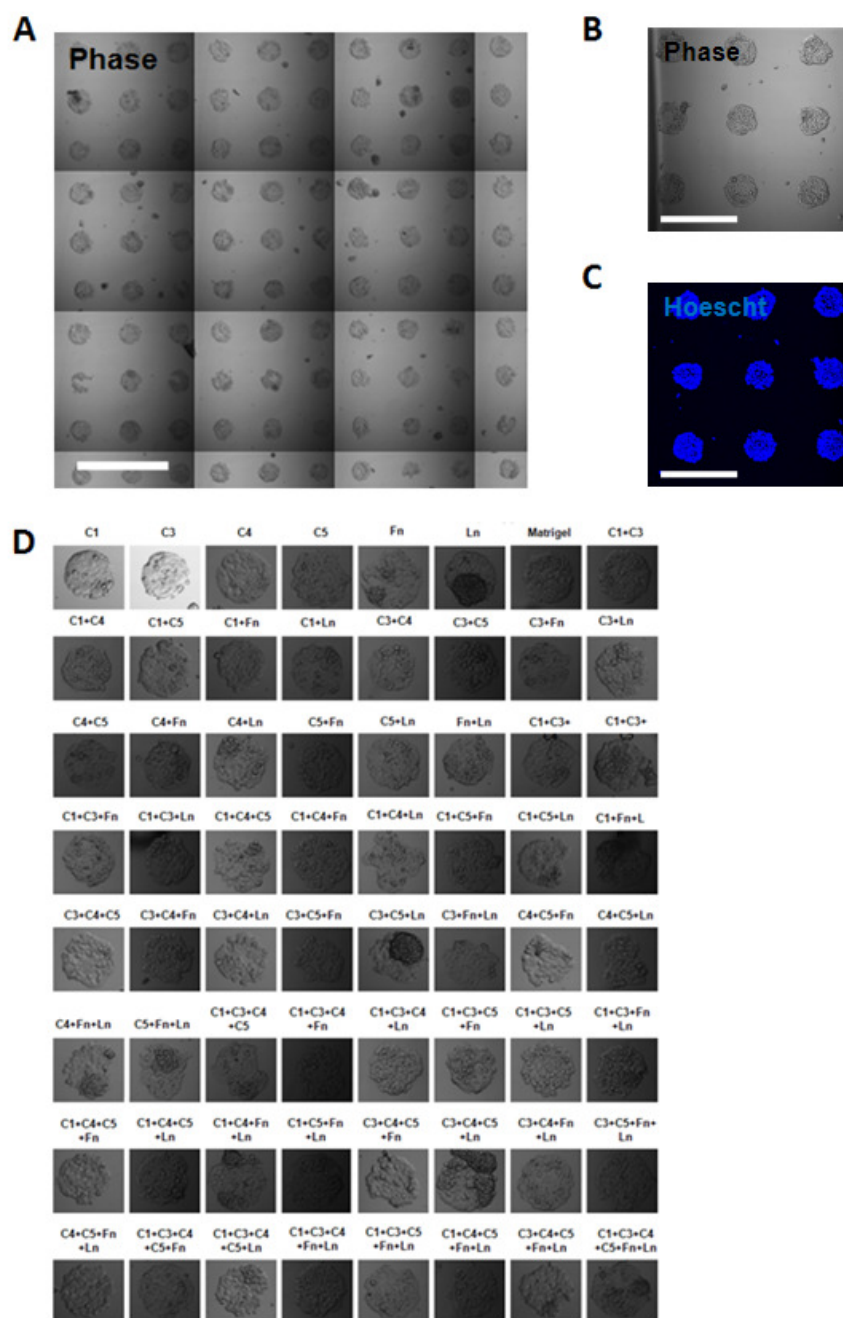
**Figure 2-2: Characterization of ECMP Deposition**

(a) Fluorescent image of SYPRO Ruby protein stained subarray containing 20 unique microenvironment conditions (250 µg/ml of protein per spot). (b) Quantitative image analysis of protein deposition reveals consistency between replicate spots (mean  $\pm$  standard deviation). (c) Characterization of individually printed ECMPs by indirect immunofluorescence. Each ECMP was printed in replicates of 10 at a concentration of 500 µg/ml. (d) Quantitative analysis of spotted fibronectin reveals a linear relationship ( $R^2 = 0.996$ ) between the spotted concentration and the measured signal.



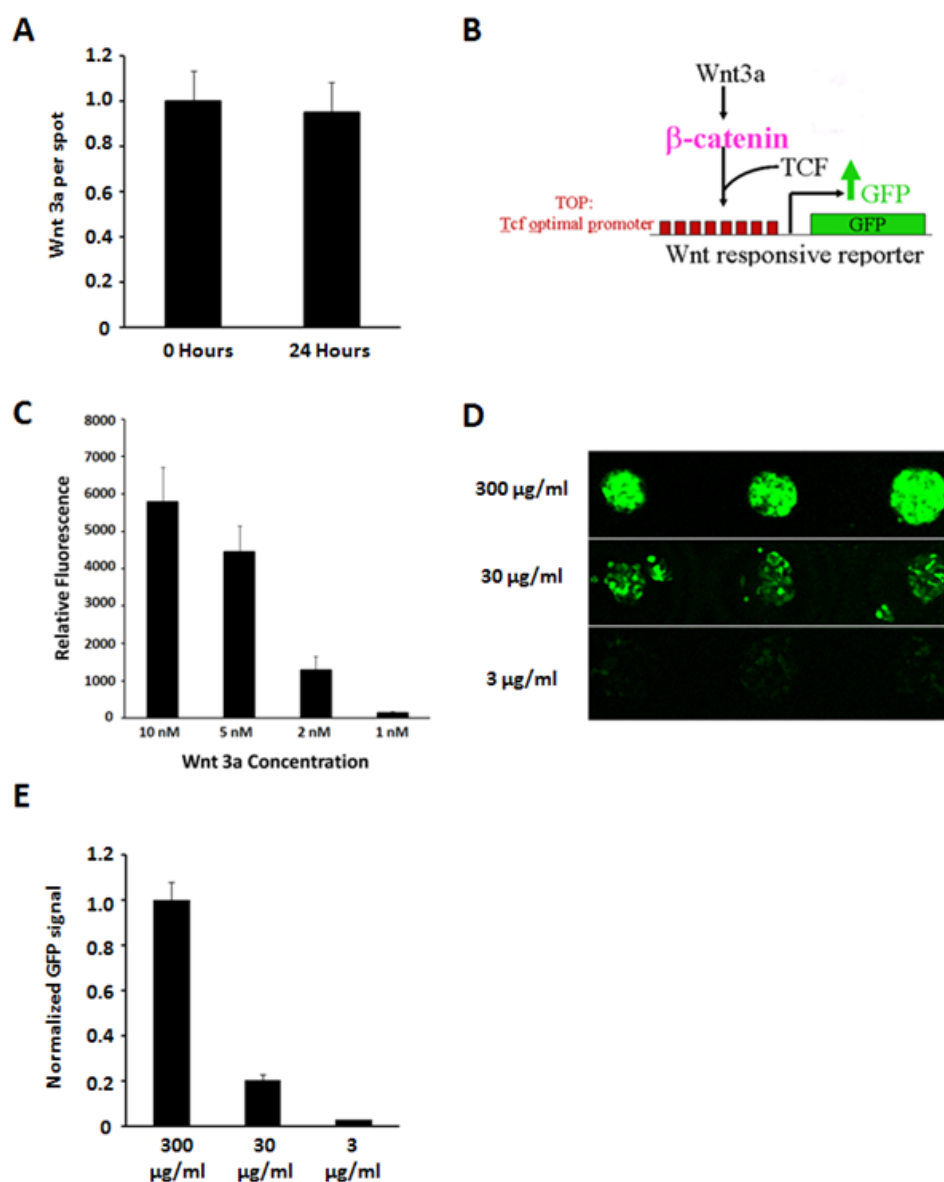
**Figure 2-3: Reproducibility of Printed Protein**

(a) Three replicate array slides were printed each with four subarrays ("sub"). Each subarray had five replicate sets. Each replicate set had five replicate spots. (b) Quantitative image analysis of protein deposition reveals consistency between replicate spots, replicate sets, subarrays, and slides (mean  $\pm$  standard deviation). Arrays were printed with fibronectin (250  $\mu$ g/ml).



**Figure 2-4: Cell Culture Compatibility—Human Embryonic Kidney (HEK) 293 Cells on ACME**

(a) Arrays were printed with fibronectin (250  $\mu\text{g}/\text{ml}$ ). Human embryonic kidney (HEK) 293 cells were cultured on arrays for 48 hours. Cells were imaged live (b,c) and stained for DNA (c). Scale bars = 900  $\mu\text{m}$  (a) and = 450  $\mu\text{m}$  (b,c). (d) Proliferation of HEK-293 on arrays of ECMPs. Representative micrographs of HEK-293 grown on combinations of ECMPs and Matrigel for 48 hours. All combinations tested support similar amounts of proliferation.



**Figure 2-5: Spotted Signaling Molecules Remain Localized and Retain Their Signaling Ability**

(a) Arrays were printed with fibronectin (250  $\mu$ g/ml) and various concentrations of Wnt3a (3  $\mu$ g/ml, 30  $\mu$ g/ml, and 300  $\mu$ g/ml). Quantitative analysis reveals that Wnt3a remains localized to the spot and does not diffuse out into the surrounding culture media. (b) Diagram of the Wnt reporter construct. Multimerized TCF binding sites comprise the Super 8X TOP Wnt responsive promoter element. A GFP gene is under the control of this Wnt responsive promoter. (c) Activity assay for canonical Wnt3a: HEK293 cells carrying the Wnt responsive GFP reporter depicted in panel B were treated with increasing amounts of Wnt3a. Wnt3a signaling saturates at concentrations between 5 to 10 nM. (d) HEK-293 cells stably transfected with the Wnt reporter TOP-GFP were seeded onto arrays and express GFP in the presence of active Wnt. (e) Quantitative analysis demonstrates that GFP expression increases linearly with spotted Wnt3a concentration

## CHAPTER 3

# INVESTIGATING THE ROLE OF THE EXTRACELLULAR ENVIRONMENT IN MODULATING HEPATIC STELLATE CELL BIOLOGY WITH ARRAYED COMBINATORIAL MICROENVIRONMENTS

### 3.1 ABSTRACT

Hepatic stellate cells (HSCs) are a major cell type of the liver that are involved in liver homeostasis. Upon liver damage, HSCs exit their normally quiescent state and become activated, leading to an increase of their proliferation, production of abnormal extracellular matrix and inflammatory mediators, and eventually liver fibrosis and cirrhosis. Current *in vitro* approaches to identify components that influence HSC biology typically investigate one factor at a time and generally ignore the complex crosstalk between the myriad of components that comprise the microenvironments of quiescent or activated HSCs. Here we describe a high throughput screening (HTS) approach to identify factors that affect HSC biology. Specifically, we integrated the use of extracellular matrix proteins (ECMPs) and signaling molecules into a combinatorial cellular microarray technology platform, thereby creating comprehensive “microenvironments”. Using this technology, we performed real-time simultaneous screening of the effects of hundreds of unique microenvironments composed of ECMPs and signaling molecules on HSC proliferation and activation. From these screens, we identified combinations of microenvironment components that differentially modulate the

HSC phenotype. Furthermore, analysis of HSC responses revealed that the influences of Wnt signaling molecules on HSC fate are dependent on the ECMP composition in which they are presented. In order to validate these observed responses using conventional approaches, we cultured HSCs in a larger format on selected microenvironments and examined their expression of specific markers of HSC activation. Collectively, our results demonstrate the utility of high-content, array-based screens to provide a better understanding of HSC biology. Our results indicate that array-based screens may provide an efficient means for identifying candidate signaling pathways to be targeted for anti-fibrotic therapies.

### **3.2 INTRODUCTION**

Quiescent hepatic stellate cells (HSCs) comprise approximately 5-10% of the cells in a healthy liver and are the primary site for retinoid storage in the body [74]. HSC fate is largely determined by the interactions between the cell and its microenvironment, i.e., the extracellular matrix (ECM) and soluble factors. Following repeated injuries, the liver undergoes a complex remodeling process, significantly altering the microenvironment of HSCs [75]. During this process, cues from the surrounding microenvironment, including activated Kupffer cells, damaged hepatocytes, platelets, endothelial and inflammatory cells, lead to the conversion of HSCs from their “quiescent” lipocyte-like progenitor state to an “activated” myofibroblast-like state [76, 77]. This transition plays a key role in hepatic fibrosis [74-76].

Since the majority of anti-fibrotic therapies aim at limiting the activation and proliferation of HSCs, understanding the influence of all microenvironmental components on HSC fate is of critical importance. Previous studies have focused on the effect of individual components of the microenvironment on HSC biology. For example, soluble



cytokines such as transforming growth factor (TGF)- $\beta$ , platelet derived growth factor (PDGF) and Wnt proteins exert potent effects on HSC activation [78-80]. With respect to liver biology, Wnt proteins are of particular interest given their highly conserved functions in regenerative and stem cell biology [81] and wound healing [82]. Even though cell-matrix interactions regulate gene expression patterns in primary hepatocytes [83-86], the influence of extracellular matrix proteins (ECMPs) on HSC proliferation and activation has been explored only to a limited extent. For example, culturing activated HSCs on Matrigel™, a commercially available matrix of undefined composition, reverts them to a partially quiescent state [87]. However, there is no study that has taken a comprehensive approach to explore the combinatorial effects of multiple microenvironmental components on the fate of HSCs. Excessive secretion and deposition of ECMP (collagen 1, 3, 4, 5, fibronectin, and laminin) and growth factors during liver injury and subsequent fibrosis [77, 88-90] suggests that HSC activation is regulated by a complex set of microenvironmental factors [90]. How these secreted components interact with each other to affect HSC activation remains unclear. Thus, a combinatorial approach is required in order to better understand HSC signaling systems. Conventional cell culture methods, such as multi-well cell culture dishes, are limited in their ability to screen the vast number of possible unique combinations of factors that may influence HSC fate. To address this problem, we [62, 63, 91] and others [64, 92] have implemented a high-throughput screening (HTS) approach to identify factors influencing cell behavior. Here, we have implemented our cellular microarray platform for the parallel exposure of HSCs to hundreds of unique combinations of microenvironment components.

In this study, we utilized this technology to perform real-time simultaneous screening of the effects of 252 unique microenvironments, composed of ECMPs (fibronectin, laminin, collagen 1, 3, 4 and 5) and signaling molecules (Wnt3a and 5a), on

HSC proliferation and activation. These studies revealed previously unidentified combinations of microenvironment components that differentially modulate the HSC phenotype. Additionally, these studies established a role for ECMPs in the *in vitro* activation process of HSCs. Furthermore, examination of interactions between multiple combinations of factors revealed that the effects of Wnt proteins on HSC fate are dependent on the ECMP microenvironment in which they are presented. Factorial analysis identified specific microenvironmental components that have the strongest influence over HSC proliferation and activation and revealed unique ECMP-ECMP and growth factor-ECMP interactions. Finally, we validated these array-based responses in traditional multi well-based culture. Together, our results demonstrate that array-based HTS provide a useful tool for not only a better understanding of HSC biology, but also for identifying candidate signaling pathways to be targeted for anti-fibrotic therapies.

### **3.3 MATERIALS AND METHODS**

#### **3.3.1 Array Fabrication and Characterization**

Arrays were fabricated as previously described in [91]. Briefly, glass slides were cleaned, silanized, and then functionalized with a polyacrylamide gel pad. Next, stock solutions of collagen I (C1), collagen III (C3), collagen IV (C4), collagen V (C5), fibronectin (Fn), and laminin (Ln) (Sigma) were prepared in an ECMP printing buffer (200 mM acetate, 10 mM EDTA, 40% (v/v) glycerol, and 0.5% (v/v) Triton X-100 in MQH<sub>2</sub>O, with pH adjusted to 4.9 using glacial acetic acid). All ECMP combinations were printed at a constant protein concentration of 250 µg/ml. Stocks of Wnt3a and Wnt5a [73] were prepared in a signaling molecule buffer (40% (v/v) glycerol, 1% (w/v) CHAPS in PBS). Final concentration of these signaling molecules in printing buffer was 30 µg/ml. Spotted Wnt activity was confirmed using human embryonic kidney cells (HEK-293) carrying a

stably integrated green fluorescent protein (GFP) reporter gene under control of a Wnt-responsive promoter [91]. Combinations of ECMPs and signaling molecules were mixed in separate 384-well plates.

A contact array (SpotArray 24; Perkin Elmer) was used to print ECMP mixtures first, followed by the signaling molecule mixtures. To control for variability, each microenvironment was printed in replicates of 5 spots. Each spot had a diameter of 150  $\mu\text{m}$  and neighboring microenvironments were separated by a center-to-center distance of 450  $\mu\text{m}$ . Spots were organized into 'subarrays' (9mm X 9mm). Each glass slide had 16 such subarrays, and each subarray contained 100 spots arranged in a 10X10 format. Thus, a single slide accommodated 1,600 spots representing 320 unique signaling microenvironments with 5 replicates each. Prior to their usage, the slides were soaked in PBS while being exposed to UVC germicidal radiation in a sterile flow hood for 10 min.

For characterization of ECMP and signaling molecule printing, the slides were fixed in 4% (w/v) paraformaldehyde (PFA) for 10 min and blocked with 1% (w/v) BSA (Sigma) and 3% (w/v) milk for 30 min at room temperature. The slides were then stained with Sypro Ruby (Probes) solution overnight, destained with 10% (v/v) methanol and 7% (v/v) acetic acid, and air dried. Additionally, slides were stained with primary antibodies mouse anti-collagen I, mouse anti-collagen III, mouse anti-collagen IV, mouse anti-collagen V, mouse anti-fibronectin, rabbit anti-laminin (Sigma), rabbit anti-Wnt3a, or rabbit anti-Wnt5a [73], diluted 1:250 in 1% BSA at 4°C overnight. The slides were subsequently washed 3 times with Tris buffered saline (TBS), incubated with a goat anti-mouse or goat anti-rabbit Alexa 647 (Invitrogen) at 1:400 for 1 hr at 37°C, washed 3 times with TBS, and air dried immediately before imaging.

### **3.3.2 Cell Isolation, Purification, and Culture**

Transgenic mice (Balb/c background) carrying a GFP gene under transcriptional control of a collagen type 1,  $\alpha 1(I)$  (Col1 $\alpha 1$ ) promoter/enhancer (Collagen-GFP Tg mice) were previously generated and are described in reference [93]. HSCs were isolated from normal livers by a 2-step collagenase-pronase perfusion of mouse livers followed by 8.2% Nycodenz (Accurate Chemical and Scientific Corporation) with a two-layer discontinuous density gradient centrifugation as previously described [94, 95]. To ensure that HSCs were not contaminated by Kupffer cells (KCs), HSCs were depleted of KCs/macrophages by magnetic antibody cell sorting (MACS; Miltenyibiotec) using anti-F4/80 Ab-(eBioscience) and CD11b-conjugated microbeads (Miltenyibiotec). This procedure resulted in HSCs with 99% purity as judged by retinoid autofluorescence. All animal procedures were approved by the University of California San Diego Institutional Animal Care and Use Committee, and met guidelines of the National Institutes of Health.

HSCs were cultured in Dulbecco's modified Eagle medium (DMEM) containing 10% fetal bovine serum (FBS), glutamine, HEPES buffer, and antibiotics. Freshly isolated HSCs were seeded ( $2.5 \times 10^5$  cells per slide) directly onto the array slides and allowed to settle on the spots for 18 hr prior to rinsing with HSC medium 3 times to remove residual cells and debris. Cell media was replaced every two days. Because the acrylamide does not permit cell adhesion, cells were confined to the printed microenvironment spots.

### **3.3.3 Slide Imaging, Quantification, and Analysis**

Live imaging of slides was performed using an automated confocal microscope (Olympus Fluoview 1000 with motorized stage and incubation chamber). Because fixing and staining protocols may cause cell detachment and alter the cell counts on each spot, arrays were stained live for DNA with Hoescht 33342 (2  $\mu\text{g/ml}$ ; Invitrogen) for 5 min on

day 5. The arrays were washed 3 times with the medium and then imaged. On all other days cell counting was done manually. Images were then quantified using GenePix software (MDS Analytical Technologies). Spots with no adherent cells were excluded from further analysis.

In order to account for variability between independent array experiments a global normalization strategy was implemented. Thus, we applied a transformation so the mean and standard deviation between independent array experiments were identical (mean = 0, standard deviation = 1). Proliferation and activation indexes were calculated for each spot as follows:

$$\text{Proliferation index (PRO)}_i = (X_i - \mu_{\text{PRO}}) / (\sigma_{\text{PRO}})$$

where  $X_i$  = day 5 cell count,  $\mu_{\text{PRO}}$  was the average of all the  $X_i$  for all the microenvironment spots on each array, and  $\sigma_{\text{PRO}}$  was the standard deviation of all the  $X_i$  for all the spots on each array.

$$\text{Activation index (ACT)}_i = (R_i - \mu_{\text{ACT}}) / (\sigma_{\text{ACT}})$$

where  $R_i = \log_2[(\text{day 5 GFP}) / (\text{day 5 cell count})]$ ,  $\mu_{\text{ACT}}$  was the average of all the  $R_i$  for all the microenvironment spots on each array, and  $\sigma_{\text{ACT}}$  was the standard deviation of all the  $R_i$  for all the spots on each array. The Hoescht signal from day 5 images was used as an estimate for the day 5 cell count.

For each ECMP combination, the fold change of Wnt protein addition (Wnt3a alone, Wnt5a alone, Wnt3a and Wnt5a together) on proliferation and activation relative to no growth factor was computed as follows:

$$\text{Proliferation fold change} = \log_2( X^{\text{Wnt}} / X^{\text{No GF}} )$$

where  $X^{Wnt}$  was the average day 5 cell count across replicate spots in presence of Wnt (Wnt3a alone, Wnt5a alone, or Wnt3a and Wnt5a together) and  $X^{No\ GF}$  was the average day 5 cell count across replicate spots when no GF was present.

$$\text{Activation fold change} = \log_2 (R^{Wnt} / R^{No\ GF})$$

where  $R^{Wnt} = (\text{average day 5 GFP across replicate spots}) / (\text{average day 5 cell count across replicate spots})$  in the presence of Wnt (Wnt 3a alone, Wnt5a alone, or Wnt3a and Wnt5a together) and  $R^{No\ GF} = (\text{average day 5 GFP across replicate spots}) / (\text{average day 5 cell count across replicate spots})$  when no GF was present. A  $\log_2$  scale was chosen so that similar increases and decreases in fold change would be treated similarly (i.e. n fold increase = -n fold decrease).

### 3.3.4 Microarray Analysis

Proliferation and activation indexes for replicate spots on each array were averaged. The proliferation and activation indexes were represented as a matrix where each row corresponded to a unique microenvironment and each column corresponded to an individual array experiment. For each array experiment, all columns were mean-centered and normalized to one unit standard deviation. The rows were clustered using Pearson correlations as a metric of similarity [96]. All clustering was performed using Gene Cluster [96]. The results were displayed using a color code with red and green representing an increase and decrease, respectively, relative to the global mean. All heat maps were created using Tree View [96].

### 3.3.5 HSC Culture on Selected ECMP Conditions

Freshly isolated HSCs were cultured for 5 days on tissue culture plates coated with selected ECMP combinations. The ECMP-coated plates were prepared by coating

tissue culture plates in the ECMPs (diluted in 10 mM acetic acid) overnight. The solution was aspirated and the plates were air-dried overnight. 250 µg/ml (10 µg/cm<sup>2</sup>) of total protein was used per plate.

### **3.3.6 qRT-PCR Analysis**

RNA was extracted by using Trizol (Invitrogen). cDNA was obtained using the Amersham kit for cDNA synthesis (Amersham Biosciences). Quantitative real time PCR (qPCR) was performed using commercially available primer-probe sets (Applied Biosystems). All samples were DNase treated before reverse transcription and quantified by comparing threshold cycle value to a serial dilution standard curve.

### **3.3.7 Data Analysis**

Main and interaction effects were calculated by performing a full factorial analysis as described in Box *et al.* (2006) using Minitab statistical software. Effects in which p-value <0.05 were considered statistically significant. Differences between probability density functions were assessed by performing one-way ANOVA using Minitab statistical software. Pearson's product moment correlation coefficients were computed between the microenvironment matched proliferation and activation indexes for each independent experiment pair. All data are presented as mean ± standard deviation.

## 3.4 RESULTS

### 3.4.1 Using Arrayed Microenvironments to Study HSC Biology

HSCs were isolated from dissociated livers of transgenic mice carrying a GFP reporter gene under control of the collagen type 1  $\alpha 1(I)$  (Col1 $\alpha 1$ ) promoter/enhancer [93, 97]. Immediately after isolation HSCs display low GFP expression, indicative of their quiescent state (Figure 3-1a). If plated onto plastic or certain ECMPs, HSCs become activated, which is readily detectable by an increase in GFP expression (Figure 3-1a). We utilized this readout of the quiescent versus activated states in combination with a cellular microarray technology previously developed in our laboratory (Figure 3-1b and [91]) to examine the effect of the matrix microenvironment on HSC quiescence and activation. Cellular microarrays comprised all possible combinations of the ECMPs fibronectin (Fn), laminin (Ln) and collagen 1, 3, 4 and 5 (C1, C3, C4, C5) for a total of 63 combinations. In later experiments, we additionally incorporated the growth factors Wnt3a and Wnt5a into the arrays (Figure 3-5). Because the polyacrylamide hydrogel does not permit cell attachment, HSCs only adhered to the sites of protein deposition.

Cellular microarrays seeded with HSCs were imaged by automated microscopy (Figure 1c), thereby permitting real-time data acquisition of HSC on the same microenvironment spot over several days (Figure 3-1c). At each time point, cell number and GFP expression on each microenvironment spot were measured. Since Col1 $\alpha 1$  expression is increased in activated HSCs, the level of GFP expression provided a direct measurement of the activation status of the HSCs on each spotted microenvironment. For each condition, we calculated an activation index value (see Materials and Methods). In addition, based upon changes in cell number over time, HSC proliferation on each microenvironment was determined and a proliferation index value was calculated (see Materials and Methods). Thus, proliferation was a lumped parameter that



measured adhesion, growth, and survival. In general, HSC proliferation and activation changed in a biphasic manner when exposed to the diverse microenvironments: a period (days 0-5) of monotonic increases in both cell number and GFP expression, followed by a plateau (day 6+) in which cell proliferation was limited by the size of the spot and GFP expression no longer increased. For this reason, we analyzed HSC proliferation and activation from days 1 to 5 only. By day 5, HSCs cultured on conditions that promoted extensive activation as measured by an increase in GFP expression had lost most retinoid-rich droplets (data not shown).

### **3.4.2 HSC Proliferation and Activation Are Modulated By ECMPs**

Using the array platform, we investigated the effects of all possible 63 combinations of six ECMPs (Ln, Fn, C1, C3, C4, C5) on HSC proliferation and activation. These six ECMPs were chosen as they are the most prevalently synthesized ECMPs during both HSC quiescence and activation [77, 88-90, 98]. Col1 $\alpha$ 1-GFP HSCs were seeded onto three independent arrays, cultured for up to 5 days, and proliferation and activation indexes were calculated (see Materials and Methods). When cultured on standard polystyrene tissue culture plates, HSCs begin to undergo rapid proliferation and expression of Col1 $\alpha$ 1 after 48 hours of culture [93]. In contrast, the changes in HSC proliferation and activation were dependent on the specific microenvironment; some microenvironments induced HSC activation (dotted line in Figures 3-2a and 3-2b) as detected by an increase in GFP expression and cell number, whereas other conditions maintained the cells in a quiescent state (solid line in Figures 3-2a and 3-2b)

In order to determine the relationships between the cellular changes on different microenvironments, the HSC responses (proliferation and activation) were displayed in a heat map, with rows representing the unique ECMP microenvironments and columns the

independent array experiments (Fig 3-2c). Both rows and columns were clustered using Pearson correlation coefficients as a measure of similarity [96]. There was modest agreement among biological repeats of independent array experiments and HSC isolations (average Pearson's correlation coefficient =  $0.5221 \pm 0.1063$ ; Table 3-1). The ECMP microenvironments were clustered into one of four main groups based on the resulting HSC responses (Figure 3-2c): (i) high proliferation and activation (red cluster), (ii) high proliferation and low activation (blue cluster), (iii) low proliferation and high activation (orange cluster), and (iv) low proliferation and low activation (green cluster). Representative members of each of these groups are shown in Figure 3-2d. Previous experiments by others showed that HSC proliferation correlated with HSC activation as measured by an increase in Col1 $\alpha$ 1 expression. Our screening identified several ECMP microenvironments that promoted HSC proliferation without the accompanying increase in Col1 $\alpha$ 1 expression, and vice versa (blue and orange clusters, respectively).

Together, the data suggest that some ECMP components differentially influence the HSC activation process. To examine the complex interactions between ECMPs and HSCs and to identify the individual components responsible for eliciting the largest changes in HSC biology, we performed a factorial analysis of the proliferation and activation indexes (Figure 3-3). The effect magnitudes for all single factor effects with their statistical significance are presented in Figure 3-3a. When the effects of each ECMP were examined individually, both C5 (p-value = 0.007) and Fn (p-value = 0.007) decreased HSC proliferation. Meanwhile, the presence of C1 (p-value = 0.022) and Ln (p-value = 0.008) correlated with increases in activation.

In order to identify interactions between the various ECMP components, we computed the two-factor interaction effects (Figure 3-3b). There were several instances where the responses to the combination of signals can be explained by the additive

effects of individual components. For example, both C1 and Ln alone and in combination (p-value = 0.048) had positive effects on activation. However, we observed instances where combinations of factors resulted in responses that could not be predicted from the effects of the single factors. For instance, Fn and Ln alone have a positive effect on activation, but they strongly decrease activation when combined (p-value = 0.003). These results indicate that predictions about interactions between molecular signals cannot be simply derived from responses of the individual components. Since both quiescent and activated HSCs reside in a complex ECMP microenvironment *in vivo*, it is significant that the effects of individual ECMPs on HSC status *in vitro* are dependent on the presence or absence of other ECMPs.

To confirm the results obtained from the arrayed microenvironment experiments, we cultured HSCs on tissue culture plates coated with different combinations of ECMPs. We chose ten ECMP combinations representing the spectrum of responses elicited by the diverse microenvironments. HSCs were cultured for five days on the various ECMP combinations and subsequently analyzed for expression of three markers of HSC activation, collagen1 $\alpha$ 1 (Col1 $\alpha$ 1), TIMP metalloproteinase inhibitor 1 (TIMP-1), and  $\alpha$ -smooth muscle actin ( $\alpha$ -SMA), by quantitative real-time PCR (Figure 3-4a). We found that the results obtained for HSC activation on the arrayed microenvironments correlated well with those observed in conventional cell culture as measured by quantitative real-time PCR for Col1 $\alpha$ 1 and TIMP-1 expression levels, with Pearson's correlation coefficient of 0.8295 and 0.8025, respectively (Figure 3-4b). The correlation between the array and RT-PCR data on  $\alpha$ -SMA expression levels was weaker with a Pearson's correlation coefficient of 0.5691 (Figure 3-4b). This reduced correlation is due to the fact that Col1 $\alpha$ 1 and  $\alpha$ -SMA expression are not simultaneously up-regulated in activated

HSCs [93]. These data demonstrate that the arrayed microenvironments are a reliable tool to explore HSC biology in response to different microenvironments.

### **3.4.3 The Role of Wnt Proteins in HSC Proliferation and Activation Is Context Dependent**

Wnt proteins have been implicated in the regulation of cellular proliferation and differentiation in virtually all developmental processes [99]. Critical to our studies, Wnt signaling has been implicated in wound healing and fibrosis in a variety of tissues [100-103]. However, the role of Wnt proteins in hepatic fibrosis, and in particular HSC proliferation, is not well established, with studies yielding conflicting results [78-80]. One explanation for the disparate results is that the effect of Wnt signaling may be significantly modulated by other microenvironmental components. Using the array platform, we sought to investigate the effects of Wnt signaling on HSC proliferation and activation in the context of the previously examined ECMP compositions. For these studies, we selected Wnt3a, which stimulates canonical Wnt/ $\beta$ -catenin signaling, and Wnt5a, which antagonizes canonical Wnt signaling.

HSCs were seeded onto arrays consisting of all possible 63 combinations of six ECMPs (C1, C3, C4, C5, Ln, and Fn) in the presence of Wnt3a alone, Wnt5a alone, Wnt3a and Wnt5a together, and no Wnt. Previously we showed that spotted Wnt proteins are retained to the spotted microenvironments and retain their biological activity [91]. HSC proliferation and activation on each microenvironment spot were measured. The proliferation and activation from individual microenvironment spots were plotted as coordinates in a proliferation versus activation plane (Figure 3-5a-d). Using the values for the global mean proliferation (106) and the global mean activation (-0.033) the plane was divided into four regions: (i) high proliferation and activation (upper right), (ii) high

proliferation and low activation (lower right), (iii) low proliferation and high activation (upper left), and (iv) low proliferation and low activation (lower left). In the absence of the Wnt proteins, the ECMP microenvironments were segregated into all four regions with a majority residing in the high proliferation/high activation and high proliferation/low activation regions (Figure 3-5a). The division of the ECMP microenvironments into the four different regions roughly corresponds to their distribution into the four clusters displayed in Figure 2c.

The addition of the Wnt proteins to the ECMP microenvironments had marked effects on HSC proliferation and activation (Figure 3-5b-d). The addition of either Wnt3a or Wnt5a resulted in a significant reduction of HSC proliferation ( $p$ -value $<0.001$ ; Figure 3-5e). When Wnt3a and Wnt5a were presented simultaneously, the effect on HSC proliferation was similar to the effect when each Wnt protein was presented individually ( $p$ -value $<0.001$ , Figure 3-5e). While Wnt3a and Wnt5a both caused reductions of HSC proliferation, they had opposite effects on HSC activation. HSC activation was increased by Wnt3a ( $p$ -value $<0.001$ ), but decreased by Wnt5a ( $p$ -value $<0.001$ ; Figure 2-6b, c and f). When presented together, Wnt3a and Wnt5a negated each other's effects on HSC activation (Figure 5d and f), consistent with previous studies demonstrating that Wnt5a antagonizes Wnt3a signaling [104].

Next, we examined whether the effect of Wnt proteins on HSC proliferation and activation was dependent on the composition of the ECMP. For each ECMP combination, we computed the fold change of Wnt protein addition (Wnt3a alone, Wnt5a alone, Wnt3a and Wnt5a together) on proliferation and activation relative to no growth factor. We discovered that the ECMP composition significantly influenced the magnitude of the response that Wnt protein addition had on proliferation and activation. Specifically, depending on the ECMP combination, the magnitude of the response could vary as

much as 75 fold. Furthermore, we indentified 14 distinct groups of ECMP microenvironments in which Wnts expert unique effects (Table 3-2). One-way clustering of the ECMP microenvironments resulted in members of the same or similar groups clustering together (Figure 3-5g). Of these 14 groups, the three largest groups consisted of ECMP microenvironments in which Wnts resulted in reduced proliferation and had the following effects on activation: (1) Wnt3a increased activation, Wnt5a decreased activation, and their combination increased activation (red cluster, Figure 3-5g), (2) Wnt3a increased activation, Wnt5a decreased activation, and their combination decreased activation (blue cluster, Figure 5g), and (3) both Wnt proteins individually and in combination decreased activation (green cluster, Figure 3-5g).

Together, these results indicate that the roles of Wnt proteins in HSC activation are significantly influenced by the specific makeup of the ECMP microenvironment in which they are presented. In order to identify specific interaction between ECMPs and Wnt proteins, the interaction effects between ECMPs and Wnt proteins were calculated (Figure 3-5h-i). For example, the presence of Ln consistently enhanced the effect of Wnt3a on HSC activation (p-value=0.031) while the presence of C4 (p-value < 0.001) and C5 (p-value=0.047) increased the effect of Wnt5a in reducing HSC activation. Although the underlying mechanisms remain to be elucidated, the complex set of observed responses demonstrates that the microenvironment components interact to fine-tune cellular responses.

## 3.5 DISCUSSION

Liver fibrosis and eventual cirrhosis is the consequence of ineffective and insufficient repair and regeneration of damaged liver tissue. Hepatic stellate cells (HSCs), a quiescent cell population comprising 5-10% of the normal liver, become activated upon liver injury and secrete ECM proteins producing a fibrotic scar that compromises liver functions. HSCs can be readily isolated and purified, and have been used to model liver fibrosis *in vitro*. However, these *in vitro* assays fail to replicate the complex microenvironment in which HSCs normally reside. Consequently most conditions in which isolated HSCs have been studied, most notably cell culture on plastic, lead to activation and rarely support their quiescent state. Here we describe a high-throughput approach in which we use arrayed cellular microenvironments to systematically and rapidly screen and identify conditions that either promote HSC activation or maintain the quiescent state.

### 3.5.1 Arrayed Combinatorial Microenvironments as a High-throughput Technology for Understanding HSC Biology

We [62, 63, 91] and others [64, 92] have used arrays of microenvironments (i.e. combinations of ECMPs, growth factors, and small molecules) for manipulating stem and progenitor cell populations. In the current study, we applied a similar technology to investigate the response of HSCs to 252 unique microenvironments composed of ECMPs and signaling molecules, with multiple replicates of each microenvironment. Using conventional cell culture methods, such as multi-well cell culture dishes, these studies would have required over 3,500 separate dishes or wells. In contrast, through the use of our array-based technology, we were able to perform these experiments on 3 microscope slides. Furthermore, our system requires 1,000 times fewer cells than typical

culture experiments. This is especially important for primary cells, such as HSCs, which are rare and difficult to isolate. Additionally, using automated microscopy to monitor activation of HSCs through the use of a Col1 $\alpha$ 1-GFP HSC reporter line, we were able to observe in real time the complex responses of HSCs to the various cellular microenvironments.

Several methodological issues might arise from cellular array-based screens. The effect of immobilization of signaling molecules has been addressed in detail [62, 64, 105]. For example, it has been previously demonstrated that mechanically spotted and immobilized matrix proteins and signaling molecules (such as Wnt proteins) remain localized and are biologically active and able to induce cellular responses [64, 91, 105]. Nonetheless, it is important to note that only the initial matrix and signaling molecule composition are specified. Cells exposed to these microenvironments remodel the underlying matrix and begin secreting their own matrix and cytokines. Even so, the observed cellular responses are a result of their exposure to the initial composition of the microenvironment. Another issue that has been addressed is the potential paracrine effects of secretion and diffusion of signaling molecules from cells on neighboring spots. By examining differences between replicates adjacent to different microenvironments, Soen *et al* (2006) did not find significant paracrine interactions between neighboring spots. Although in the current study we did not randomize the placement of replicates within a single array (i.e. 5 replicates were clustered together on the same array), we did vary the location of replicates on independent arrays in order to minimize any bias that might result from topographical effects. However, the possibility of subtle paracrine and edge effects remains. Nonetheless, these effects can be normalized by averaging randomly placed replicates at the cost of increasing intra- and inter- experimental variability.



Additional technical issues, such as inter-experiment variability and validation in traditional culture formats, which could affect the utility of obtained data were addressed in this study. To address the issue of variability between independent array experiments, we computed the Pearson's correlation coefficients between the microenvironment-matched proliferation and activation indexes for each independent experiment pair. The average inter-experiment correlation was  $0.5221 \pm 0.1063$ . The modest correlation between independent array experiments can be explained by the inherent variability of cell based assays. For example, other cell based assays such quantitative real-time PCR show similar amounts of variability between independent biological replicates [106]. Additional sources of variability include subtle deviations in array fabrication, cell isolation, staining, and imaging between independent array experiments. Nonetheless, by using statistical analysis of multiple replicates of each condition we were able to identify specific microenvironmental components that play a role in HSC biology. Furthermore, using traditional multi-well plate format we validated the data obtained from the array experiments, thus demonstrating that the array technology presented in this study is a practical and reliable tool for rapidly investigating the effects of large number of factors on HSC fate.

### **3.5.2 ECMPs Control HSC Proliferation and Activation**

The majority of studies involving HSCs have mainly focused on the role of signaling molecules on HSC proliferation and activation. However, the extracellular matrix can induce numerous structural and signaling changes within a cell [107-109]. Our study demonstrated that ECMPs also significantly modulate HSC proliferation and activation. When presented individually, collagen 1 (C1) was the only ECMP that induced significant HSC proliferation and activation, consistent with the finding that

HSCs express and secrete excessive C1 upon activation. Other ECMPs, such as fibronectin (Fn) or laminin (Ln) alone, prevented proliferation and activation. These results are in concert with previous liver fibrosis studies demonstrating a shift in ECMP composition from one heavy in basement membrane components such as Fn to one rich in C1 [90, 98, 110, 111].

In contrast to single compositions, combinations of ECMPs to create more comprehensive microenvironments yielded a wide range of effects: some microenvironments promoted activation, while others maintained quiescence. Importantly, several combinations of ECMPs resulted in responses that could not be anticipated from the additive effects of the individual proteins. In fact, there were several instances where responses to combinations of ECMPs were opposite to the responses to the individual ECMPs. Our statistical analysis suggests that these responses result from the complex synergistic and antagonistic interactions that may occur between various ECMP signaling pathways. Similar crosstalk between ECMPs has been reported in several other contexts[112, 113].

In contrast to previous studies, the level of correlation between HSC proliferation and our indicator of activation, Col $\alpha$ 1-GFP expression, was relatively weak [76, 93]. This unexpected finding suggests that cellular responses may be significantly influenced by the compositions and complexity of the microenvironment. Through the use of multi-factorial statistical analysis, we showed that these results could be attributed to the dominance of certain ECMPs in influencing either HSC proliferation or activation. Similarly, other studies have demonstrated that certain ECMPs are responsible for specific and often opposing cellular responses[114]. For example, the switch between growth and differentiation in primary hepatocytes is regulated by different cell-matrix interactions[83, 115].

Although additional studies are required to understand the underlying mechanisms of the effects of these ECMPs on HSCs, these *in vitro* experiments suggest that ECMPs could play a critical role *in vivo* in regulating both the activated and quiescent HSC phenotypes. In addition, these experiments indicate that the proliferation and activation status of HSCs can be manipulated *in vitro* by varying the composition of the extracellular microenvironment.

### **3.5.3 Wnt Proteins Interact with ECMPs to Influence HSC Biology**

The role Wnt proteins play in the HSC proliferation and activation is not well established. Previous research has shown that expression of both canonical (Wnt3a) and noncanonical (Wnt5a) Wnt genes, receptors (Fz-1 and Fz-2), and co-receptors (LRP6 and Ryk) are induced in culture activated HSCs compared with quiescent HSCs [79]. Other studies have implicated canonical Wnt signaling in promoting either HSC quiescence [78] or activation [80]. However, we found that in the presence of Wnt3a, HSC activation as measured by Col1 $\alpha$ 1-GFP expression was significantly enhanced, whereas the presence of Wnt5a led to a significant reduction in Col1 $\alpha$ -GFP expression. Furthermore, when presented together, Wnt3a and Wnt5a negated each other's effect, and the levels of Col1 $\alpha$ 1-GFP expression were similar to those in the absence of both Wnt proteins. This is consistent with the observation that Wnt5a antagonizes Wnt3a signaling. Interestingly, the presence of either Wnt protein led to a significant decrease in HSC proliferation.

It is well established that integrin binding can influence growth factor signal transduction[116, 117]. Similarly, we also demonstrated that the degree to which either the canonical or noncanonical Wnt signaling pathways influences HSC fate is dependent on the ECMP microenvironment in which they are presented. We identified several

significant interactions that occur between ECMPs and Wnt proteins. For example, the presence of Ln in the microenvironment enhanced the effect of Wnt5a in maintaining HSC quiescence. This observation has significant implications for any *in vitro* cell studies: the precise composition of the extracellular environment in which cells are cultured can alter the cellular responses to experimental manipulations. Providing an *in vitro* culture milieu that closely resembles the *in vivo* microenvironment may be critically important in studying the signaling effects of growth factors and assessing the effect of small molecules and drugs.

#### **3.5.4 Implications for Culture Activation of HSCs**

We have recently demonstrated that *in vitro*-cultured HSCs require a specific environment to resemble the characteristics of *in vivo*-activated HSCs [97]. Moreover, the spontaneous activation of HSCs cultured on plastic limits the *in vitro* study on quiescent HSCs. Thus, improvement of HSC culture activation will lead to more physiologic models of HSC activation and thus be useful in improving our understanding of the role HSCs play in the fibrotic process. The data presented here demonstrate that ECMPs may represent an important component that regulates HSC status. However, other aspects such as three-dimensionality have been shown to play a critical role in the microenvironment and can affect cell function [118, 119]. In the future, specific ECMP combinations may be used to create 3D culture systems *in vitro*[120] to study characteristics of quiescent HSCs, or conversely to provide a proper environment for an *in vivo*-like HSC activation. Nonetheless, knowledge about the ECMP combinations that are able to maintain quiescence or promote activation will provide new approaches to understanding HSC biology and liver fibrosis.

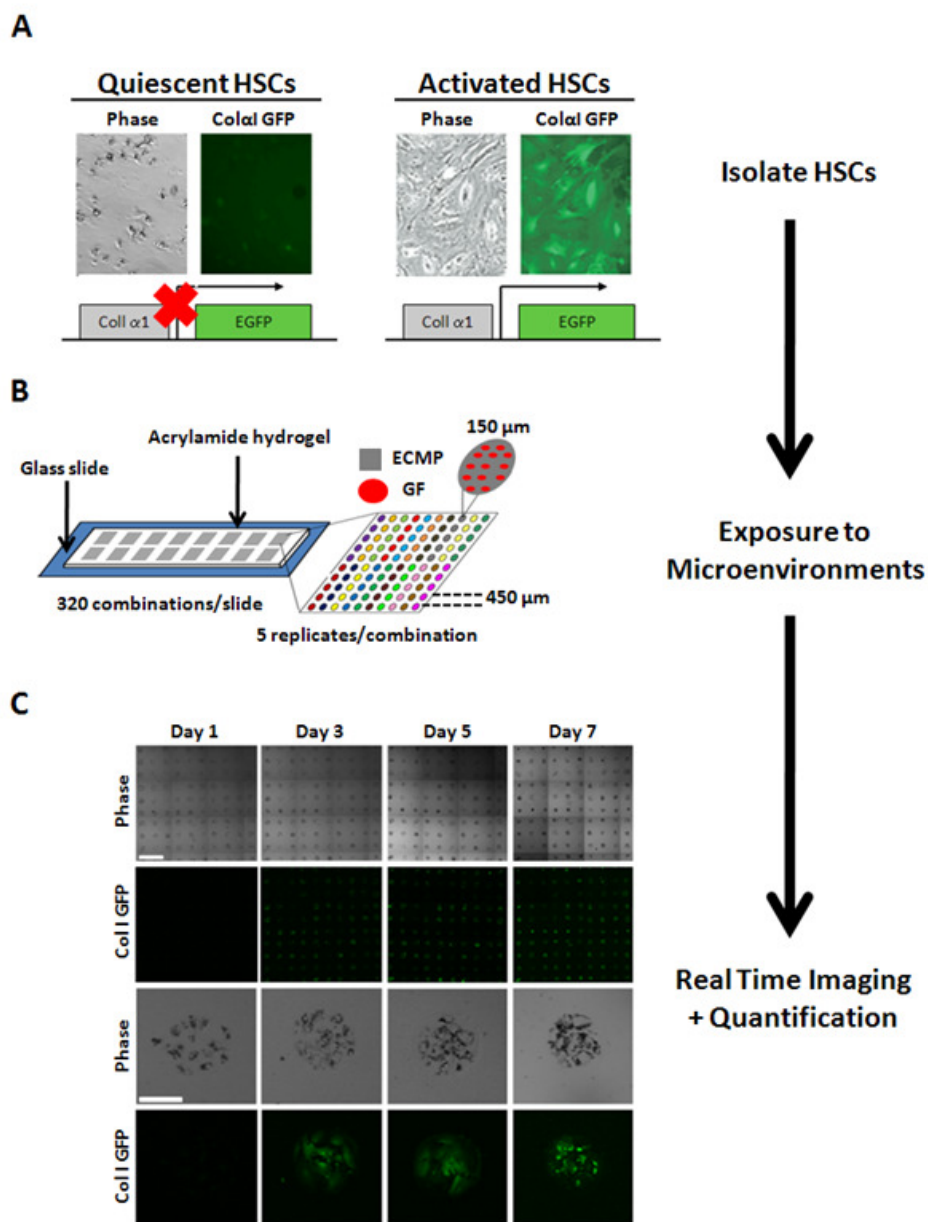
### 3.6 CONCLUSION

In this study, we utilized a high-throughput combinatorial array platform to perform the real-time simultaneous screening of hundreds of unique microenvironments composed of ECMPs and signaling molecules on HSC proliferation and activation. From these screens we identified a novel role for ECMPs and Wnt proteins in the HSC activation process. In general, the presence of C5 and Fn in the microenvironment decreases HSC proliferation, while the presence of C1 and Ln in the microenvironment increases HSC activation. Wnt3a enhances HSC activation and Wnt5a reduces HSC activation, whereas the presence of either Wnt proteins reduces HSC proliferation. Our results demonstrate that high-throughput array-based screens provide a useful tool for not only a better understanding of HSC biology but also may be useful as a rapid and efficient therapeutical strategy for identifying anti-fibrotic therapies.

### 3.7 ACKNOWLEDGEMENTS

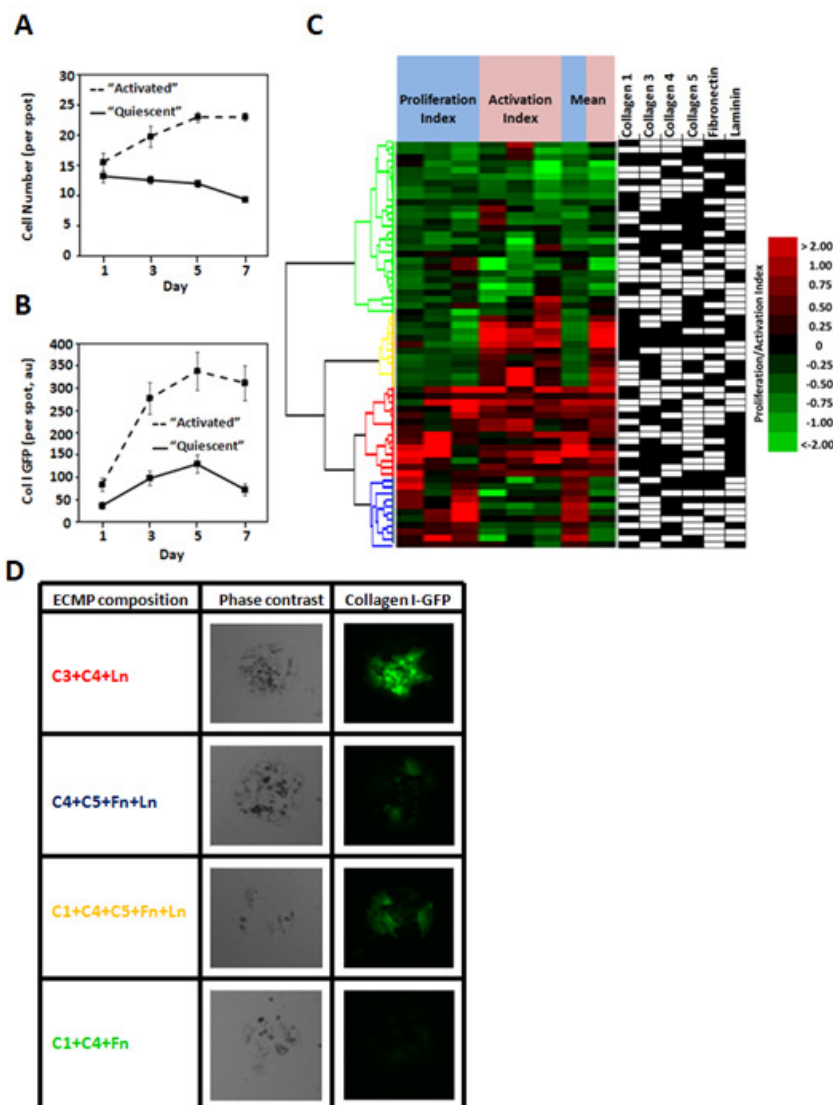
D.A.B. was supported by funding from the University of California Biotechnology Research and Education Program (2007-006). This research was supported in part by the California Institute of Regenerative Medicine (RS1-00172-1) to S.C. and K.W., NHLBI Research Grant HL080518 to S.C., NIAAA Center Grant P50 AA011999 to D.A.Brenner, NIDDK Research Grant DK072237 to D.A.Brenner, and NIGM Research Grant GM041804 to D.A.Brenner.

The text and figures in Chapter 3 are in part reproductions from: Brafman DA, De Minicis S, Seki E, Brenner DA, Willert K, Chien S. Investigating the role of the extracellular environment in modulating hepatic stellate cell biology with arrayed combinatorial microenvironments. 2009. Integ Bio. *In review*. The dissertation author was the primary researcher and author pertaining to this work.



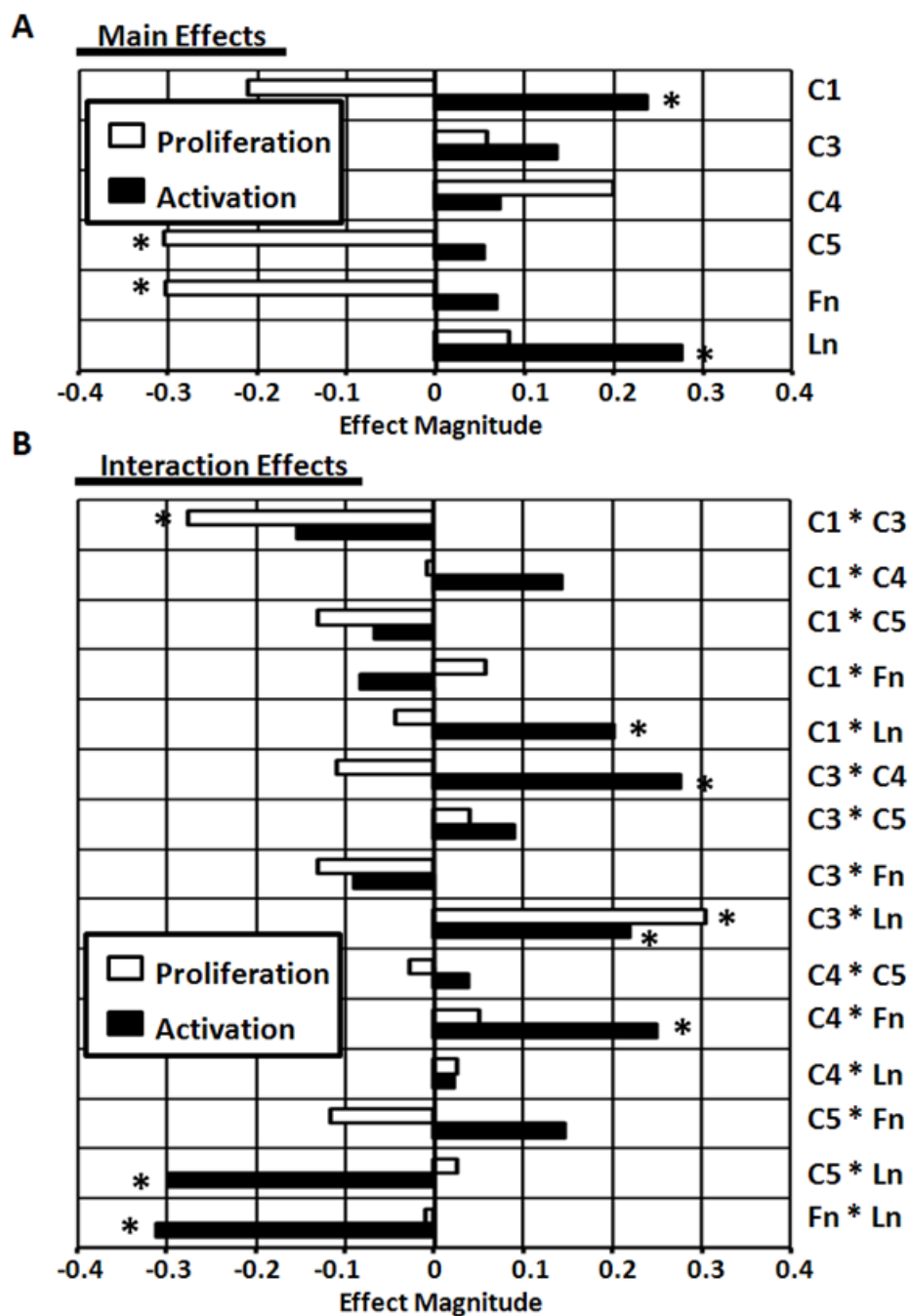
**Figure 3-1: High Throughput Combinatorial Array Technology.**

(a) Hepatic stellate cells (HSCs) isolated from livers of healthy mice transgenic for a gene encoding green fluorescent protein (GFP) under transcriptional control of the collagen1 $\alpha$ (I) (Col1 $\alpha$ 1) promoter/enhancer displayed retinoid autofluorescence, little GFP expression, and morphology characteristic of quiescent HSCs. (b) Freshly isolated HSCs were seeded on arrayed microenvironments consisting of pre-mixed combinations of extracellular matrix proteins (ECMPs) and signaling molecules arranged in 16 subarrays consisting of a 10X10 matrix of spots. Each combination was printed in five replicates. (c) Cellular arrays were imaged by automated microscopy. HSCs were tracked in real time on each microenvironment spot over the course of 7 days. Scale bar for 10x10 matrix = 900  $\mu$ m. Scale bar individual spots = 75  $\mu$ m.



**Figure 3-2: Effect of ECMPs on HSC Proliferation and Activation.**

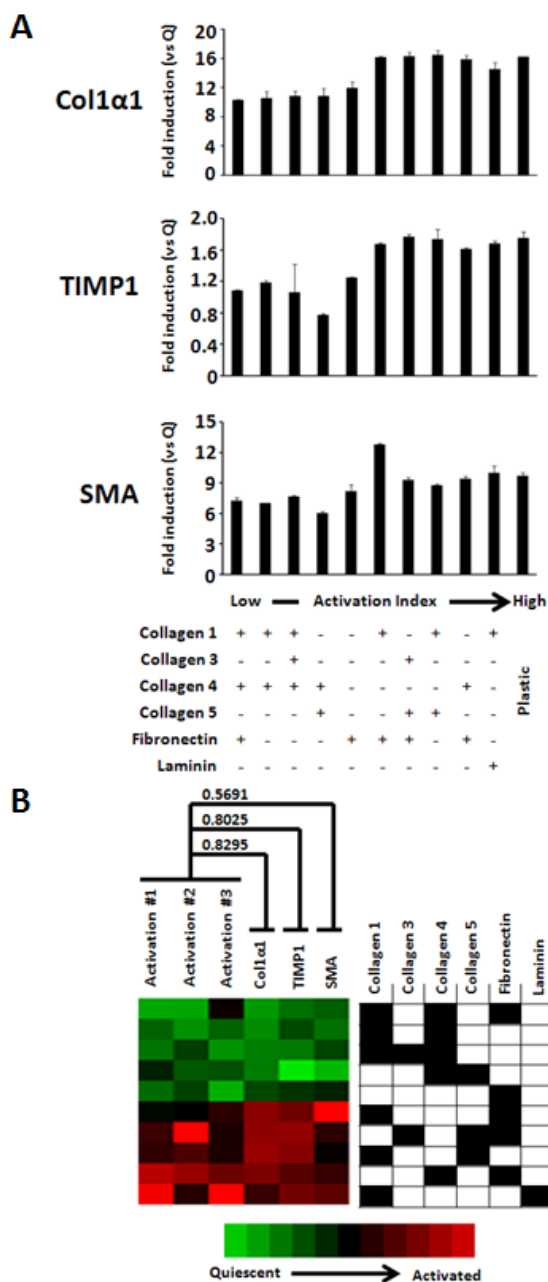
HSC proliferation (a) and activation (b) were measured on ECMP microenvironments. Some microenvironments induced HSC activation (dotted line in a and b) as detected by an increase in GFP expression and cell number, whereas other conditions maintained the cells in a quiescent state (solid line in a and b) (c) Heat map representing the mean proliferation indexes and the mean activation indexes of each ECMP condition (rows) for each independent array experiment (columns). The last two columns represent the mean of the three independent array experiments. Columns were mean centered and scaled to one unit standard deviation. The ECMPs present in each experimental condition are shown as black boxes in the six columns to the right of the heat map. Two-way cluster analysis of each experiment was performed with respect to ECMP conditions using Pearson correlation as a similarity metric. The ECMP microenvironments were clustered into one of four main groups based on the resulting HSC responses that were promoted: (i) high proliferation and activation (red cluster), (ii) high proliferation and low activation (blue cluster), (iii) low proliferation and high activation (orange cluster), and (iv) low proliferation and low activation (green cluster). (d) Phase contrast and Col1 $\alpha$ 1 GFP images illustrating representative members of each cluster.



**Figure 3-3: Identification of ECMPs Having Prominent Effect on HSC Proliferation and Activation.**

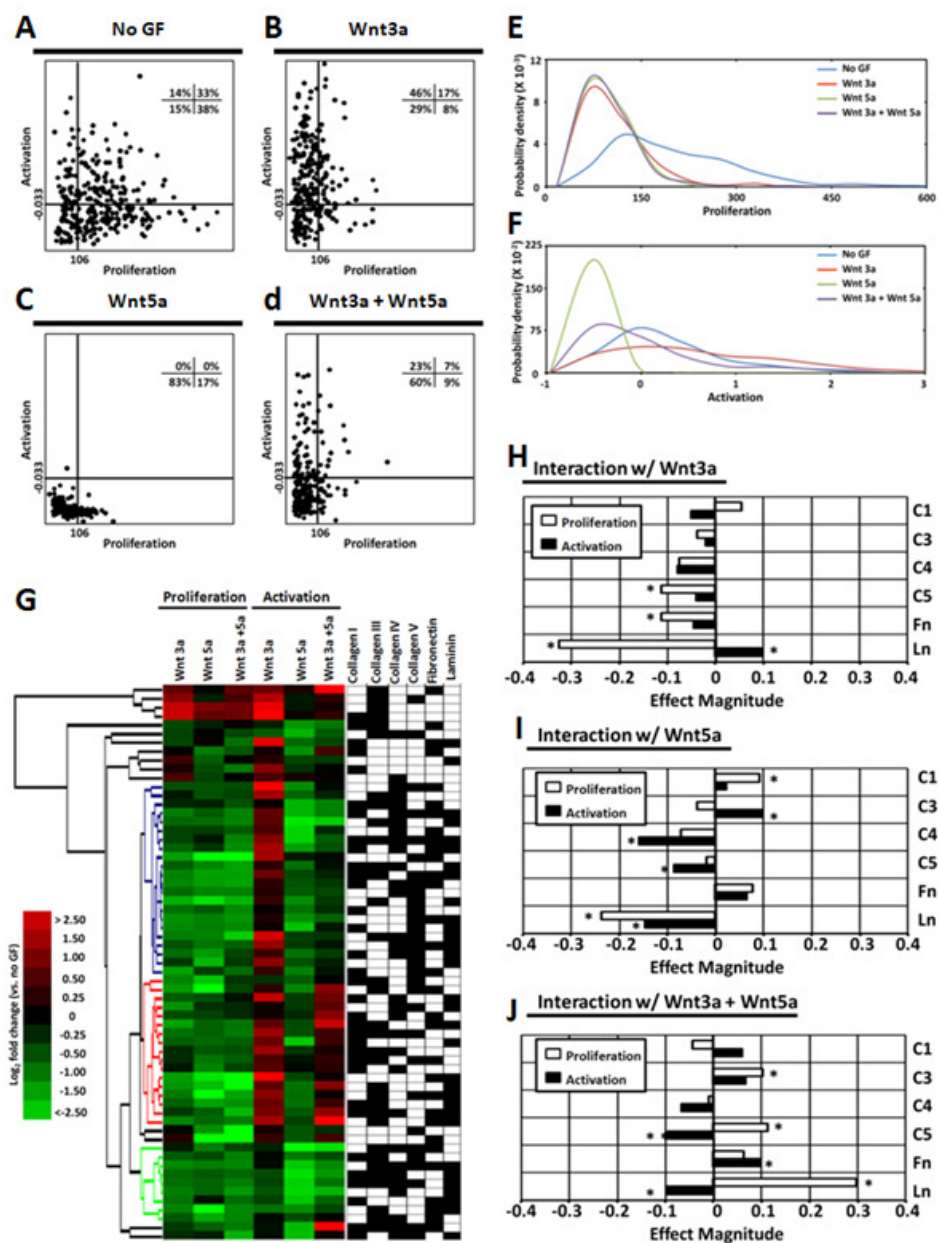
(a) Magnitude of the main effects of a factorial analysis reveals that specific ECMP components have significant dominance in influencing HSC proliferation and activation (\* $p < 0.05$ ). (b) Magnitude of the two factor interaction effects of a factorial analysis reveals crosstalk that occurs between various ECMPs (\* $p < 0.05$ ).





**Figure 3-4: Confirmation of Array-based Data.**

(a) Expression of collagen1 $\alpha$ 1 (Col1 $\alpha$ 1), tissue metalloproteinase inhibitor 1 (TIMP-1), and  $\alpha$ -smooth muscle actin ( $\alpha$ -SMA) of HSCs grown on different ECMP microenvironments. Results are expressed as fold induction  $\pm$  standard deviation in comparison with quiescent HSCs. (b) Comparison of HSC activation on the arrayed microenvironments, measured by normalized Col1 $\alpha$ 1-GFP expression, with the quantitative real-time PCR data reveals that data obtained from conventional culture experiments are consistent with data obtained from the microarray experiments.



**Figure 3-5: Effect of Wnt Proteins on HSC Proliferation and Activation.**

Proliferation (day 5 cell count) versus activation ( $\log_2[\text{day 5 GFP} / \text{day 5 cell count}]$ ) plots for all microenvironments without Wnt proteins (a), with Wnt3a (b), with Wnt5a (c), and with both Wnt3a and Wnt5a (d). Probability density functions reveal Wnt proteins reduce HSC proliferation (e), Wnt 3a enhances HSC activation (red trace, f), and Wnt 5a reduces HSC activation (green trace, f). (g) Heat map representing the  $\log_2$  fold change of Wnt protein addition (columns; Wnt3a alone, Wnt5a alone, Wnt3a and Wnt5a together) to each ECMP microenvironment (rows) on proliferation and activation relative to no growth factor. (h-j) Magnitude of the interaction effects between ECMPs and Wnt proteins demonstrate that Wnt proteins interact with ECMPs to influence HSC proliferation and activation ( $*p < 0.05$ ).

**Table 3-1: Reproducibility Between Biological Repeats.** Pearson's product moment correlation coefficients of proliferation and activation indexes of biological repeats of independent array experiments and HSC isolations.

## Proliferation

	<b>Array 1</b>	<b>Array 2</b>	<b>Array 3</b>
<b>Array 1</b>		0.5005	0.3503
<b>Array 2</b>			0.6486

## Activation

	<b>Array 1</b>	<b>Array 2</b>	<b>Array 3</b>
<b>Array 1</b>		0.6221	0.5075
<b>Array 2</b>			0.5033

**Table 3-2: Groupings of ECMP Microenvironments.**

ECMP microenvironments were placed into groups in which Wnts exert unique effects on HSC proliferation and activation. '+' indicates an increase of proliferation/activation relative to no growth factor, while '-' indicates a decrease of proliferation/activation relative to no growth factor.

Group	Size	Proliferation			Activation		
		Wnt 3a	Wnt 5a	Wnt 3a + Wnt 5a	Wnt 3a	Wnt 5a	Wnt 3a + Wnt 5a
1	1	+	+	+	+	+	+
2	1	+	-	+	-	-	-
3	1	+	-	+	+	+	+
4	1	+	-	+	+	-	+
5	1	+	-	-	+	+	+
6	2	+	-	-	+	-	+
7	2	+	-	-	+	-	-
8	1	+	+	-	+	-	-
9	1	+	+	-	-	-	-
10	1	+	-	+	-	-	-
11	16	+	-	-	+	-	+
12	23	+	-	-	+	-	-
13	3	+	-	-	-	-	+
14	9	+	-	-	-	-	-

## **CHAPTER 4**

# **DEFINING LONG-TERM MAINTENANCE CONDITIONS OF HUMAN EMBRYONIC STEM CELLS WITH ARRAYED CELLULAR MICROENVIRONMENT TECHNOLOGY**

### **4.1 ABSTRACT**

The optimization of defined growth conditions is necessary for the development of clinical application of human embryonic stem cells (hESCs). Current research has focused on developing defined media formulations for long-term culture of hESCs with little attention on the establishment of defined substrates for hESC proliferation and self-renewal. Presently available technologies are insufficient to address the full complement of factors that may regulate hESC proliferation and maintenance of pluripotency. Here, we report the application of a multi-factorial array technology to identify fully defined and optimized culture conditions for the proliferation of hESCs. Through the systematic screening of extracellular matrix proteins (ECMPs) and other signaling molecules, we developed and characterized a completely defined culture system for the long-term self-renewal of three independent hESC lines. In the future, the novel array platform and analysis procedure presented here will be applied towards the directed differentiation of hESCs and maintenance of other stem and progenitor cell populations.

## 4.2 INTRODUCTION

Development and maintenance of multi-cellular life forms involves complex interactions between cells and biomolecules that mediate cell-cell and cell-matrix contact. Due to the vast number of molecules used in biological systems and furthermore the virtually limitless possible combinations of these molecules, it has been extremely difficult to identify sets of conditions that specifically affect in a biologically relevant manner the behavior of any cell type *in vitro*. With the derivation of human embryonic stem cells (hESCs) [66], it has for the first time become conceivable to study various aspects of human development at the cellular level in a culture dish. In addition, hESCs represent an infinite supply of cellular “raw-material” for future cell-based therapies, drug testing and disease modeling. The *in vitro* culture conditions and the cellular microenvironments that either promote hESC expansion or their specific differentiation have either not been developed or not been defined.

Conventional cell culture methods, such as multi-well cell culture dishes, are limited in their ability to screen the vast number of possible combinations of factors that may influence hESC behavior. The establishment of high-throughput screens with hESCs will be important for a broad range of applications from basic understanding of the role of certain signaling networks in self-renewal to the development of novel therapeutic treatments, such as cell replacement of damaged, diseased or dead tissues. Based on previous array technologies [62, 63], we integrated the use of ECMPs and signaling molecules into a cellular microarray technology platform, thereby creating comprehensive “microenvironments” that closely resemble the *in vivo* environment in which cells reside.

In recent years there have been a large number of research studies to identify the optimal hESC culture conditions. Most hESC culture protocols utilize mouse or human feeders that secrete a combination of many uncharacterized factors, some of which are critical to the maintenance of the pluripotent state [16] while others promote their differentiation. More recently, several protocols for the “feeder-free” culture of hESCs have been described [17]. These methods generally involve the use of extracellular matrices, such as Matrigel™ (BD), to provide a suitable cell adhesion substrate and media that have been conditioned on mouse or human feeder layers [18]. However, both Matrigel and conditioned media (CM) contain undefined components of non-human origin, making the cells cultured in these conditions unsuitable for any future therapeutic applications. Several groups have reported the successful use of combinations of factors to replace the need for CM [20-24, 28-30], and only a few studies have been performed to replace Matrigel with extracellular matrix proteins (ECMPs) such as fibronectin, laminin, or vitronectin [31-34]. These previous attempts to define the optimal culture conditions for hESCs, however, were made with random variations of a few ECMPs and other signaling molecules without systematically assessing the optimal conditions required for the long-term culture of hESCs. While ECMPs interact in a complex manner to regulate ESC proliferation, maintenance of pluripotency, and differentiation [35, 36], these interactions have not been studied systematically in hESCs.

With the novel multi-factorial array technology presented here, we systematically defined an optimal combination of ECMPs that supports long-term propagation of several hESC lines in an undifferentiated state. Furthermore, we have developed several computational tools to process the large data sets produced in these experiments and to extract the critical data points so that the optimal conditions can be verified

independently in conventional cell culture format. Our study demonstrates the feasibility of using high-throughput array-based screens to identify ECMPs, growth factors (GFs), and other signaling molecules that may affect hESC fate.

## **4.3 MATERIALS AND METHODS**

### **4.3.1 Array Fabrication**

Glass slides (75mm x 25mm x 1mm) were washed with 100% acetone, 100% methanol, and ten times in Millipore water (MQH<sub>2</sub>O) to remove residual debris and oils. The slides were etched overnight in 0.05 N NaOH, rinsed five times with MQH<sub>2</sub>O, and dried with filtered compressed air and in vacuum oven (65°C, 20 psi) for 1 hr. The slides were then silanized in a 2% solution of 3-(trimethoxysilyl)propyl methacrylate in anhydrous toluene overnight, rinsed in toluene, dried with compressed air, and baked for 1 hr in a vacuum oven (65°C, 20 psi).

A stock solution of 10% (w/v) acrylamide, 0.55% (w/v) bis-acrylamide, 10% (w/v) photoinitiator I2959 (200 µg/ml in 100% methanol; Igacure 2959, Ciba Specialty Chemicals) was prepared. Subsequently, 100 µl of this stock solution was placed on a silanized slide and covered with a 75mm x 25 mm coverslip (Bellco Glass). The slide was then exposed to 1.5 mW/cm<sup>2</sup> 365-nm ultraviolet A light for 7 min and immersed in MQH<sub>2</sub>O for 10 min. The coverslip was then removed, leaving a thin (~75 µm) polyacrylamide gel pad. The polyacrylamide slides were soaked in MQH<sub>2</sub>O for 48 hr to remove residual unpolymerized acrylamide and photoinitiator, and then dehydrated on a hot plate (40°C) for 10 min.

Stock solutions of human collagen I, collagen III, collagen IV, collagen V, fibronectin, and laminin (Sigma) were prepared in an ECMP printing buffer (200 mM



acetate, 10 mM EDTA, 40% (v/v) glycerol, and 0.5% (v/v) triton X-100 in MQH<sub>2</sub>O, with pH adjusted to 4.9 using glacial acetic acid). All ECMP combinations were printed at a constant protein concentration of 250 µg/ml. We discovered that signaling molecules were largely inactive in the ECMP spotting buffer (data not shown). Hence, stocks of bFGF (Invitrogen), BMP-4 (Invitrogen), retinoic acid (Sigma) and Wnt3a [73] were prepared in a signaling molecule buffer (40% (v/v) glycerol, 1% (w/v) CHAPS in PBS). Final concentrations of these signaling molecules in printing buffer were 30 µg/ml for bFGF, 100 µg/ml for BMP, and 300 µg/ml for retinoic acid. Signaling molecules printed using this buffer retained their signaling ability. Combinations of ECMPs and signaling molecules were mixed in separate 384-well plates.

SMP 3.0 spotting pins (Telechem) were washed with 90% ethanol. All printings were performed with a SpotArray 24 (Perkin Elmer) at room temperature with 65% relative humidity. ECMP mixtures were printed first, followed by the signaling molecule mixtures. The acrylamide substrate served to retain the printed proteins to the spots. To control for variability, each microenvironment was printed in replicates of 5 spots. Each spot had a diameter of 150 µm and neighboring microenvironments were separated by a center-to-center distance of 450 µm. Spots were organized into 'subarrays' (9mm X 9mm). Each glass slide had 16 such subarrays, and each subarray contained 100 spots arranged in a 10 X 10 format. Thus, a single slide accommodated up to 320 unique signaling microenvironments with 5 replicates each. Prior to their use, slides were soaked in PBS while being exposed to UVC germicidal radiation in a sterile flow hood for 10 min.

### **4.3.2 Cell Culture**

The following media were used: MEF and HEK-293 (1X high glucose DMEM, 10% fetal bovine serum, 1% (v/v) L-glutamine penicillin/streptomycin); H9/WA09 hESCs (1X DMEM-F12, 20% (v/v) Knockout Serum Replacement, 1% (v/v) non-essential amino acids, 0.5% (v/v) glutamine, 120  $\mu$ M 2-mercaptoethanol [Sigma]); Hues1 and 9 hESCs (1X Knockout DMEM, 10% (v/v) Knockout Serum Replacement, 10% (v/v) human plasmanate (Talecris Biotherapeutics), 1% (v/v) non-essential amino acids, 1% (v/v) penicillin/streptomycin, 1% (v/v) Gluta-MAX, 55  $\mu$ M 2-mercaptoethanol [Sigma]). All media components are from Invitrogen unless indicated otherwise. H9, Hues9, and Hues1 hESC lines were maintained on feeder layers of mitotically inactivated mouse embryonic fibroblasts ( $2 \times 10^4$ /cm<sup>2</sup>; Global Stem). All hESC cultures were supplemented with 30 ng/ml bFGF (Invitrogen). MEF-CM was produced by culturing the appropriate hESC medium on MEFs for 24 hr. StemPro consisted of the StemPro supplement (Invitrogen) diluted in DMEM-F12 with 2% (v/v) BSA (Millipore) and 55  $\mu$ M 2-mercaptoethanol. Cultures of H9s were routinely passaged in clumps by exposure to dispase (2 mg/ml; Invitrogen) for 5 min, followed by three rinses with the H9 media, and then collection by gentle scarping. Colonies were further broken up by gentle pipetting prior to plating onto fresh MEF cultures. Hues9 and Hues1 were routinely passaged as single cells by exposure to acutase (Millipore) for 5 min, followed by one rinse with media and centrifugation at 200 x g. Cells were then resuspended and plated.

HEK-293 were passaged ( $2.5 \times 10^5$  cells per slide) directly onto the array slides and allowed to settle on the spots for 18 hr prior to rinsing with HEK-293 medium 3 times to remove residual cells and debris. Prior to seeding onto the arrays, hESCs were cultured for two passages on Matrigel (BD Sciences) with MEF-CM supplemented with 30 ng/ml bFGF to remove residual feeder cells. HESCs were then acutase-passaged onto the array slides ( $5.0 \times 10^5$  cells per slide) and allowed to settle on the spots for 18

hr prior to rinsing with the medium one time to remove unattached cells and debris. Cell media was replenished daily. Due to the non-fouling nature of the acrylamide, cells were confined to the printed microenvironment spots.

### **4.3.3 Slide Staining, Imaging and Quantification**

For characterization of ECMP and signaling molecule printing, the slides were fixed in 4% (w/v) paraformaldehyde (PFA) for 10 min and blocked with 1% (w/v) BSA (Sigma) and 3% (w/v) milk for 30 min at room temperature. The slides were then stained with Sypro Ruby (Probes) solution overnight, destained with 10% (v/v) methanol and 7% (v/v) acetic acid, and air dried. Additionally, slides were stained with primary antibodies mouse anti-collagen I, mouse anti-collagen III, mouse anti-collagen IV, mouse anti-collagen V, mouse anti-fibronectin, rabbit anti-laminin, rabbit anti-bFGF, mouse anti-BMP-4 (Sigma), or rabbit anti-Wnt3a [73], diluted 1:250 in 1% BSA at 4°C overnight. The slides were subsequently washed 3 times with Tris buffered saline (TBS), incubated with a goat anti-mouse or goat anti-rabbit Alexa 647 (Invitrogen) at 1:400 for 1 hr at 37°C, washed 3 times with TBS, and air dried immediately before imaging.

Because fixing and staining protocols may cause cell detachment and alter the cell counts on each spot, arrays were stained live for DNA with Hoescht 33342 (2 µg/ml; Invitrogen) for 5 min. The arrays were washed 3 times with the medium and then imaged. After live imaging, the arrays were fixed in 4% PFA for 5 min at 4°C, followed by 10 min at room temperature. Immediately before staining, the cells were permeabilized with 0.2% (v/v) Triton-X-100 and blocked with 1% (w/v) BSA and 3% (w/v) milk for 30 min. The slides were stained with the primary antibodies rabbit anti-Oct3/4a or rabbit anti-Nanog (Santa Cruz) diluted 1:200 in 1% BSA overnight at 4°C, washed 3 times with TBS, and incubated with goat anti-rabbit Alexa 647 at 1:400 for 1 hr at 37°C. Nucleic

acids were stained using the Cy3 equivalent POPO-3 (Invitrogen) for 5 min at room temperature. The slides were then washed 3 times with TBS and air dried immediately before imaging.

Live imaging of slides was performed using an automated confocal microscope (Olympus Fluoview 1000 with motorized stage and incubation chamber). Imaging of fixed slides was performed using a confocal DNA microarray scanner (Scanarray 400) at 5- $\mu$ m pixel resolution. Sypro Ruby stain was imaged using a Scanarray 4000 (Perkin Elmer) with 546-nm laser excitation and a 617-nm emission filter. The POPO-3 nucleic acid stain (Cy3 equivalent) was imaged using a 543-nm laser excitation and 570-nm emission filter. The Alexa 647 (Cy5 equivalent) was imaged using a 633-nm excitation laser and 670-nm emission filter. Each subarray was individually imaged using a focus height that gave the maximum signal in the Z-direction for each channel at the center of the array. Images were then quantified using GenePix software (MDS Analytical Technologies).

#### **4.3.4 Long Term hESC Culture on Defined Conditions**

H9, Hues9 and Hues1 were cultured on Matrigel<sup>TM</sup> (BD) with MEF-CM supplemented with 30 ng/ml bFGF for 2 passages to remove residual MEFs. The human ECMP coated plates were prepared by coating tissue culture plates in the ECMP (diluted in 10mM acetic acid) overnight, followed by air drying. 10 ug of total protein was plated per cm<sup>2</sup> of culture dish surface. During these studies we used two lots of collagen I, two lots of collagen IV, three lots of fibronectin, and three lots of laminin without noticeable differences in the quality of the hESC cultures. HESCs were passaged at a density of 5 x 10<sup>4</sup> cells/ml onto human ECMP or Matrigel coated plates. MEF-CM or StemPro and bFGF were changed daily. Cell viability was assessed using a Trypan Blue exclusion

assay. Fixation and immunostaining with Hoescht, Oct3/4a, and Nanog were performed using the procedures described above for fixation and immunostaining of array slides.

#### **4.3.5 Karyotype Analysis**

For each cell line, cytogenetic analysis was performed on 20 metaphase cells using standard protocols for G-banding (Cell Line Genetics).

#### **4.3.6 Embryoid Body Formation**

Cells were treated with 5  $\mu$ M of ROCK inhibitor (Y27632, Sigma) 24 hr before EB formation. Cells were trypsinized, transferred into untreated V-shaped 96-well plate (5 x 10<sup>3</sup> cell/well) and centrifuged at 950 x g to form compact colonies of cells. After 24 hr, the cell clumps were transferred using a P1000 pipet to ultra-low binding 6-well plate. After 7 days, the EBs were replated onto Matrigel-coated plates for an additional 14 days.

#### **4.3.7 RT-PCR Analysis**

RNA isolation was performed using TRIzol (Invitrogen). 1  $\mu$ g of RNA was treated with DNase I (Invitrogen), and reverse transcription was carried out using qScript cDNA Supermix (Quanta BioScience). Q-PCR was performed on a 7900HT Fast Real-Time PCR System (Applied Biosystems) using TaqMan Gene Expression Assay probes (Applied Biosystems) and TaqMan Fast Universal PCR Master Mix (Applied Biosystems). PCR products were separated and visualized by gel electrophoresis. Amplification of GAPDH and omission of RT served as positive and negative controls, respectively. Taqman gene expression assay primers (Applied Biosystems) were used.

### **4.3.8 Data Analysis**

All values were presented as mean  $\pm$  standard deviation. Effect magnitude was calculated as previously described [121]. Clustering analysis was performed using Gene Cluster (Eisen) and all heat maps were created using Treeview (Eisen).

## **4.4 RESULTS**

### **4.4.1 Arrayed Cellular Microenvironments to Study hESC Fate**

The layout of the arrayed cellular microenvironments is described in Fig. 4-1. Using a DNA microarray spotting instrument, we deposited protein mixtures onto hydrogel-coated glass microscope slides. A single slide carries 1,600 spots arranged in 16 10x10 matrices (Fig. 4-1a). Each protein spot, or microenvironment, is 150  $\mu$ m in diameter and each protein mixture is spotted in replicates of five so that one slide carries 320 unique conditions. In this work we spot multiple extracellular matrix proteins (ECMPs; collagen I, III, IV and V, fibronectin, laminin), growth factors (GFs; bFGF, BMP-4, and Wnt3a), and small molecules (retinoic acid).

Prior to seeding onto the arrayed cellular microenvironments, hESCs were cultured in feeder-free conditions [17] and assessed for their characteristic morphology, maintenance of markers of pluripotency, and normal karyotype. To seed the arrays, hESCs were trypsinized into single cells, and cell suspensions were allowed to settle onto the microenvironments for 18 hrs. Thereafter, medium was replaced to remove non-adhering cells and debris. Passaging methods that result in cell clumps rather than single cells (e.g. manual dissection or Collagenase IV treatment) did not produce cell suspension suitable for seeding the arrays. Consequently, we utilized mainly the Hues lines (D. Melton, HHMI, Harvard), which have been adapted to enzymatic single cell

passaging. To ensure maximum cell survival, we tested various enzymatic passaging methods. We found that Accutase™ (Chemicon) treatment resulted in fully dissociated suspensions that adhered well to the arrayed microenvironment spots. Seeding the array slides with  $5 \times 10^5$  cells allowed for the attachment of 10-20 cells per spot and provided sufficient area for subsequent growth. After 5 days of growth, various parameters of cell behavior, such as proliferation and pluripotency, were quantified by microscopy and microarray imaging (Fig. 4-1 b-g).

#### **4.4.2 Individual ECMPs Differentially Support hESC Proliferation in a Concentration-dependent Manner**

We have used single ECMPs such as laminin and fibronectin as substrates with mixed results for the long-term maintenance of hESCs (data not shown). Here we assessed the ability of single ECMPs to support hESC proliferation. Hues1 and Hues9 were cultured on arrays of single ECMPs (collagen I, collagen III, collagen IV, collagen V, fibronectin, and laminin) at varying concentrations (500, 250, and 125  $\mu\text{g/ml}$ ) and Matrigel (250  $\mu\text{g/ml}$ ). After 5 days of growth, cell arrays were fixed and stained for DNA (Fig. 4-2a and 4-2b). Since total DNA is directly reflective of cell number, we used this measure to assess relative proliferative rates.

Among the ECMPs studied, only high concentrations of fibronectin and laminin (500  $\mu\text{g/ml}$ ) were able to support hESC proliferation at levels comparable to Matrigel (250  $\mu\text{g/ml}$ ) for both Hues1 and Hues9. Collagen I supported moderate amounts of proliferation in both cell lines tested while collagen IV supported moderate amounts of proliferation in only Hues9 and collagen III supported moderate amounts of growth in only Hues1. These findings suggest that single ECMPs differentially support various hESC lines. Collagen V did not support extensive growth at any concentration in both

cell lines. In general, each ECMP supported hESC proliferation in a concentration-dependent manner with the highest amount of proliferation typically occurring at the highest concentration of ECMPs tested. As a whole, these results indicate that single ECMPs are not the optimal defined substrates to support hESC growth.

To ensure individual ECMPs were functional and able to support growth of other more robust cell types, we seeded the arrays with HEK-293 cells (Fig. 4-2c). The individual ECMPs were able to support the growth of HEK-293, but the levels of proliferation of HEK-293, unlike the hESCs, did not show significant trends of changes with concentration variations for all individual ECMPs.

#### **4.4.3 Effect of ECMP Composition on hESC Proliferation and Maintenance of Pluripotency**

MEFs deposit a complex mixture of ECMPs, including various collagens, laminin, and fibronectin, thereby creating a substrate that supports attachment and proliferation of undifferentiated hESCs [122]. Likewise, Matrigel is a complex mixture containing multiple ECMPs (e.g. collagen IV and laminin) that is able to support long-term culture of hESCs [123]. However, the identity of the essential matrix components required for undifferentiated proliferation of hESCs is unknown. Since single ECMPs only marginally supported hESC growth, we sought to systematically assess the effect of multiple ECMPs on hESC proliferation.

Using the array platform, we investigated the effects of all possible combinations of six ECMPs (collagen I, collagen III, collagen IV, collagen V, laminin, and fibronectin) on hESC proliferation. Hues1 and Hues9 were cultured on arrays carrying all 63 combinations of 6 ECMPs, as well as Matrigel, in the presence of MEF-CM. The total protein concentration for each spotted combination remained constant at 250 µg/ml.



After 5 days of growth, cell arrays were stained and imaged live for DNA. A Proliferation Index (PRO<sub>i</sub>) was calculated for each spot:

$$\text{PRO}_i = \frac{X_i - \mu_{\text{DNA}}}{\sigma_{\text{DNA}}}$$

where  $X_i$  is the log<sub>2</sub> of the DNA signal for the spot,  $\mu_{\text{DNA}}$  is the average of the log<sub>2</sub> DNA signals for all spots on each array, and  $\sigma_{\text{DNA}}$  is the standard deviation of the log<sub>2</sub> DNA signals for all spots on each array. Proliferation Indexes from replicate spots (n=5 per ECMP condition) were averaged ( $\mu_{\text{PRO}}$ ) for each array.

To assess the proliferative responses of hESCs to each ECMP condition,  $\mu_{\text{PRO}}$  values were displayed in a heat map with rows corresponding to various ECMP conditions and columns representing three independent array experiments (Fig. 4-3a). The rows and columns were clustered using Pearson correlation as a similarity metric and displayed using a color code with red and green pixels representing higher and lower proliferation, respectively, relative to the global average ( $\mu_{\text{PRO}}=0$ ) (Fig. 4-3a). The biological response of hESCs to the ECMP combinations could be segregated into one of four main groups: i) high proliferation in both Hues1 and Hues9 (red cluster), ii) high proliferation in Hues9 only (blue cluster), iii) high proliferation in Hues1 only (orange cluster), iv) low proliferation in both Hues1 and Hues9 (green cluster), corresponding to the four main regions of the proliferation space (Fig. 4-3b and 4-3c). With the exception of one condition (C1 + Fn), the results of independent array experiments were in good agreement with each hESC line displaying similar trends and tight clustering (Pearson's Correlation Coefficient of 0.805 for Hues9 cluster, Pearson's Correlation Coefficient of 0.838 for Hues1 cluster).

All ECMP conditions promoting high proliferation in both Hues1 and Hues9 (red cluster) contained either fibronectin (Fn) or laminin (Ln), confirming previous studies that

demonstrated the importance of these ECMPs in promoting hESC proliferation [17, 31, 124]. However, fibronectin or laminin alone resulted in relatively low proliferation (green cluster). Since the total amount of protein present was the same for individual ECMPs and combinations of ECMPs, it can be concluded that certain combinations of ECMPs better support hESC proliferation than individual ECMPs. Furthermore, Matrigel (Mgel) was less effective at maintaining a high proliferation index relative to most combinations of ECMPs. To ensure that the effect of ECMP composition on cell proliferation was specific to hESCs, we seeded the arrays with HEK-293 cells. All combinations of ECMPs supported very similar levels of HEK-293 proliferation.

To determine the effect of ECMP composition on maintenance of pluripotency in addition to proliferation, Hues9 were fixed after five days of growth and stained for the stem cell markers Oct4 and Nanog (Fig. 4-4). These markers are specifically expressed in undifferentiated hESCs and become quickly down-regulated as cells enter differentiation programs [16, 125].

For each spot, the ratio ( $R_i$ ) of the  $\log_2$  of the Oct3/4a or Nanog signal and the DNA signal was calculated. From this ratio a Pluripotency Index ( $PLU_i$ ) was calculated for each spot:

$$PLU_i = \frac{R_i - \mu_{ratio}}{\sigma_{ratio}}$$

where  $R_i$  was the ratio for the spot,  $\mu_{ratio}$  was the average of the ratios for all spots on each array, and  $\sigma_{ratio}$  was the standard deviation of the ratios for all spots on each array. Each spot was assigned a coordinate (PRO, PLU) to determine the relationship of hESC proliferation to the maintenance of pluripotency.

Pluripotency Indexes from replicate spots ( $n=5$  per ECMP condition) were averaged ( $\mu_{PLU}$ ) for each ECMP condition on the array. The  $\mu_{PRO}$  and  $\mu_{PLU}$  were

displayed in a heat map with rows corresponding to individual ECMP conditions and columns representing independent array experiments to determine the effects of each ECMP condition on hESC proliferation and maintenance of pluripotency (Fig. 4-4a). The ECMP conditions were segregated into one of four main groups: i) high maintenance of pluripotency and high proliferation (red cluster), ii) high maintenance of pluripotency and low proliferation (blue cluster), iii) low maintenance of pluripotency and high proliferation (orange cluster), iv) low maintenance of pluripotency and low proliferation (green cluster) (Fig. 4-4b and 4-4c). The results showed good agreement between experiments (Pearson's correlation coefficient 0.723 for pluripotency cluster).

No single ECMP resulted in high values for both proliferation and maintenance of pluripotency. However, collagen I alone (C1), fibronectin alone (F), and laminin alone (L) all resulted in high maintenance of pluripotency. This ability to support maintenance of pluripotency is consistent with the use of both fibronectin and laminin for culture of hESCs. Matrigel (Mgel) also supported maintenance of pluripotency but was unable to support high amounts of proliferation.

Principal component analysis revealed that certain ECMP components, particularly laminin, had dominant effects in terms of proliferation and maintenance of pluripotency (Fig. 4-5). All ECMPs had a positive effect on proliferation, indicating that combinations of ECMPs provide a better proliferative environment than single ECMPs. Additionally, laminin was the only component that had a positive effect on both proliferation and maintenance of pluripotency.

#### **4.4.4 Effect of GFs and Small Molecules on hESC Proliferation and Maintenance of Pluripotency**

To demonstrate the feasibility of future array-based screens of hESCs involving signaling molecules, we utilized human basic fibroblast growth factor (bFGF), bone morphogenetic protein-4 (BMP4), and retinoic acid (RA). It has been demonstrated that bFGF is a factor critical for the maintenance of pluripotency of hESCs [20], while BMP4 and RA promote differentiation of hESCs [126]. Arrays spotted with various combinations of ECMPs and signaling molecules were seeded with hESCs. After five days of growth, proliferation and maintenance of pluripotency were assessed. Higher proliferation and survival of hESCs was evident when bFGF was present along with the ECMP combination (Fig. 4-6a-d). There was no difference in hESC proliferation whether bFGF was included directly in the microenvironment spot or added exogenously to the growth media (data not shown). On the other hand, the presence of BMP4 or RA reduced both proliferation and maintenance of pluripotency (Fig. 4-6e-f), consistent with the role of these factors in hESC differentiation. Furthermore, hESCs on microenvironments with BMP4 or RA quickly lost expression of markers of pluripotency and quickly acquired the fibroblast-like morphology of differentiating hESCs. Together, these results demonstrate that the spotted signaling molecules retain their signaling activity and can influence hESC behavior. These finding also suggest that this screening technology may be applicable to other signaling molecules.

A major goal of our studies was to identify the ECMP conditions that support long-term culture of hESCs in fully defined conditions. Previous experiments were performed in the presence of MEF-CM, a poorly defined environment for the culture of hESCs. Therefore, we performed array experiments in which we replaced MEF-CM with unconditioned media (UCM). Overall, the absence of CM leads to decreases in proliferation and pluripotency maintenance. This suggests that the ECMPs cannot compensate for certain soluble factors that are present in CM and that promote hESC

proliferation and maintenance of pluripotency. Future array-based screens will be useful to identify such factors.

Our previous experiments demonstrated that the ECMP composition has a significant effect on hESC proliferation and maintenance of pluripotency. Likewise, the experiments we performed with BMP4 and RA demonstrate that the ECMP composition also significantly affects the efficacy of these molecules in promoting differentiation (Fig. 4-6 g). Specifically, BMP4 or RA paired with specific ECMP combinations resulted in higher amounts of hESC differentiation. In the future, such knowledge will be useful for designing more efficient directed differentiation protocols.

#### **4.4.5 Long-term Culture of hESCs in Completely Defined Conditions**

To determine the ECMP conditions appropriate for further testing of their ability to maintain long-term hESC culture, the mean  $\mu_{\text{PRO}}$  and  $\mu_{\text{PLU}}$  values from all independent array experiments were calculated. Based on these values, the combination of collagen I, collagen IV, fibronectin, and laminin (I+IV+F+L) was chosen because it promoted the highest proliferation (mean  $\mu_{\text{PRO}}=1.41 \pm 0.25$ ) and maintenance of pluripotency (mean  $\mu_{\text{PLU}}=1.57 \pm 0.19$ ). When hESCs were cultured in a larger tissue culture format over 14 days (3 passages), removal of any one of the four ECMP components decreased the total cell number and also the expression of markers of maintenance of pluripotency (Fig. 4-7a). Removal of collagen I and laminin also significantly decreased the expression of pluripotency markers. These findings suggest that the combination of collagen I, collagen IV, fibronectin, and laminin promotes hESC proliferation and maintenance of pluripotency. Additionally, data from these experiments in conventional culture systems were consistent with data obtained from the cell array experiments (Fig. 4-7b-d).

We next tested whether the combination of collagen I, collagen IV, fibronectin, and laminin (I+IV+Fn+Ln) could sustain long-term self-renewal of hESCs without loss of pluripotency markers, genomic integrity, and differentiation potential. Hues1, Hues9, and H9 were cultured on I+IV+Fn+Ln in the presence of MEF-CM supplemented with bFGF for 15, 10, and 10 passages, respectively. Because MEF-CM contains undefined components, Hues 9 and H9 were also cultured for 10 passages on I+IV+Fn+Ln in the presence of a defined medium, StemPro (a commercially available medium containing bFGF, IGF1, Heregulin and ActivinA, Invitrogen) [28]. In all conditions, hESCs were found to grow in compact colonies with no morphological differentiation (Fig. 4-8a-d). Under these culture conditions, hESCs exhibited a growth rate slightly higher (passaging every 5-6 days at 1:6) than conventional cultures grown on feeder cells or on Matrigel with MEF-CM (passaging every 6-7 days at 1:6). Maintenance of pluripotency was assessed by immunostaining (Fig. 4-8e-h) and quantitative RT-PCR for stem cell markers Oct4 and Nanog (Fig. 4-8i-j). HESCs grown on I+IV+Fn+Ln maintained expression of these pluripotency markers equivalent to that of hESCs grown on Matrigel. Karyotypic analysis revealed that cells grown on I+IV+Fn+Ln maintained genetic stability (Fig. 4-8k-l).

Finally, to determine their differentiation potential, hESCs grown on I+IV+Fn+Ln were differentiated via embryoid body (EB) formation. After 3 weeks, EBs were analyzed for expressions markers of pluripotency as well as ectoderm, endoderm, mesoderm, and trophoectoderm differentiation (Fig. 4-9a). The results showed that hESCs grown on I+IV+Fn+Ln retained the ability to differentiate into the three germ layers (Fig. 4-9b-c). Together, these results confirmed the ability of I+IV+Fn+Ln to support long-term culture of hESCs in defined media conditions.

## 4.5 DISCUSSION

### 4.5.1 Defined Matrix for the Long-term Proliferation of hESCs

In the current study, we established a novel microarray technology and leveraged conventional DNA microarray statistical analysis tools to systematically identify a defined substrate for long-term culture of hESCs. It is well established that proliferation and maintenance of pluripotency of hESCs is in large part dependent on signaling through soluble biomolecules [20-22, 24, 26, 34, 127]. As a result, most studies have focused on creating defined media [28, 29, 128] rather than on defining the composition of the ECMPs. However, since signaling molecule responses are affected by interactions between the cell and its matrix, it is equally important to develop defined matrices that support cell growth. Given the complex makeup of Matrigel and diversity of the ECMPs secreted by mouse or human feeders, a defined matrix supportive of hESCs would most likely be composed of several ECMPs. Furthermore, recent studies have shown that hESCs express integrin receptors for collagens, laminin, and fibronectin and that mouse and human feeder layers secrete several ECMPs, including collagen I, collagen IV, fibronectin, and laminin [33]. These findings suggest that interactions between hESCs and the ECMPs regulate stem cell behavior. Thus, we systematically screened in a concentration-varying and combinatorial manner six common ECMPs (collagen I, collagen III, collagen IV, collagen V, laminin, and fibronectin) that may potentially influence hESC self renewal. From our initial screens, we identified several substrates that were able to support short-term hESC proliferation and maintenance of pluripotency. Of all the possible ECMP combinations, including all previously tested and published ECMP combinations, we identified one substrate, composed of human collagen I, collagen IV, fibronectin, and laminin that performed significantly better. We then demonstrated that this novel substrate was able to sustain the long-term culture of three

independently derived stem cell lines (Hues1, Hues9, and H9), while maintaining their morphology, expression of pluripotent stem cell markers, genetic stability, and differentiation potential. Furthermore, we verified that this substrate was compatible with MEF-CM or other defined media such as StemPro (Invitrogen). We also demonstrated the necessity of each component of this substrate, as removal of any one of these components had negative effects on hESC culture.

#### **4.5.2 High-throughput Platform for Screening Signaling Molecules to Direct hESC Fate**

Given the paucity of studies investigating the effect of the matrix proteins on hESC fate, the studies conducted here largely focused on ECMPs. However, we also demonstrated the feasibility of future-array based screens with signaling molecules. Many developmental GFs and morphogens (such as Wnts, FGFs and Hedgehogs) interact with the cell surface and/or ECM, thereby restricting their signaling range and modulating their activities [129-131]. Additionally, current studies in hESCs focus on one signaling molecule at a time and largely ignore the role of ECMPs in regulating GF signaling response. Therefore, we incorporated a number of GFs (bFGF, BMP-4) and small molecules (retinoic acid) directly into the spotted microenvironments. We confirmed the biological activity of these spotted factors: bFGF by its ability to maintain hESCs in a highly proliferative and pluripotent state, and BMP-4 and retinoic acid by their ability to induce hESC differentiation. Incorporation and immobilization of GFs and small molecules into spotted microenvironments have the additional benefit of increasing the throughput of the screening technology.

#### **4.5.3 Investigations with Arrayed Based High-throughput Approaches**



Several studies have used array-based systems to screen factors that may influence cell fate [62, 63, 122, 123, 125, 132]. However, our technology is the only array-based platform that has been used to screen microenvironments composed of ECMPs and signaling molecules on hESC fate. Flaim et al. used an array technology to investigate the effect of ECMPs on hepatocytes and mouse ES cells [62, 63]. However, that technology relied on the addition of signaling molecules to the surrounding media, thereby limiting the throughput and the complexity of the microenvironments that could be screened. Meanwhile, Soen et al. (2006) used a cellular microarray to examine the regulation of human neural precursors and found that Wnt and Notch co-stimulation maintained the cells in an undifferentiated state [64]. Our platform distinguishes itself in three major ways: (1) We routinely print multiple ECMPs to create a more complex microenvironment. In the referenced publication only one ECMP is used at a time. (2) In previous studies, proteins are covalently attached directly to aldehyde-derivatized slides. In contrast, we spot proteins on a hydrogel, which serves to immobilize the proteins non-covalently and prevents their diffusion. Previous experiments in which we attempted to covalently cross-link Wnt3a produced an inactive protein (K.W. data not shown); as a result we believe that non-covalent immobilization is critical to maintain maximal biological activity. (3) Our spotted microenvironments are significantly smaller, thus allowing a larger number of conditions to be screened per slide. Finally, Anderson et al. (2004) utilized arrayed artificial biomaterials to study polymer-cell interaction [65]. While this platform was able to characterize many conditions that facilitate stem cell interactions with these synthetic polymers, these synthetic microenvironments do not contain signaling molecules that are instructive in cell fate choice.

Although array-based studies generate large data sets, the potential use of this data may be limited by several methodological issues, which we have addressed in this

study. These include i) reproducibility of data between independent array screens, ii) statistical analysis of the generated data to achieve outcome assessment, and iii) validation of data in traditional tissue culture formats. Reproducibility is an essential characteristic of any array-based platform [133]. Our independent array experiments generally had Pearson correlation coefficients  $>0.80$ . For comparison, the reported correlation coefficients between technical replicates of high-end oligonucleotide arrays such as Affymetrix or Agilent are  $\approx 0.90$  [134]. The slightly lower correlation coefficients in our array system are explained by the inherent variability of living cells as well as subtle deviations in fixation, staining, and imaging of the cellular arrays among independent experiments. Nonetheless, by using statistical analysis of multiple replicates of each condition and of each experiment, we were able to identify highly reproducible conditions for maintaining hESC pluripotency. The usefulness of array-generated data to address a specific question largely depends on the methods used for data analysis. Previously, principal component analysis (PCA) was employed to identify the individual components responsible for the measured change in cellular fate [62, 63]. However, PCA does not sufficiently allow for the identification of specific conditions responsible for the most prominent changes in cellular fate. Here, we have demonstrated that array data from these experiments can be analyzed using the same clustering algorithms that are used to analyze DNA microarray data. By utilizing these clustering algorithms, we have been able to identify several substrates capable of supporting hESC culture. Furthermore, we confirmed that the results obtained from our array system are in agreement with those obtained in traditional culture system.

Recently, traditional high-throughput screening assays (HTS) have been implemented to screen for the discovery of single small molecules that sustain hESC self-renewal [49]. Several compounds were identified as promoting short-term hESC

self-renewal, but none were identified as being able to sustain long-term hESC proliferation and maintenance of pluripotency. The array technology presented here is advantageous to traditional HTS because our system requires 1,000 times less reagent and cell number than typical HTS. This is especially important because of the expense of certain proteins and small molecules and the rarity of certain cell types (e.g. cancer and hematopoietic stem cells). In the current array format we were able to simultaneously screen 320 unique conditions. However, the technology can be adapted to simultaneously screen on the order of 1,000 unique conditions and thus achieving similar screening capacities as typical HTS.

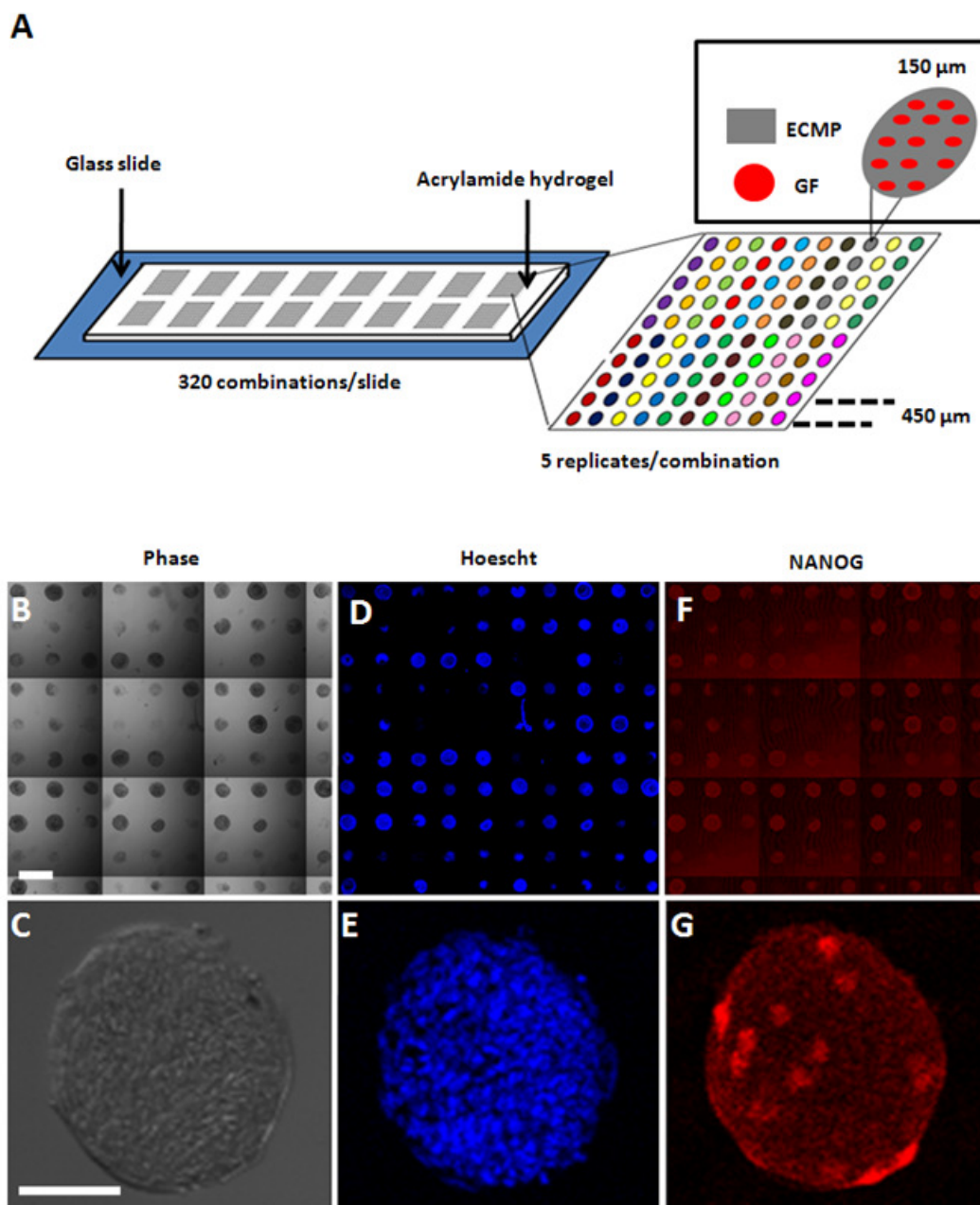
#### **4.6 CONCLUSION**

In summary, with data generated from this array system, we have developed and characterized a completely defined culture system for the long-term self-renewal or defined differentiation of hESCs. We demonstrate that the novel technology platform and analysis procedure described here can be broadly utilized as a cellular screening tool. This system will be useful for future hESC scientific research, including the elucidation of differentiation protocols, as well as the identification of culture conditions of rare and recalcitrant primary cell populations, such as adult stem and progenitor cells and cancer stem cells.

#### **4.7 ACKNOWLEDGEMENTS**

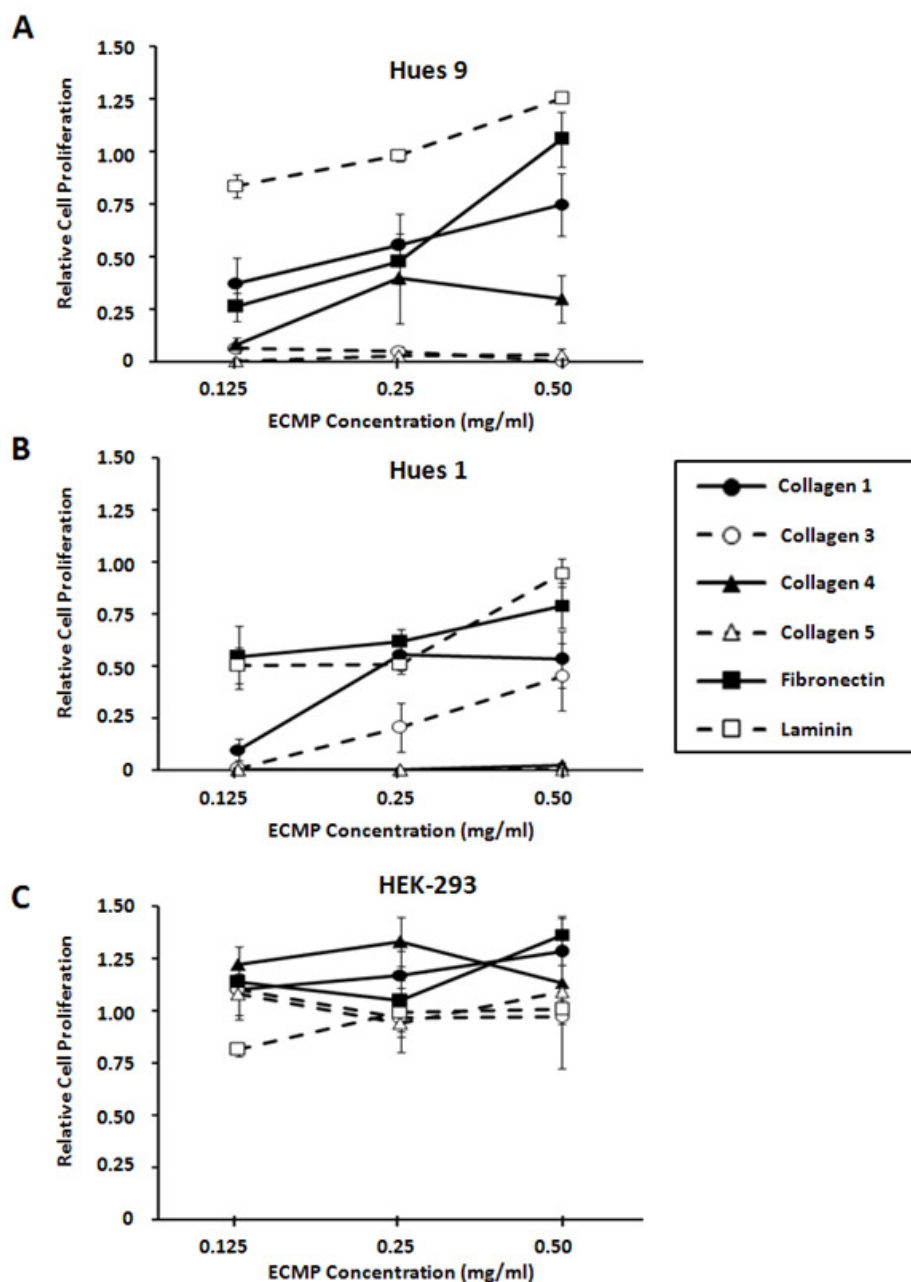
D.A.B. was supported by funding from the University of California Biotechnology Research and Education Program (2007-006). This research was supported in part by the California Institute of Regenerative Medicine (RS1-00172-1) to S.C. and K.W., and NHLBI Research Grant HL080518 to S.C.

The text and figures in Chapter 4 are in part reproductions from: Brafman DA, Shah KD, Fellner T, Chien S, Willert K. Defining long-term maintenance conditions of human embryonic stem cells with arrayed cellular microenvironment technology. *Stem Cell Dev.* 2009. 18(8). The dissertation author was the primary researcher and author pertaining to this work.



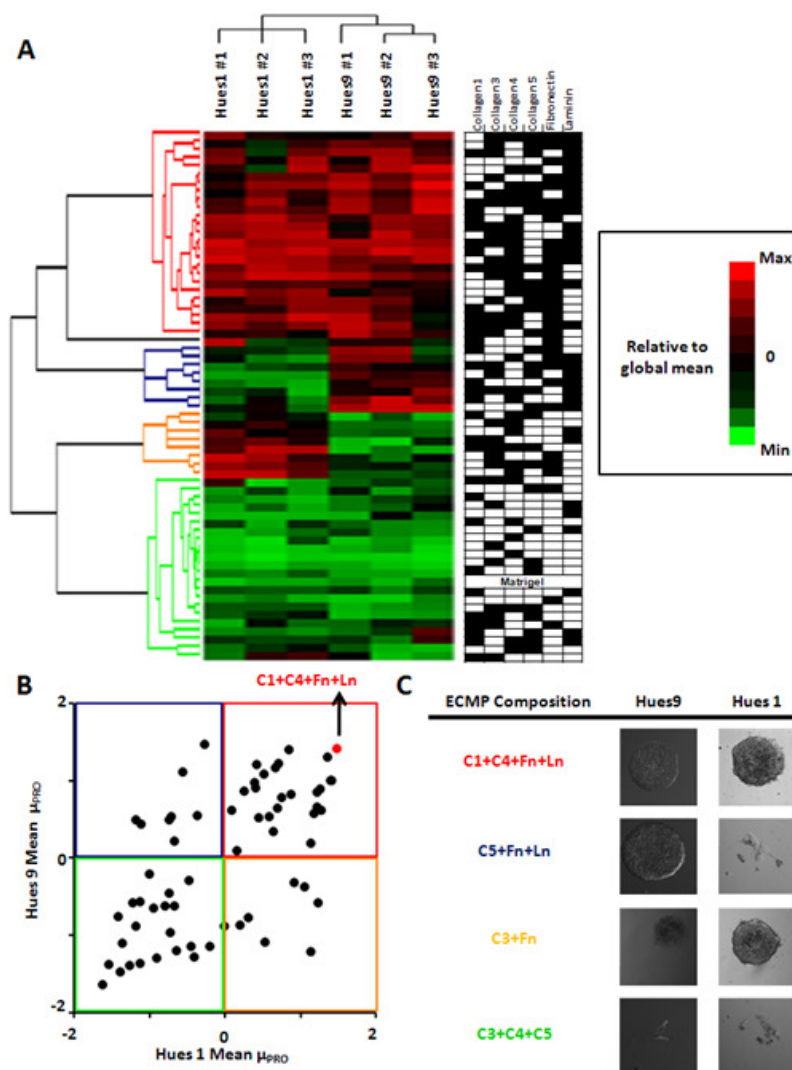
**Figure 4-1: Cellular Microarray Technology Platform.**

(a) Typical layout of arrayed cellular microenvironments. Arrays of pre-mixed combinations of extracellular matrix proteins (ECMPs) and signaling molecules are arranged in 16 subarrays consisting of a 10X10 matrix of spots. Each combination was printed in five replicates. Human embryonic stem cells (hESCs) were cultured on the arrays for 96 hours. Cells were imaged live (b-c) and then fixed and stained for DNA (d-e), NANOG (f-g), and OCT3/4a (not shown). Scale bars=450  $\mu\text{m}$  (b,d,f) and =75  $\mu\text{m}$  (c,e,g).



**Figure 4-2: HESC Proliferation As a Function of ECMP Substrate Concentration.**

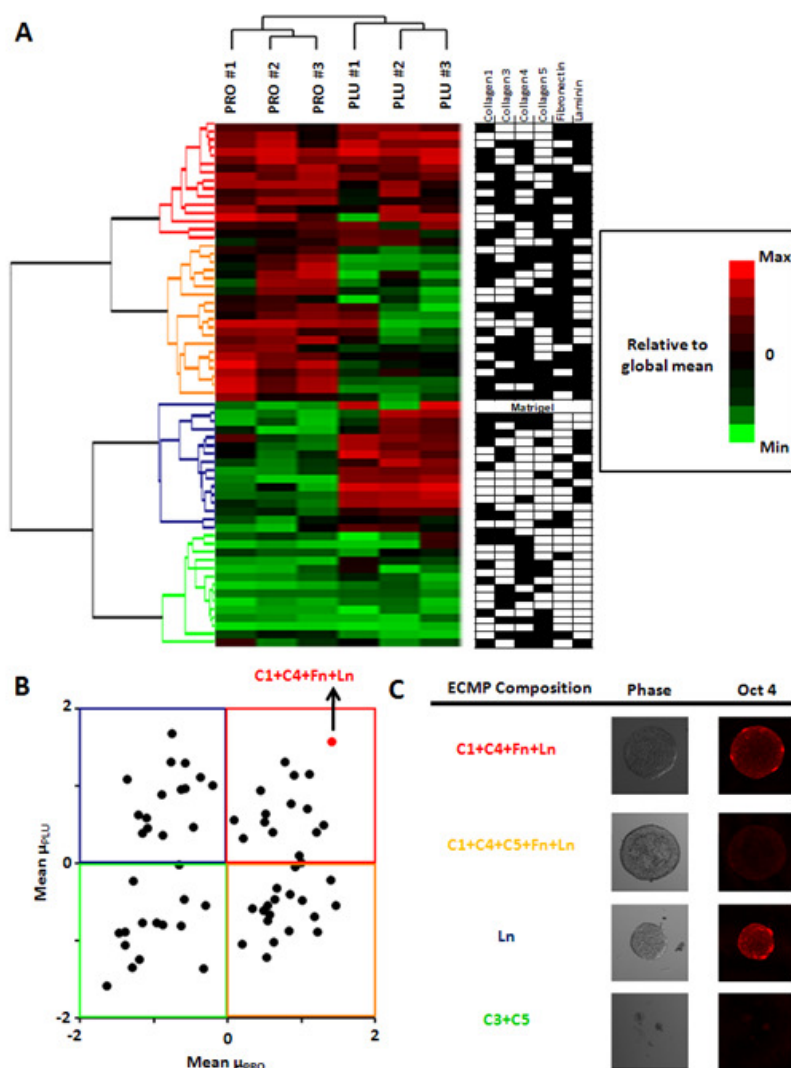
(a) Hues9, (b) Hues1, and (c) HEK-293 cell proliferation after 5 days on Matrigel and various concentrations of collagen I, collagen III, collagen IV, collagen V, fibronectin, and laminin. Cells were stained live for DNA and the signal was quantified to obtain a measurement of proliferation. Cell proliferation levels were normalized to cell proliferation levels on Matrigel (250  $\mu$ g/ml). Data were collected and displayed as mean  $\pm$  standard deviation.



**Figure 4-3: Effect of ECMP Composition on hESC Proliferation.**

(a) Heat map representing the mean proliferation indexes ( $\mu_{PRO}$ ) of each ECMP combination (rows) for each independent array experiment (columns). Columns were scaled to a unit standard deviation. Three independent array experiments were conducted for each hESC type, i.e. Hues9 and Hues1. The ECMPs present in each experimental condition are shown as shaded boxes in the six columns to the right of the heat map. Two-way cluster analysis of each experiment with respect to ECMP condition was performed using Pearson correlation as a similarity metric. Clustering resulted in segregation of the ECMP combinations into four main groups: i) high proliferation in both Hues1 and Hues9 (red cluster), ii) high proliferation in Hues9 only (blue cluster), iii) high proliferation in Hues1 only (orange cluster), iv) low proliferation in both Hues1 and Hues9 (green cluster). (b) Mean Proliferation Indexes ( $\mu_{PRO}$ ) from independent array experiments on the same cell line were averaged and plotted in a proliferation plane whose coordinates were the average Hues1 Proliferation Index and the average Hues9 Proliferation Index. The plane was divided into four regions that corresponded roughly to the four main clusters of the proliferation heat map. (c) Phase contrast images illustrating representative members of each of these clusters.

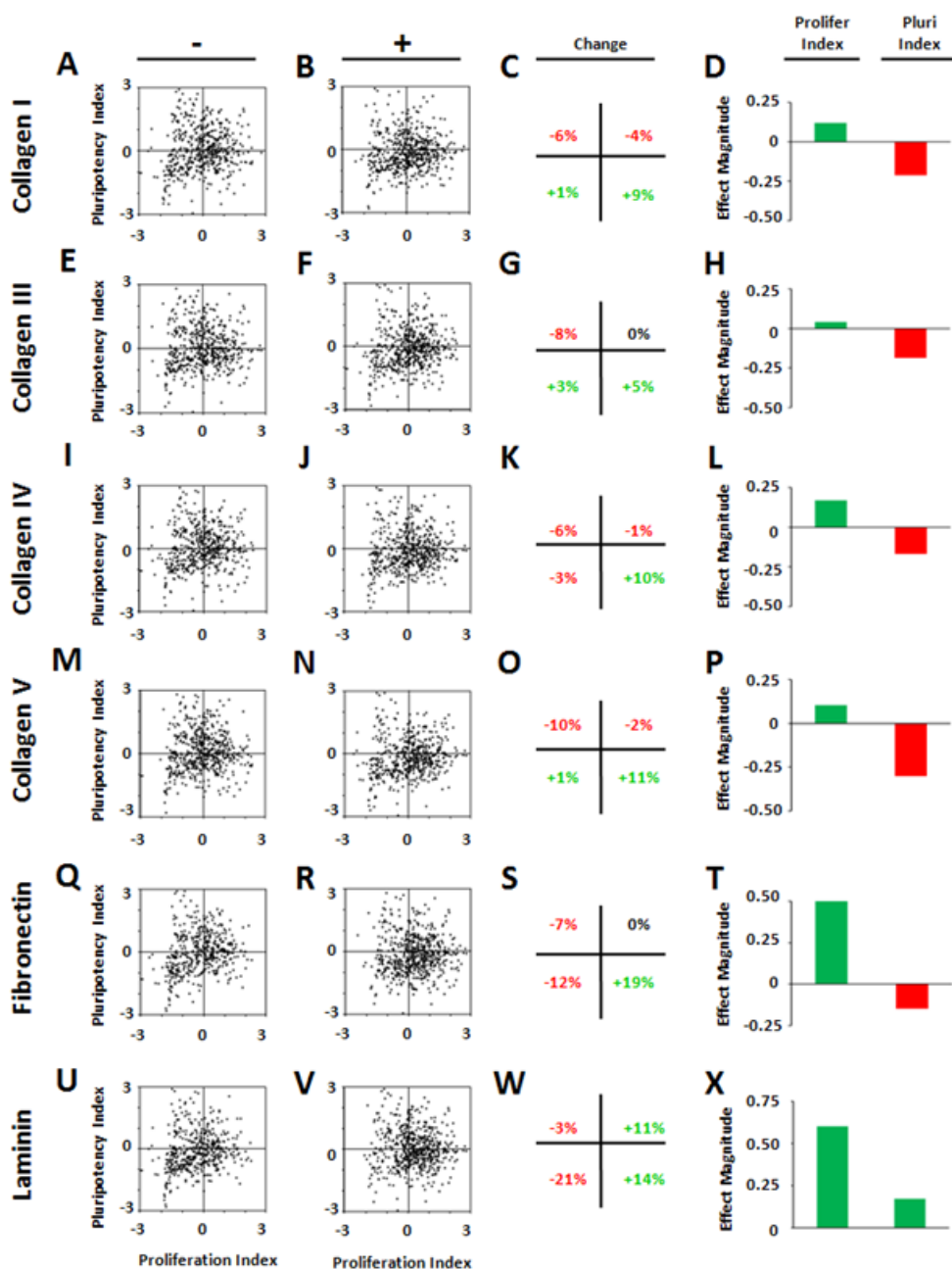




**Figure 4-4: Effect of ECMP Composition on hESC Proliferation and Maintenance of Pluripotency.**

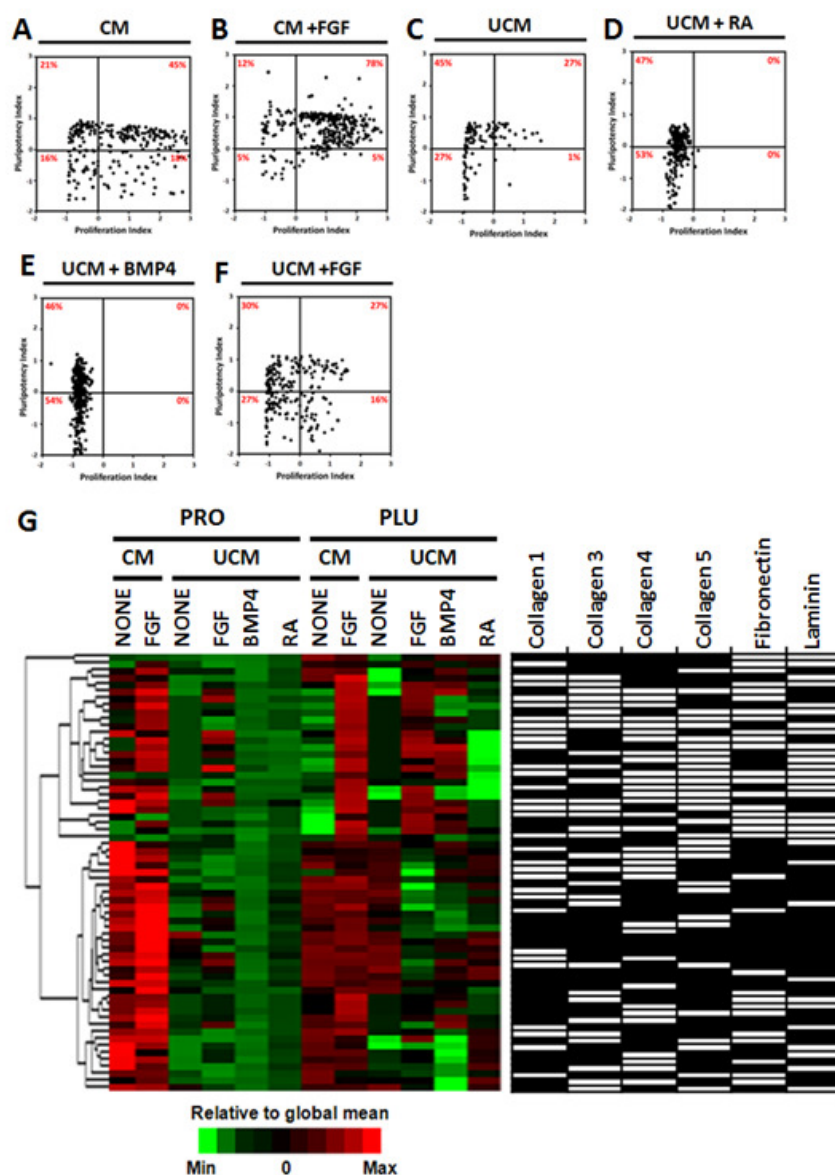
(a) Heat map representing the mean proliferation indexes ( $\mu_{PRO}$ ) and the mean pluripotency indexes ( $\mu_{PLU}$ ) of each ECMP condition (rows) for each independent array experiments (columns). Columns were scaled to a unit standard deviation. The ECMPs present in each experimental condition are shown as shaded boxes in the six columns to the right of the heat map. Two-way cluster analysis of each experiment was performed with respect to ECMP conditions using Pearson correlation as a similarity metric. The ECMP conditions clustered into four groups i) high maintenance of pluripotency and high proliferation (red), ii) high maintenance of pluripotency and low proliferation (blue), iii) low maintenance of pluripotency and high proliferation (orange), iv) low maintenance pluripotency and low proliferation (green). (b) The mean proliferation indexes ( $\mu_{PRO}$ ) and the mean pluripotency indexes ( $\mu_{PLU}$ ) for each ECMP condition were averaged across all independent array experiments and plotted in a proliferation versus pluripotency space defined by these values. The ECMP conditions were grouped into four regions that corresponded to the four clusters of the heat map. (c) Phase contrast images and corresponding immunocytochemical analysis for Oct4 illustrating representative members of each of these clusters. Phase contrast images illustrating representative members of each of these clusters.





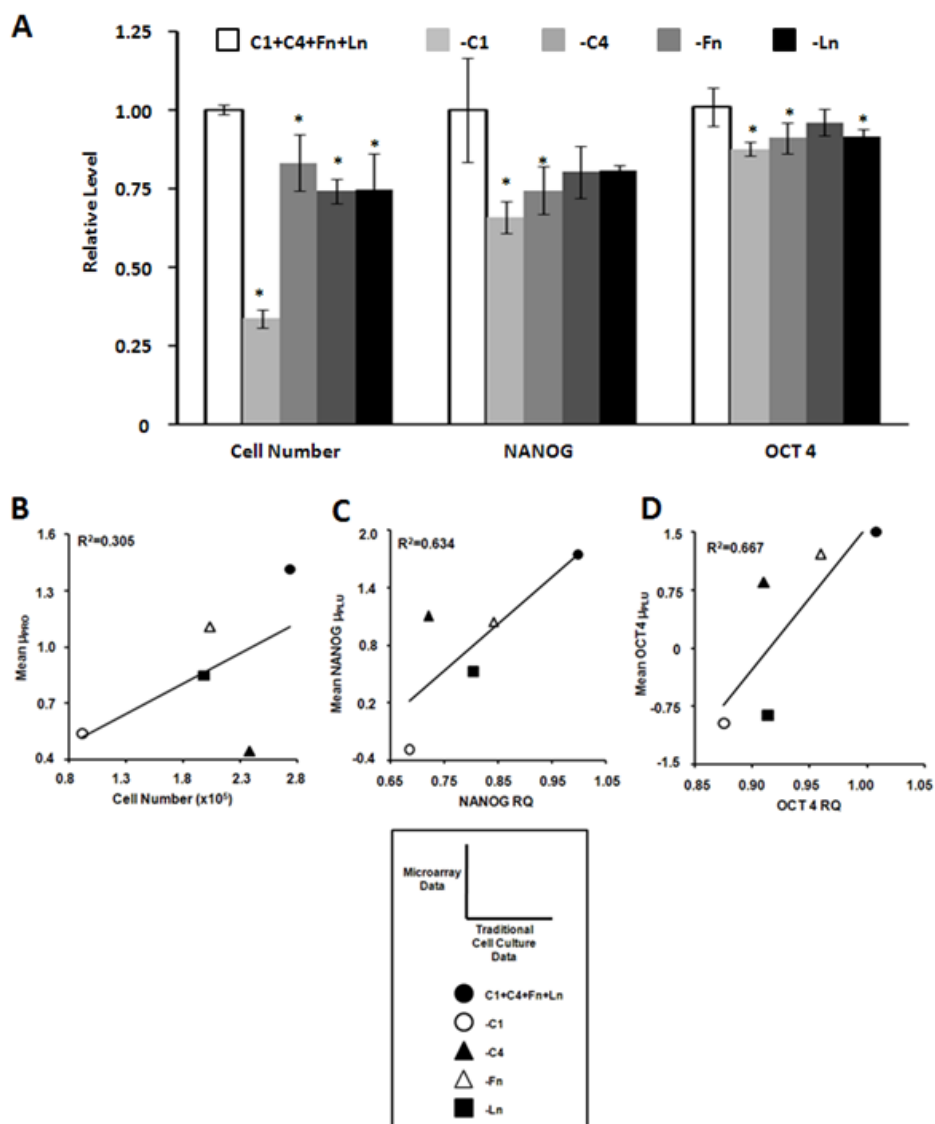
**Figure 4-5: Principle Component Analysis of ECMP Effects on Proliferation and Maintenance of Pluripotency of hESC.**

Proliferation versus pluripotency plots of all ECMP combinations (a, e, i, m, u) without and (b, f, j, n, r, v) with specified component. (c, g, k, o, s, w) The change in the number of ECMP spots in each quadrant of the proliferation versus pluripotency space when the specified component is added was calculated. (d, h, l, p, t, x) The effect magnitude of each component on hESC proliferation and maintenance of pluripotency was calculated.



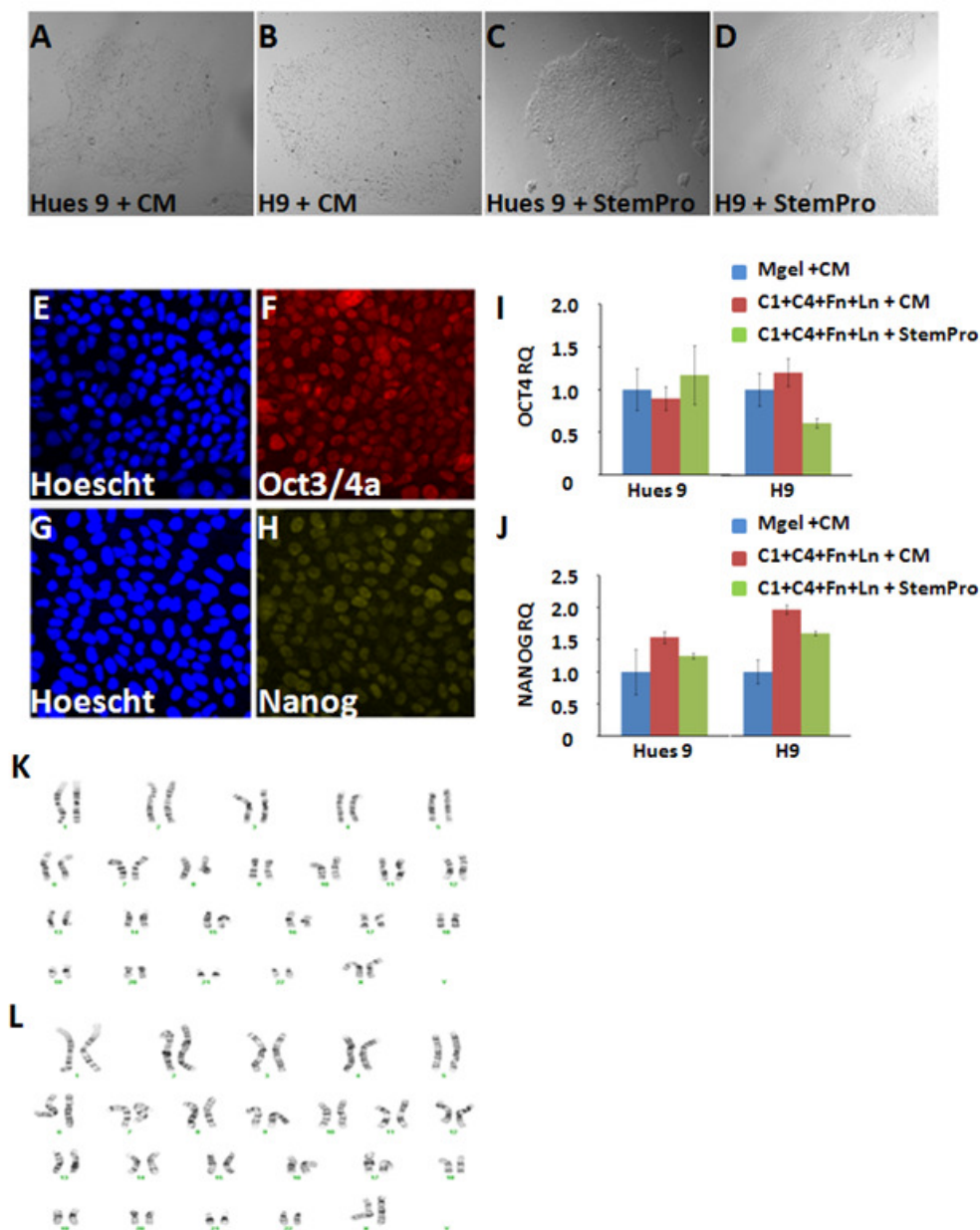
**Figure 4-6: Spotted Signaling Molecules Modulate hESC Fate.**

Various ECMP combinations were spotted along with signaling molecules FGF, BMP-4, and retinoic acid (RA). HESCs were seeded onto the arrays in the presence (CM) or absence (UCM) of conditioned media. Proliferation and maintenance of pluripotency were assessed after 5 days of growth. Proliferation versus pluripotency plots of all ECMP combinations with (b) conditioned media with no spotted signaling molecule (CM), (c) conditioned media with spotted FGF (CM + FGF), (d) unconditioned media with no spotted signaling molecule (UCM), (e) unconditioned media with spotted FGF (UCM + FGF), (f) unconditioned media with spotted BMP-4 (UCM + BMP4), and unconditioned media with spotted RA (UCM + RA). The percentage of ECMP combinations in each quadrant of the proliferation versus pluripotency space are listed in red. (g) Heat map representing results of hESCs grown on arrays consisting of signaling molecules and ECMP combinations.



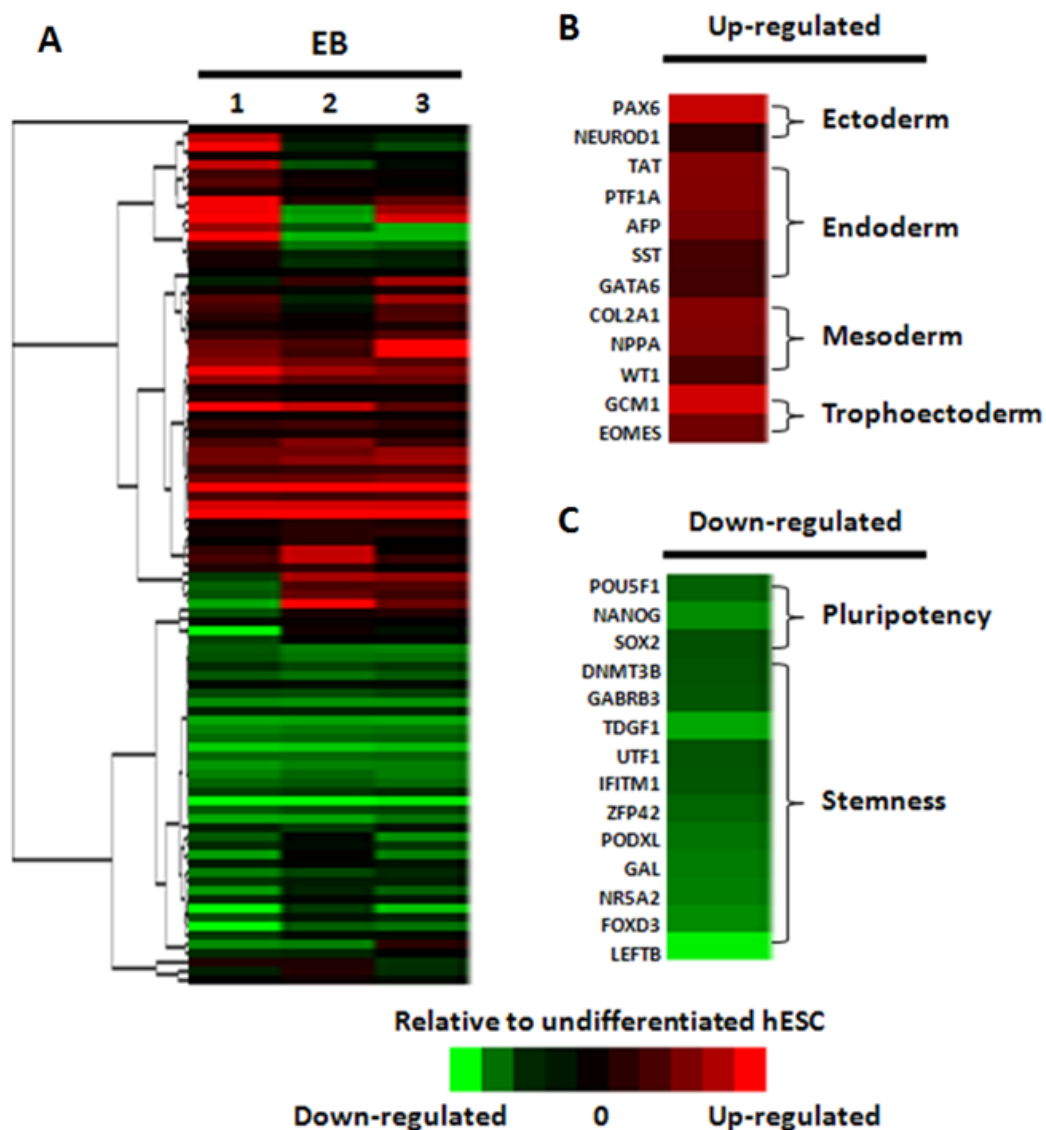
**Figure 4-7: Identification of Optimal ECMP Condition for Long-term Culture of hESCs.**

From microarray experiments, the combination of collagen I, collagen IV, fibronectin, and laminin (I+IV+F+L) was identified as an ECMP condition that would promote hESC proliferation and maintenance of pluripotency. Hues9 were grown in triplicate wells of a 6 well-plate coated with I+IV+F+L and also minus each of the components: collagen I (-C1), collagen IV (-C4), fibronectin (-Fn), and laminin (-Ln). (a) After 14 days of growth (3 passages), cells were counted and analyzed by quantitative RT-PCR for expression of hESC markers OCT4 and NANOG. Data were normalized to I+IV+F+L and reported as mean  $\pm$  standard deviation. \*: significantly different (two-tailed t-test,  $p < 0.05$ ) from C1+C4+Fn+Ln. Array data (y-axis) and data from traditional cell culture (x-axis) were compared for hESCs grown on I+IV+F+L (blue) and also minus each of the components: collagen I (-C1; red), collagen IV (-C4; green), fibronectin (-Fn; purple), and laminin (-Ln; blue). (b) cell count vs. mean  $\mu_{PRC}$  (c) relative quantity of NANOG expression vs. mean NANOG  $\mu_{PLU}$  (d) relative quantity of OCT4 expression vs. mean OCT  $\mu_{PLU}$ .



**Figure 4-8: An Optimized ECMP Composition (C1+C4+Fn+Ln) Supports Long-term Culture of hESCs in Defined Conditions.**

(a,c) Hues9 and (b,d) H9 cultured on I+IV+Fn+Ln in MEF-CM (a,b) and StemPro for 10 passages (c,d). (e-h) Immunostaining for stem cell markers and DNA of H9 cultured on C1+C4+Fn+Ln in StemPro for 10 passages. Quantitative RT-PCR for expression levels of (i) Oct4 and (j) Nanog of Hues9 and H9 grown on Matrigel in MEF-CM, I+IV+Fn+Ln in MEF-CM, and C1+C4+Fn+Ln in StemPro. Expression levels were normalized to hESCs grown on Matrigel in MEF-CM and displayed as mean  $\pm$  standard deviation. (k-l) Karyogram of H9 cultured for 7 passages on C1+C4+Fn+Ln in StemPro showing a normal diploid 46,xx karyotype.



**Figure 4-8: Differentiation Potential of hESC Grown on Defined Matrix.**

(a) Heat map displaying qRT-PCR analysis of pluripotency and differentiation markers of H9 grown on C1+C4+Fn+Ln in StemPro for 10 passages after differentiation via embryoid body (EB) formation. Data displayed as  $\log_{10}$  of the relative quantity. Data show (b) increase in expression of markers of ectoderm, endoderm, mesoderm, and trophoectoderm (red) and (c) decrease in expression of markers of pluripotency and stemness (green) of differentiated hESCs relative to undifferentiated hESCs.

## CHAPTER 5

# SYNTHETIC POLYMERS SUPPORT LONG-TERM HUMAN EMBRYONIC SELF-RENEWAL

### 5.1 ABSTRACT

Advances in research on human embryonic stem cells (hESCs) will have major impacts on the quality of life of millions of people with health problems such as cancer, cardiovascular disease, and neurodegenerative disorders (e.g. Alzheimer's and Parkinson's diseases). With their ability to develop into virtually all adult cell types, hESCs represent the "raw material" for many cell-based therapies. To realize the full potential of hESCs in regenerative medicine requires the design of materials that can be used for (1) establishment of well-defined culture conditions for hESC growth and differentiation, (2) cost-effective protocols for hESC expansion, and (3) the derivation of new pluripotent stem cell lines under completely defined conditions. Here, we have developed a technology platform, for the real-time simultaneous screening of thousands of synthetic biomaterials on cell attachment, proliferation, differentiation and gene expressions. We have utilized this technology to develop and characterize a completely defined synthetic culture system for the long-term self-renewal of hESCs. In the future, this technology will facilitate research on the directed differentiation of hESC into specific mature cell types, such as neurons, cardiomyocytes, pancreatic islets, and other cells, that can be applied in the treatment of a variety of debilitating human diseases.



## 5.2 INTRODUCTION

Human embryonic stem cells (hESCs) can differentiate into virtually all mature cell types, which may be useful in the treatment of various incurable diseases. However, many challenges remain before such therapies can become a reality: (a) lack of well-defined conditions for derivation and expansion of clinical grade hESCs, (b) insufficient systematic control over conditions that regulate hESC behavior, and (c) inability for large-scale production of hESCs in defined conditions needed for human therapy and drug screening. The derivation and proliferation of hESCs depend on their microenvironment, including the chemical composition and physical characteristics of the extracellular matrix (ECM) and the presence of growth factors (GFs). We and others have identified unique factors and signaling pathways that regulate hESC self-renewal in order to develop fully defined, animal free culture systems for the long-term self-renewal of hESCs [20-24, 28-30]. However, these culture systems rely on recombinant or purified human proteins are expensive, difficult to isolate, subject to batch-to batch variation and, thus, not suitable for large scale expansion of hESCs.

Biomaterials could provide an inexpensive, easily produced, and reliable alternative for *in vitro* hESC expansion. Polymeric biomaterials have been utilized as substrates for the growth of variety of different cell types [135]. Specifically, biomaterials have been used for the expansion of many human adult stem cell and progenitor populations such as hematopoietic [136-139], mesenchymal [37-41], and neural stem cells [42]. However, biomaterial based expansion of hESCs has not been successful [43, 44] because there is no established set of principles or properties that can assist in prediction of which polymers would support hESC expansion.

Typically, the engineering of new bioactive materials has involved a candidate-based approach in which individual polymers are fabricated, tested, and redesigned.

Recently, high throughput approaches have been developed to screen libraries of polymeric biomaterials on cell fate [65, 140-146]. Here, we describe the development of an array based high-throughput method for investigating the effects of thousands of polymeric biomaterials on hESC fate. Using this technology, polymers with varying chemical compositions and functional properties (e.g. molecular weight, charge, hydrophobicity, and wettability) were screened for their ability to promote hESC proliferation and pluripotency. From these screens we identified several polymers with defined physicochemical properties that could be utilized for the long-term expansion and maintenance of large numbers of hESCs.

## **5.3 MATERIALS AND METHODS**

### **5.3.1 Polymer Array Fabrication**

Glass slides were coated with acrylamide as previously described in [91]. Briefly, glass slides were cleaned, silanized, and then functionalized with a polyacrylamide gel pad. . Polymers (Sigma and Polysciences) were dissolved in the appropriate solvent (DMSO, DMF, or toluene) at five different concentrations (15  $\mu\text{M}$ , 7.5  $\mu\text{M}$ , 3.75  $\mu\text{M}$ , 1.875  $\mu\text{M}$ , and 0.9375  $\mu\text{M}$ ) and placed in polypropylene 384-well plates.

A contact array (SpotArray 24; Perkin Elmer) was used to print polymers. The printing conditions were a 1000ms inking time and a 250 ms stamping time. To control for variability, each polymer was printed in replicates of 5 spots. Each spot had a diameter of 150-200  $\mu\text{m}$  and neighboring microenvironments were separated by a center-to-center distance of 450  $\mu\text{m}$ . A single slide carried 6,400 spots arranged in 16 20x20 matrices so that one slide carried 1280 unique biomaterial conditions. Slides were inspected manually under a light microscope consistent and uniform polymer deposition.



Prior to their use, slides were soaked in PBS while being exposed to UVC germicidal radiation in a sterile flow hood for 10 min.

### 5.3.2 Cell Culture

The following media were used: H1299 (1X high glucose DMEM, 10% fetal bovine serum, 1% (v/v) L-glutamine penicillin/streptomycin); H9/WA09 hESCs (1X DMEM-F12, 20% (v/v) Knockout Serum Replacement, 1% (v/v) non-essential amino acids, 0.5% (v/v) glutamine, 120  $\mu$ M 2-mercaptoethanol [Sigma]); Hues 9 hESCs (1X Knockout DMEM, 10% (v/v) Knockout Serum Replacement, 10% (v/v) human plasmanate (Talecris Biotherapeutics), 1% (v/v) non-essential amino acids, 1% (v/v) penicillin/streptomycin, 1% (v/v) Gluta-MAX, 55  $\mu$ M 2-mercaptoethanol [Sigma]). All media components are from Invitrogen unless indicated otherwise. Hues9 hESC lines were maintained on feeder layers of mitotically inactivated mouse embryonic fibroblasts ( $2 \times 10^4/\text{cm}^2$ ; Chemicon). All hESC cultures were supplemented with 30 ng/ml bFGF (Invitrogen). MEF-CM was produced by culturing the appropriate hESC medium on MEFs for 24 hr. StemPro consisted of the StemPro supplement (Invitrogen) diluted in DMEM-F12 with 2% (v/v) BSA (Millipore) and 55  $\mu$ M 2-mercaptoethanol. Hues9 were routinely passaged as single cells by exposure to acutase (Millipore) for 5 min, followed by one rinse with media and centrifugation at 200 x g. Cells were then resuspended and plated.

H1299 were passaged ( $5.0 \times 10^5$  cells per slide) directly onto the array slides and allowed to settle on the spots for 18 hr prior to rinsing with HEK-293 medium 3 times to remove residual cells and debris. Prior to seeding onto the arrays, hESCs were cultured for two passages on Matrigel (BD Sciences) with MEF-CM supplemented with 30 ng/ml bFGF to remove residual feeder cells. HESCs were then acutase-passaged onto the

array slides ( $1.5 \times 10^6$  cells per slide) and allowed to settle on the spots for 18 hr prior to rinsing with the medium one time to remove unattached cells and debris. Cell media was replenished daily. Due to the non-fouling nature of the acrylamide, cells were confined to the printed microenvironment spots.

### 5.3.3 Slide Staining, Imaging and Quantification

Because fixing and staining protocols may cause cell detachment and alter the cell counts on each spot, arrays were stained live for DNA with Hoescht 33342 (2  $\mu\text{g}/\text{ml}$ ; Invitrogen) for 5 min. The arrays were washed 3 times with the medium and then imaged. After live imaging, the arrays were fixed in 4% PFA for 5 min at 4°C, followed by 10 min at room temperature. Live imaging of slides was performed using an automated confocal microscope (Olympus Fluoview 1000 with motorized stage and incubation chamber). Slides were imaged as 3 x 3 arrays at 10x magnification using a focus height that gave the maximum signal in the Z-direction for each channel at the center of the array. Images were then quantified using GenePix software (MDS Analytical Technologies).

Polymer hydrogel slides and polymer acrylamide coated slides were fixed in 4% PFA for 5 min at 4°C, followed by 10 min at room temperature. Immediately before staining, the cells were permeabilized with 0.2% (v/v) Triton-X-100 and blocked with 1% (w/v) BSA and 3% (w/v) milk for 30 min. The slides were stained with the primary antibodies rabbit anti-Oct3/4a or rabbit anti-Nanog (Santa Cruz) diluted 1:200 in 1% BSA overnight at 4°C, washed 3 times with TBS, and incubated with goat anti-rabbit Alexa 647 at 1:400 for 1 hr at 37°C. Nucleic acids were stained for DNA with Hoescht 33342 (2  $\mu\text{g}/\text{ml}$ ; Invitrogen) for 5 min at room temperature. The slides were then washed 3 times with TBS and air dried immediately before imaging.

### 5.3.4 Oct4-GFP Reporter Line

The lenti construct that was used to generate the Oct4-GFP reporter line was kindly provided by Dr. Alexey Terskikh. High titer lenti was produced as previously described [147, 148]. Hues9 were infected overnight with lenti Oct4-GFP and single clones were isolated and screened for (i) stable GFP expression levels, (ii) low GFP expression levels after EB formation and (iii) rapid decrease in GFP expression upon removal of MEF-CM.

### 5.3.5 Polymer Hydrogel Fabrication

Glass slides (75mm x 25mm x 1mm) were washed with 100% acetone, 100% methanol, and ten times in Millipore water (MQH<sub>2</sub>O) to remove residual debris and oils. The slides were etched overnight in 0.05 N NaOH, rinsed five times with MQH<sub>2</sub>O, and dried with filtered compressed air and in vacuum oven (65°C, 20 psi) for 1 hr. The slides were then silanized in a 2% solution of 3-(trimethoxysilyl)propyl methacrylate in anhydrous toluene overnight, rinsed in toluene, dried with compressed air, and baked for 1 hr in a vacuum oven (65°C, 20 psi).

A stock solution of 20% (w/v) acrylic acid or acrylamido-methyl-propane sulfonate, 1% (w/v) bis-acrylamide, 10% (w/v) photoinitiator I2959 (200 µg/ml in 100% methanol; Igacure 2959, Ciba Specialty Chemicals) was prepared. Subsequently, 100 µl of this stock solution was placed on a silanized slide and covered with a 75mm x 25 mm coverslip (Bellco Glass). The slide was then exposed to 1.5 mW/cm<sup>2</sup> 365-nm ultraviolet light for 7 min and immersed in MQH<sub>2</sub>O for 10 min. The coverslip was then removed, leaving a thin (~75 µm) polymer hydrogel pad. The polymer hydrogel slides were soaked

in MQH<sub>2</sub>O for 48 hr to remove residual unpolymerized monomer and photoinitiator, and then dehydrated on a hot plate (40°C) for 10 min.

### 5.3.6 Polymer Coated Slide Fabrication

Acrylamide coated glass slides were coated with 15 µM poly(methyl vinyl ether-alt-maleic anhydride) or poly(styrene-alt-maleic acid). Slides were then dried on a hot plate (60°C) until solvent evaporation. This was repeated 5 times until a thin layer of polymer had formed on top of the acrylamide coated glass slide.

### 5.3.7 Polymer Coated Slide Fabrication

RNA was isolated from cells using TRIzol (Invitrogen), and treated with DNase I (Invitrogen) to remove traces of DNA. Reverse transcription was performing by means of qScript cDNA Supermix (Quanta Biosciences). Quantitative PCR was carried out using TaqMan probes (Applied Biosystems) and TaqMan Fast Universal PCR Master Mix (Applied Biosystems) on a 7900HT Real Time PCR machine (Applied Biosystems). Taqman gene expression assay primers (Applied Biosystems) were used. Markers of pluripotency assayed were *OCT4*, *NANOG*, and *SOX2*. Gene expression was normalized to 18S rRNA levels. The  $2^{-\Delta\Delta Ct}$  was used to determine normalized gene expression levels relative to Hues9 grown on Matrigel. All reactions were performed in triplicate.

### 5.3.8 Data Analysis

All values were presented as mean  $\pm$  standard deviation. Minitab statistical software was used for all statistical analysis.  $p < 0.05$  was considered statistically significant.

## **5.4 RESULTS**

### **5.4.1 Polymer Microarrays to Study Cell Fate**

We used a contact DNA microarray spotting instrument to deposit nano-liter amounts of polymer onto acrylamide coated glass microscope slides. Several printing parameters such as inking and printing time were optimized in order to create a uniform distribution of the polymer spots within the array. Polymers were dissolved in the appropriate solvent (DMSO, DMF, or toluene) and deposited onto the acrylamide coated slides. The polymers interpenetrated with the acrylamide coating and became fixed in place after solvent evaporation (Figure 5-1e-f). Furthermore, the acrylamide coating inhibited cell growth in the spaces between different polymers. A single slide carried 6,400 spots arranged in 16 20x200 matrices (Figure 5-1c). Each polymer spot was 150-200  $\mu\text{m}$  in diameter and each polymer mixture was spotted in replicates of five so that one slide carried 1280 unique conditions. Polymer spots showed consistent size between replicate spots and non-replicate spots (Figure 5-1e-f).

As proof of principle, we tested this polymer array on an immortalized cell line (H1299, non-small cell lung carcinoma cells). Unlike hESCs, this cell line is capable of robust growth on tissue cultured treated plastic. Cells were seeded onto to polymer arrays and analyzed 48 hours later for adhesion and growth. In general, cells attached and spread on the majority of the polymers. Additionally, the polymers supported H1299 proliferation in a concentration-dependent manner with the highest amount of proliferation typically occurring at the highest concentration of the polymer tested. However, there were incidences where high polymer concentrations exhibited cytotoxic effects. Figure 5-3 displays a subset of the polymers that supported H1299 growth.

### **5.4.2 Polymer Microarray Screens with HESCs**

Prior to seeding onto the arrayed cellular microenvironments, hESCs were cultured in feeder-free conditions [17] and assessed for their characteristic morphology (Figure 5-1a), maintenance of markers of pluripotency (Figure 5-1b-c), and normal karyotype (data not shown). Bioactive polymers typically mediate cellular adhesion through two mechanisms: (1) Electrostatic interactions with the polymer surface lead to cellular immobilization [145]. (2) Physiosorption of extracellular matrix proteins (from the surrounding media) by the polymer promotes interactions with membrane bound integrin which leads to cell adhesion[149]. Recent studies have shown that that mouse and human feeder layers condition media contains several soluble ECMPs, including collagen I, collagen IV, fibronectin, and laminin [33]. In order to eliminate undefined absorption of these soluble ECMPs we performed all of our screens in the presence of a defined medium, StemPro (a commercially available medium containing bFGF, IGF1, Heregulin and ActivinA, Invitrogen). Thus, any observed interactions between polymers and hESCs would be reproducible and independent of soluble ECMP concentrations.

To seed the arrays, hESCs were trypsinized into single cells, and cell suspensions were allowed to settle onto the microenvironments for 18 hrs. Thereafter, medium was replaced to remove non-adhering cells and debris. Seeding the array slides with  $1 \times 10^6$  cells allowed for the attachment of 10-20 cells per spot and provided sufficient area for subsequent growth. After 5 days of growth, various parameters of cell behavior, such as proliferation and pluripotency, were quantified by microscopy and microarray imaging (Figure 5-1 g-h).

In order to have a real-time measure of pluripotency, we generated a hESC line (Hues9) with a GFP gene under an Oct4 promoter (Oct4-GFP). The Oct4-GFP hESCs lose both GFP expression and their compact-colony morphology completely in five days in the absence of conditions that promote maintenance of pluripotency. To validate our

assay for detecting small changes in GFP expression, we seeded arrays with defined mixtures of constitutively expressing GFP hESCs and non-fluorescent hESCs. After 5 days of culture, the arrays were imaged. Qualitatively, the average GFP signal from an array increased in a linear manner as the proportion of GFP cells in the mixture increased (Figure 5-2).

### **5.4.3 Subset of Polymers Support HESC Proliferation and Maintenance of Pluripotency**

Using this array technology, we screened a library of diverse polymers (Table 1). The library contained a diverse set of polymers that varied in their molecular weight, charge, hydrophobicity, wettability, and functionality. Each polymer was screened at five different concentrations (15  $\mu$ M, 7.5  $\mu$ M, 3.75  $\mu$ M, 1.875  $\mu$ M, and 0.9375  $\mu$ M). Spotted Matrigel served as a positive control. The screen was performed three times on independent polymer array slides to ensure reproducibility of results.

The Oct4-GFP values were normalized to total cell number (estimated by Hoechst stain). These values were analyzed and rank ordered for repeated high hits compared to Matrigel. Several polymers supported limited hESC growth, but only four polymers demonstrated the consistent ability to support proliferation and maintenance of pluripotency at similar levels as Matrigel (Figure 5-4 a). All four polymers were hydrophilic and two were maleic anhydride co-polymers. However, these two characteristics were not sufficient by themselves to support hESC proliferation as several hydrophilic and maleic anhydride co-polymers failed to support even limited amounts of hESC growth.

Since polymer molecular weight influences the growth in other contexts [150], poly(methyl vinyl ether-alt-maleic anhydride) (PMVE-alt-MA) and polyacrylic acid (pAA)

were selected for molecular weight based analysis. Hues9 were cultured on arrays of PMVE-alt-MA and PAA at varying molecular weights and concentrations. In general, the polymers supported hESC proliferation in a concentration-dependent manner with the highest amount of proliferation typically occurring at the highest concentration of the polymer tested. However, hESC proliferation was strongly dependent on the molecular weight of the polymer. For example, PAA supported the highest amount of hESC proliferation at a molecular weight of  $4.5 \times 10^5$  and did not support significant levels of hESC proliferation at higher or lower molecular weights (Figure 5-4 b-c). Likewise, PMVE-alt-MA supported the highest amount of hESC proliferation at a molecular weight  $1.08 \times 10^6$  (Figure 5-4 d-e). Increasing or decreasing the molecular weight of pMVE-alt-MA also reduced the amount of hESC growth that was supported. As a whole, these results indicate that polymer molecular weight influences hESC growth.

In order to determine if this response was specific to hESCs, we seeded the arrays with H1299 cells (Figure 5-5 a-b). The polymers were able to support the growth of H1299s, but the levels of proliferation of H1299s, unlike the hESCs, did not show significant changes with concentration or molecular weight variations for PAA or PMVE-alt-MA.

#### **5.4.4 Long-term Culture of HESCS on Defined Polymers**

We next tested whether the hit polymers identified could sustain long-term self-renewal of hESCs without loss of pluripotency markers and genomic integrity. Coating multi-well dishes with solutions of the hit polymers did not result in sufficient amounts of polymer deposition (data not shown). Thus, we tested two types of alternative culture systems: (1) two-dimensional (2D) polymer hydrogels and (2) polymer coated acrylamide slides.



PAA and PAMPS hydrogels were synthesized using a photo-polymerization technique (Figure 5-6a). HUES9 were cultured on these polymer hydrogels using typical trypsin passage. On both hydrogels, hESCs were found to grow in compact colonies with no morphological differentiation (Figure 5-6b-c). Additionally, hESCs displayed a high amount of Oct4 expression, indicating their maintenance of pluripotency (Figure 5-6b-c). However, on these hydrogels hESCs exhibited a growth rate significantly lower than conventional cultures grown on feeder cells or on Matrigel with MEF-CM. Furthermore, high variability among the fabricated hydrogels resulted in inconsistent, uneven hESC adhesion. Thus significant expansion of hESCs on these hydrogels beyond 5 passages was not achieved.

Acrylamide coated glass slides were coated with solutions of PMVE-alt-MA ( $M_w=1.25 \times 10^6$ ) and PS-alt-MA ( $M_w=3.50 \times 10^5$ ) (see Materials and Methods). Non-coated glass slides were unable to retain significant amounts of the polymers (data not shown). Only PMVE-alt-MA coated slides produced significant hESC adhesion. Furthermore, PMVE-alt-MA coated slides were able to support consistent hESC expansion beyond 5 passages. Under these culture conditions, hESCs exhibited their characteristic morphology (Figure 5-7a) and a growth rate similar to conventional cultures grown on feeder cells or on Matrigel with MEF-CM. Maintenance of pluripotency was assessed by immunostaining (Figure 5-7a) and quantitative RT-PCR for stem cell markers Oct4, Nanog, Sox2 and (Figure 5-7b). hESCs grown on PMVE-alt-MA maintained expression of these pluripotency markers equivalent to that of hESCs grown on Matrigel. Karyotypic analysis revealed that cells grown on PMVE-alt-MA maintained genetic stability (Figure 5-7c). Together, these results confirmed the ability of PMVE-alt-MA to support long-term culture of hESCs in defined media conditions.

## **5.5 DISCUSSION**

### **5.5.1 Biomaterial Based Expansion of hESCs**

Developing defined conditions for the long-term propagation and expansion of hESCs has been a major challenge in hESC research. hESCs can be co-cultured with mouse or human feeders that secrete a combination of many uncharacterized factors which are essential for the maintenance of the pluripotent state [16]. Feeder-free culture conditions have been utilized [17] but these methods generally involve the use of extracellular matrices, such as Matrigel™ (BD), to provide a suitable cell adhesion substrate and media that have been conditioned on mouse or human feeder layers to provide the necessary soluble factors to maintain pluripotency [18]. For cell-based therapies, hESCs need to be cultured in defined and reproducible conditions that are devoid of animal-derived components.

It is well established that signals from the microenvironment, such as physical structure and chemical composition of the underlying extracellular matrix, influence numerous structural and signaling changes within a cell [107-109]. However, much of the research carried out on hESCs has focused on soluble signals and their effects on hESC fate [28, 29, 128]. As a result, several groups have reported the successful use of combinations of soluble factors to replace the need for conditioned media [20-24, 28-30]. Since signaling molecule responses are affected by interactions between the cell and its matrix, we [91] and others [151-154] have investigated the effect of the underlying extracellular matrix on influencing hESC fate. Subsequently, various ECMP combinations have been used for the propagation of hESCs [31-34]. However, these culture systems utilize purified and recombinant proteins which are expensive, thus making large scale expansion of hESCs using these systems cost-prohibitive.

Biologically active polymers are inexpensive and have been used for culture and expansion of several adult and progenitor cell populations [44]. We therefore reasoned that biologically active polymer might provide be an alternative for long-term hESC proliferation and expansion. However, little research has been performed on using synthetic biomaterials for hESC culture. Most studies have focused on the promotion of differentiation mainly using mouse or non-primate ESCs [15, 44, 155, 156]. Additionally, all of these studies employed a candidate based approach in which a limited diversity of polymers was investigated. Thus, we systematically screened in a concentration-varying a library of bioactive that may potentially influence hESC self renewal. From our initial screens, we identified several polymers that were able to support short-term hESC proliferation and maintenance of pluripotency. We identified one polymer, PMVE-alt-MA, that was able to sustain the long-term culture of hESCs while maintaining their morphology, expression of pluripotent stem cell markers and genetic stability. Furthermore, we verified that this substrate was compatible with MEF-CM or other defined media such as StemPro (Invitrogen). To our knowledge, this is the first time in which a completely synthetic matrix has been used for the long-term culture of hESCs.

### **5.5.2 PMVE-alt-MA Promotes HESC Proliferation in the Absence of Exogenous ECMPs**

Cellular adhesion can occur through two mechanisms: (1) binding of soluble factors and extracellular matrix proteins and non-specific interactions with the physical and chemical features of the underlying substrate [157]. Both of these interactions have been exploited to for the *in vitro* culture of numerous cell types. Most commonly, extracellular matrix proteins such as collagen, fibronectin, and laminin can be used to facilitate cell adhesion through integrin binding. On the other hand, surfaces coated with

bioactive polymers such as poly L-lysine can mediate cellular adhesion in the absence of integrin binding through electrostatic interactions. Nonetheless, adhesion and growth of hESCs on surfaces devoid these initial cell-matrix interactions has not been previously achieved [155]. Here, we report a polymer substrate, PMVE-alt-MA, that is able to support hESC proliferation independent of exogenously added ECMPs. However, during hESC growth on these polymers extensive remodeling of the substrate by the cells occurs. So, although we have demonstrated that this polymer fosters initial hESC adhesion independent of cell matrix interactions, we cannot rule out additional contributions from adsorption of proteins secreted from the growing hESCs. Further investigation of the mechanism by which this polymer promotes hESC proliferation will aide in the future development of biomaterials that can be used for culture other recalcitrant cell populations.

### **5.5.3 Polymer Microarrays to Modulate HESC Fate**

Despite continual advances in hESC research, the *in vitro* culture conditions that promote specific differentiation have either not been developed. Extensive research has demonstrated that characteristics of the microenvironment such as chemical functionality and hydrophobicity play critical roles in regulating cell fate [156, 158-160]. For example, the adhesion of cultured human endothelial progenitor cells varies based on surface charge. Likewise, mesenchymal stem cell differentiation can be directly influenced by controlling substrate wettability. However, precise control over the microenvironment is difficult to achieve with complex ECMPs and other signaling molecules which cannot be easily modified. Thus an important goal of hESC research is to design synthetic materials repeatable control over the microenvironment to influences cell fate. The diversity of biomaterials and lack of systems for the screening of large polymer libraries

have made it difficult to apply a synthetic materials approach to hESC research. Here, we describe the development of an array based high-throughput technology for investigating and characterizing thousands of hESC-biomaterial interactions. This technology provides a robust method for systematically identifying materials that alter the local microenvironment, thereby providing more control over proliferation and directed differentiation of hESCs.

In summary, with data generated from this array system, we have developed and characterized a completely defined culture system for the long-term self-renewal or defined differentiation of hESCs. We demonstrate that the novel technology platform and analysis procedure described here can be broadly utilized as a cellular screening tool. This system will be useful for future hESC scientific research, including the elucidation of differentiation protocols, as well as the identification of culture conditions of rare and recalcitrant primary cell populations, such as adult stem and progenitor cells and cancer stem cells.

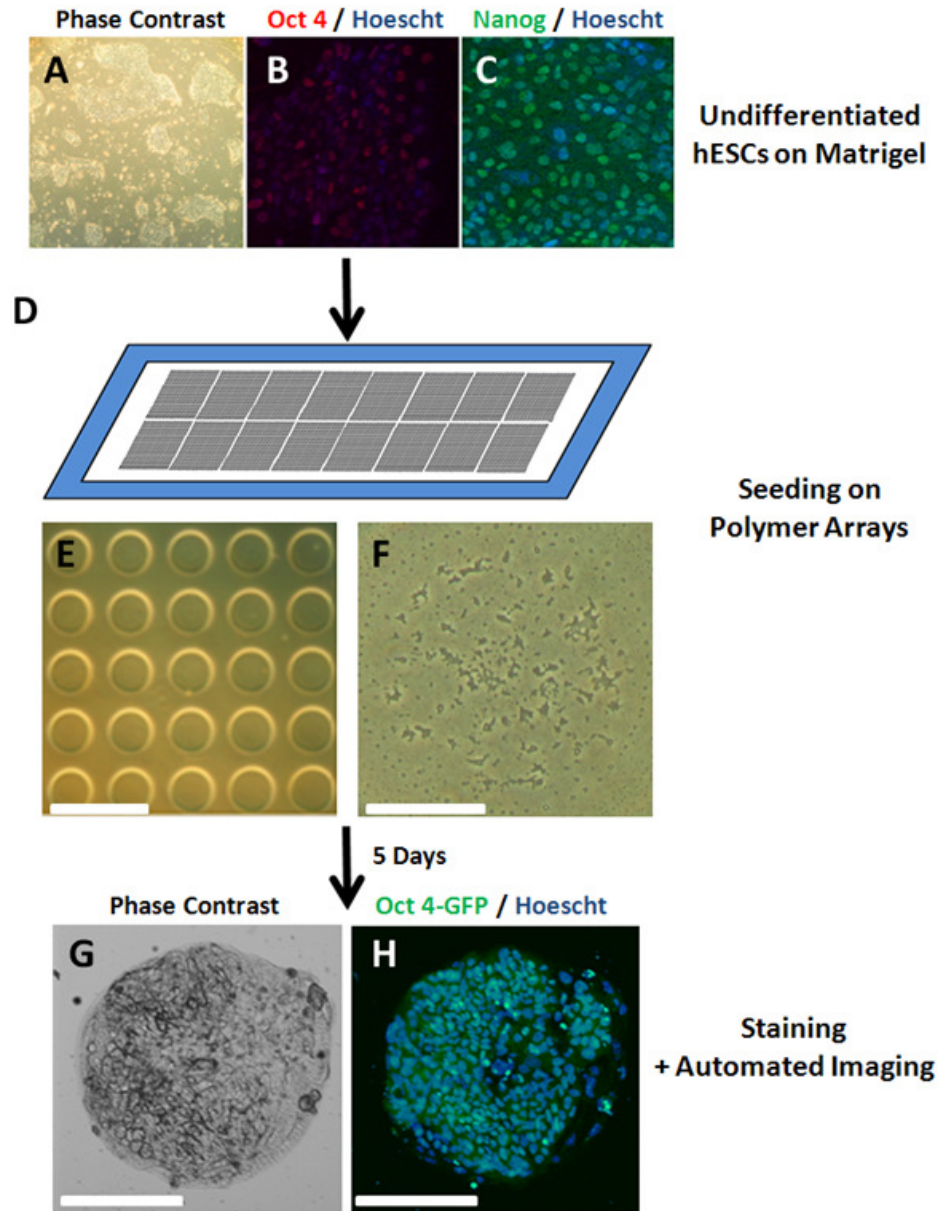
## **5.6 CONCLUSION**

In summary, using a high-throughput systematic approach we have developed and characterized a completely defined synthetic culture system for the long-term self-renewal of hESCs. The novel technology will be of significant value to many lines of scientific inquiry, including: (1) developing protocols for the directed differentiation of hESCs and other pluripotent cells into specific cell types, (2) identifying growth conditions for primary cells (e.g. adult or cancer stem cells), which at present are impossible to expand *ex vivo*, (3) controlling the microenvironment, or niche, of various stem cell populations.

## 5.7 ACKNOWLEDGEMENTS

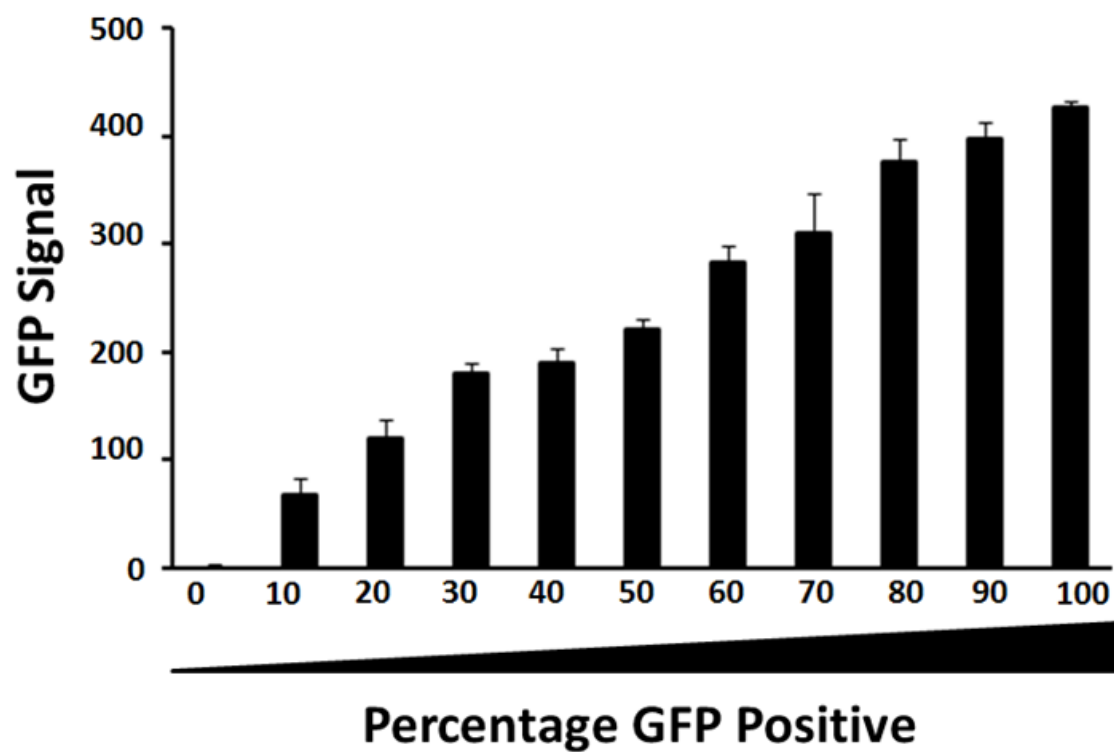
D.A.B. was supported by funding from the University of California Biotechnology Research and Education Program (2007-006). This research was supported in part by the California Institute of Regenerative Medicine (RS1-00172-1) to S.C. and K.W., and NHLBI Research Grant HL080518 to S.C.

The text and figures in Chapter 5 are in part reproductions from: Brafman DA, Chang J, Shah KD, Varghese S, Willert K, Chien S. Synthetic polymers support long term human embryonic stem cell self-renewal. 2009. *In preparation*. The dissertation author was the primary researcher and author pertaining to this work.



**Figure 5-1: Schematic Representation of Polymer Array Assay.**

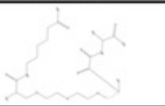
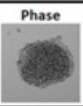
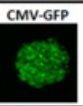
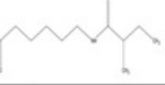
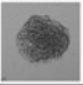
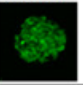

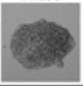
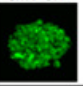
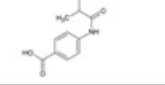
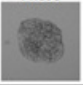
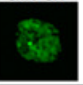
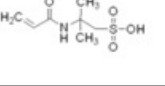
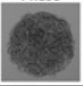
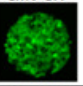
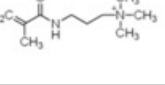
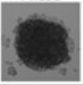
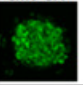
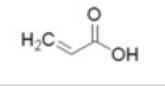
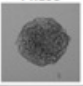
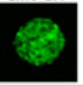
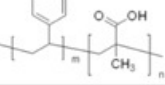
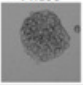
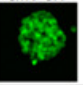
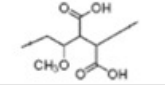
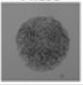
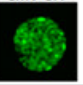
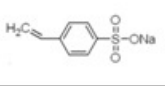
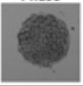
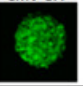
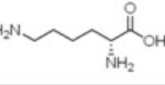
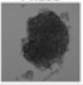
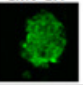
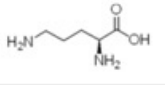
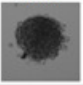
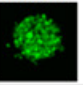
HESCs maintained on Matrigel prior to seeding on the arrays exhibit typical (a) undifferentiated cell morphology and express high levels of pluripotency markers (b) Oct4 and (c) Nanog. (d) HESCs are globally seeded onto polymer arrays consisting spotted polymers arranged in 16 subarrays consisting of a 20X20matrix of spots. (e) Each combination was printed in five replicates (scale bar = 450  $\mu\text{m}$ ). (f) Each polymer spot had a diameter of 150  $\mu\text{m}$  ( scale bare = 75  $\mu\text{m}$ ). HESCs were grown on the polymer arrays for 5 days and imaged in real time by automated microscopy. HESCs were assessed for their (g) characteristic morphology and (h) proliferation (Hoescht) and maintenance of pluripotency (Oct4).



**Figure 5-2: Validation of GFP Detection.**

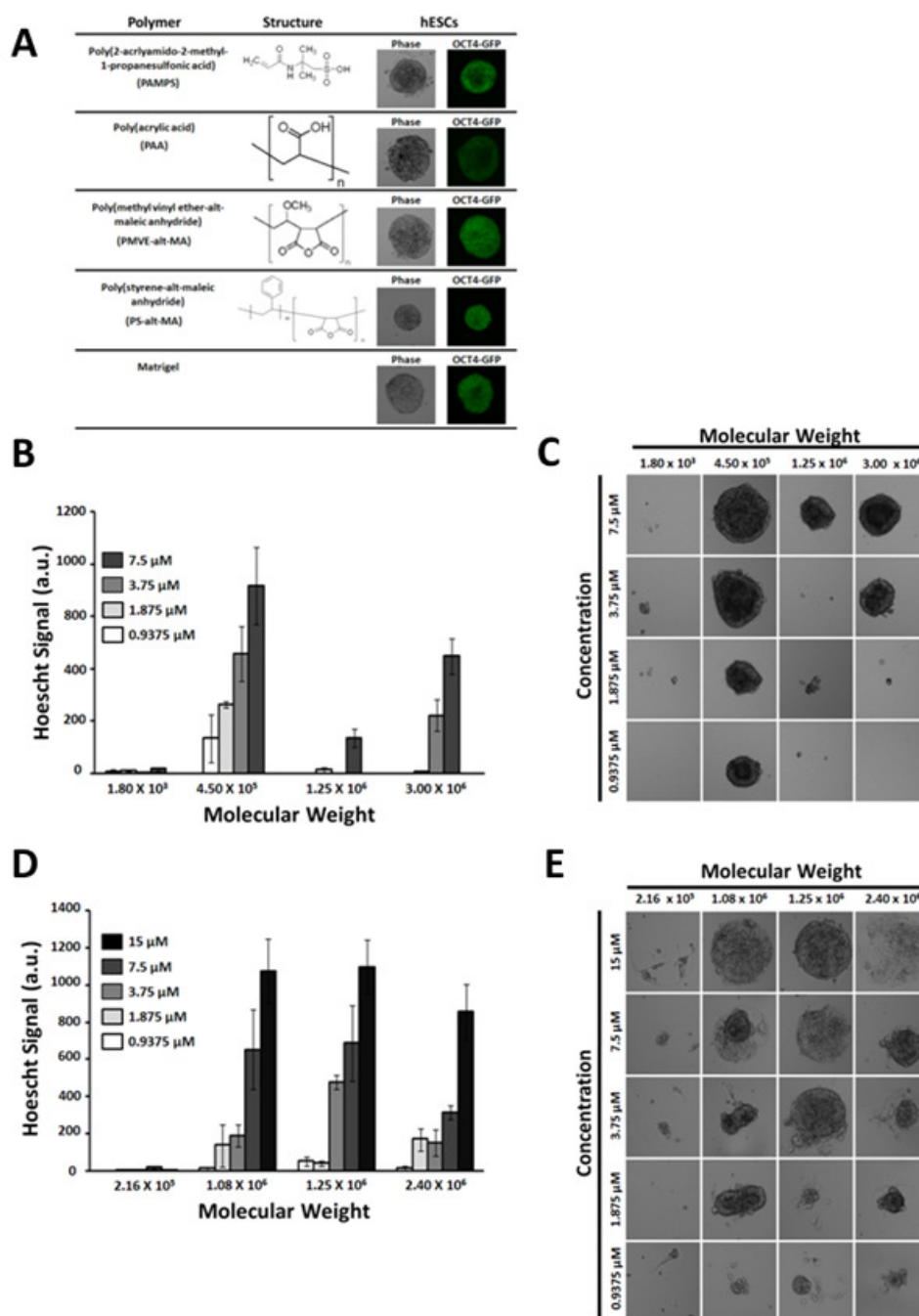
To validate our assay for detecting small changes in GFP expression, polymer arrays were seeded with defined mixtures of constitutively expressing GFP hESCs and non-fluorescent hESCs. After 5 days of culture, the arrays were imaged. The average GFP signal from an array increased in a linear manner as the proportion of GFP cells in the mixture increased.



Polymer	Structure	H1299	
Poly[(2-acrylamido glycolic acid)-co-(ethylene glycol)-co-(caproic acid)] (AGA-co-PEG-co-CA)			
Poly(acryloyl-6-amino caproic acid) (PA6ACA)			
Poly(acryloyl-2-acrylamido glycolic acid) (PA2AGA)			
Poly(acryloyl-4-aminobenzoic acid) (PA4ABA)			
Poly(2-acrylamido-2-methyl-1-propanesulfonic acid) (PAMPS)			
Poly[3-(methacryloylamino)propyl(trimethylammonium)] (PMAAPTMA)			
Poly(acrylic acid) (PAA)			
Poly(styrene-co-methacrylic acid) (PS-co-MA)			
Poly(methyl vinyl ether-alt-maleic anhydride) (PMVE-alt-MA)			
Poly(sodium 4-styrenesulfonate) (PS4SS)			
Poly(D-lysine) (PDL)			
Poly(L-ornithine) (PLO)			

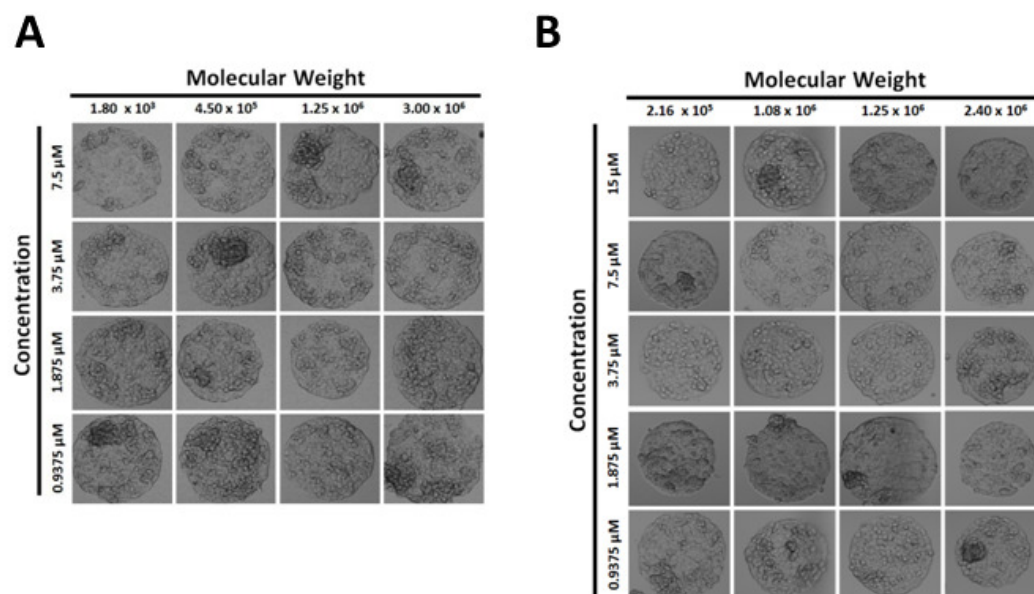
**Figure 5-3: Sample of H1299 “Hits” on Polymer Arrays.**

As proof of principle non-small lung carcinoma cells (H1299) were seeded onto polymer arrays. Several different classes of polymers were able to support H1299 attachment and growth.



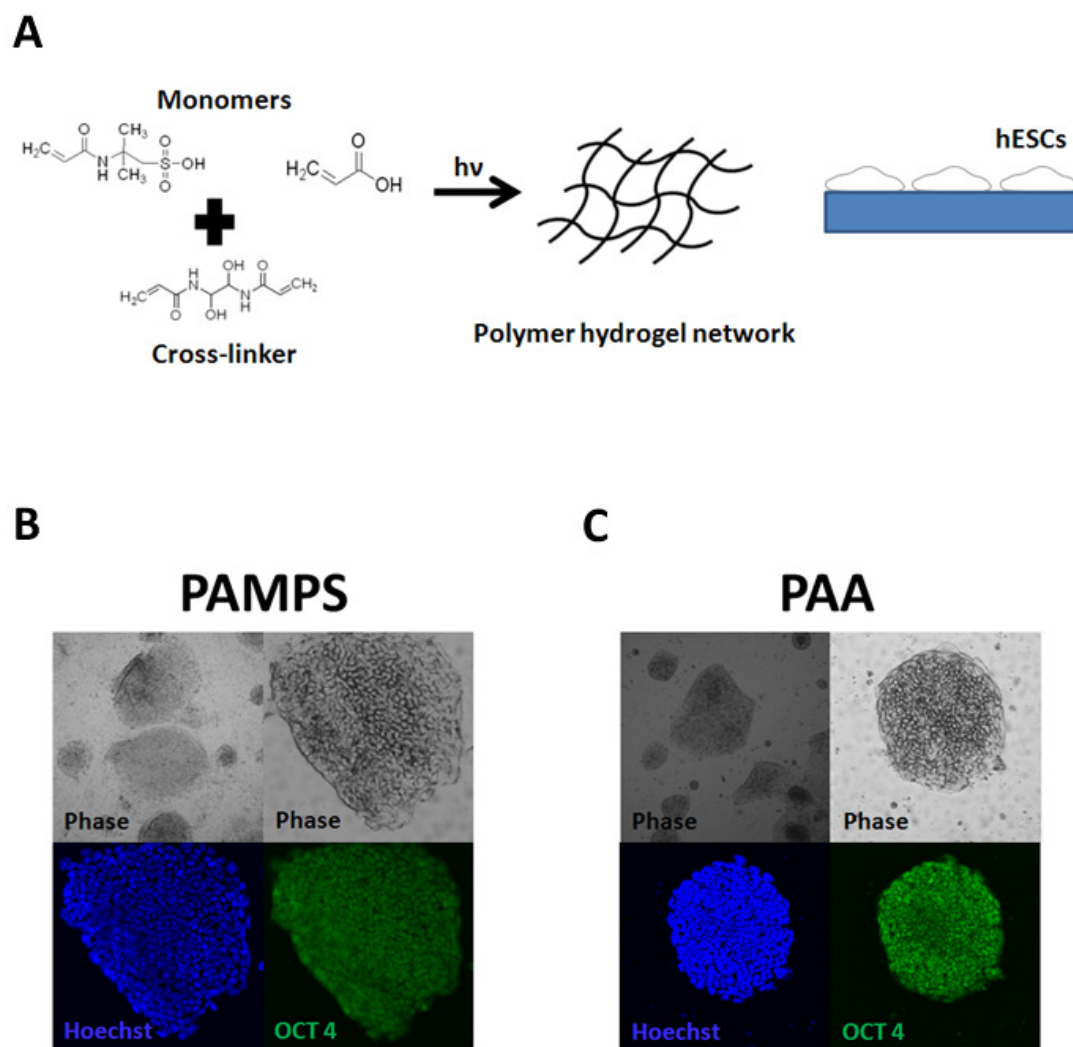
**Figure 5-4: Synthetic Polymers Supporting hESC Proliferation and Maintenance of Pluripotency.**

(a) Four polymer hits were identified that supported levels of hESC proliferation and maintenance of pluripotency similar to those on Matrigel. Two hits, (b,c) poly(acrylic acid) and (d,e) poly(methyl vinyl ether-alt-maleic anhydride), were selected for molecular weight based analysis. Quantification of hESC proliferation reveals the influence of polymer molecular weight.



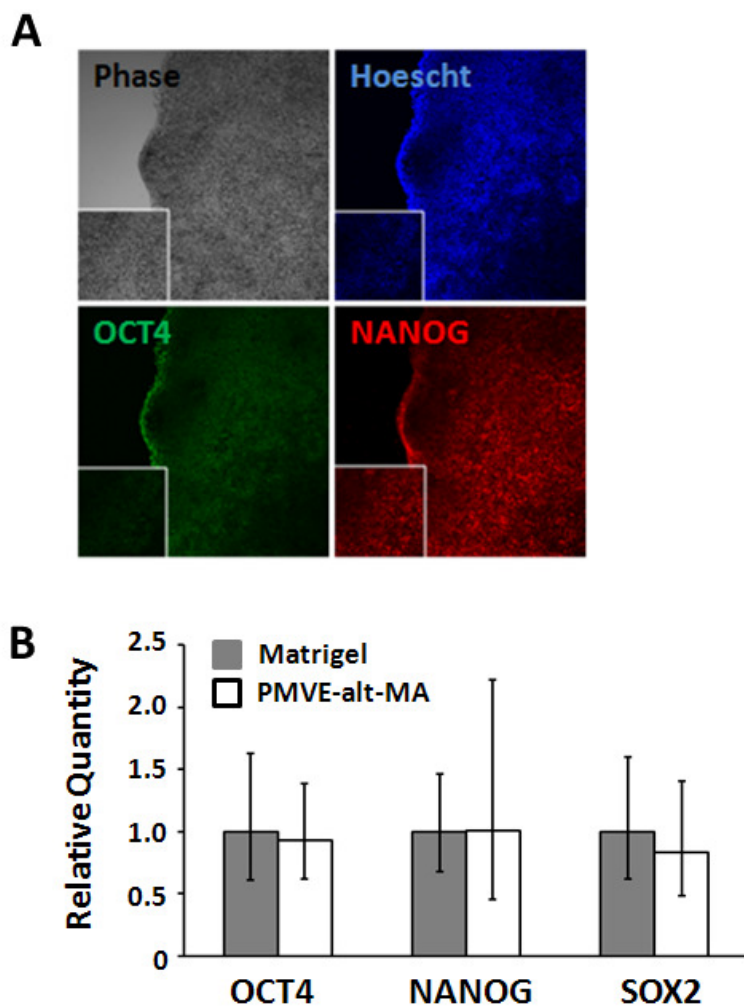
**Figure 5-5: Influence of Molecular Weight on Cell Proliferation Is Specific to HESCs.**

H1299s were seeded onto arrays consisting of varying molecular weights and concentrations of (a) poly(acrylic acid) and (b) poly(methyl vinyl ether-alt-maleic anhydride). Neither polymer molecular weight nor concentration had an effect of H1299 proliferation.



**Figure 5-6: Short Term Propagation of hESCs on Polymer Hydrogels .**

(a) Poly(acrylamido-methyl-propane sulfonate) (PAMPS) and poly(acrylic acid) (PAA) hydrogels were fabricated using a photo-polymerization technique. Phase contrast images and immunostaining for stem cell markers and DNA of HUES 9 cultured on (b) PAMPS and (c) PAA hydrogels for 3 passages.



**Figure 5-7: Long-term Culture of HESCs on Defined Substrates .**

(a) Phase contrast images and immunostaining for stem cell markers and DNA of Hues9 cultured on poly(methyl vinyl ether-alt-maleic anhydride) (PMVE-alt-MA) coated slides passages in StemPro for 5 passages. Quantitative RT-PCR for expression levels of Oct4, Nanog, and Sox2 of Hues9 on Matrigel in MEF-CM and PMVE-alt-MA in StemPro for 5 passages. Expression levels were averaged across 3 biological replicates and were normalized to hESCs grown on Matrigel in MEF-CM.



**Table 5-1: Polymer Microarray Design.**  
Polymers used for microarray synthesis.

1 Poly(ethylene glycol-co-acryloyl glycolic caproic acid)	47 Poly(ter-butyl methacrylate)
2 Poly(acryloyl-6-amino caproic acid)	48 Poly(2-hydroxyethyl methacrylate)
3 Poly(acryloyl-2-acrylamido glycolic acid):	49 Poly(benzyl methacrylate)
4 Poly(2-hydroxyethyl methacrylate)	50 Poly(2-(dimethylamino)ethyl methacrylate)
5 Poly(N-isopropylacrylamide)	51 Poly(4-vinylphenol-co-methyl methacrylate)
6 Poly(trimethylene carbonate)	52 Poly(ethylene-co-glycidyl-methacrylate)
7 Poly(acryloyl- 4-aminobenzoic acid)	53 Poly(cyclohexyl methacrylate)
8 Poly(acrylamido-methyl-propane sulfonate)	54 Poly(tert-butyl acrylate-co-ethyl acrylate-co-methacrylic acid)
9 Poly([3-(Methacryloylamino)propyl]dimethyl(3-sulfopropyl)ammonium hydroxide)	55 Poly(ethylene-co-methyl acrylate-co-glycidyl methacrylate)
10 Poly([3-(Methacryloylamino)propyl]trimethylammonium chloride)	56 Poly(ethylene-co-acrylic acid)
11 Poly(ethylene-co-acrylic acid)	57 Poly(ethylene-co acrylic acid)
12 Poly(acrylic acid)	58 Poly(vinyl alcohol)
13 Poly(L-lactide)	59 Poly(vinylphosphonic acid)
14 Poly(D-lactide)	60 Poly(vinyl sulfate) potassium salt
15 Poly (DL-lactide-co-glycolide) 85:15	61 Poly(4-vinylpyridine hydrochloride)
16 Poly (DL-lactide-co-glycolide) 75:25	62 Poly(4-vinylphenol)
17 Poly (DL-lactide-co-glycolide) 65:35	63 Poly(4-vinylpyridine) crosslinked
18 Poly (DL-lactide-co-caprolactone) 86:14	64 Poly(vinyl -co-ethylene)
19 Poly (DL-lactide-co-caprolactone) 40:60	65 Poly(vinyl butyral-co-vinyl alcohol-co-vinyl acetate)
20 Polycaprolactone	66 Poly(ethylene-co-vinyl acetate-co-carbon monoxide)
21 Poly(3-hydroxybutyric acid-co-3-hydroxyvaleric acid)	67 Poly(allylamine hydrochloride)
22 Poly(3-hydroxybutyric acid)	68 Poly(anetholesulfonic acid)
23 Poly(propylene carbonate)	69 Poly(epoxysuccinic acid)
24 Poly(methyl vinyl ether-alt-maleic anhydride), hydrophillic	70 Poly(1,4-butylene terephthalate)
25 Poly(sodium 4-styrenesulfonate)	71 Poly(styrene-co-4-bromostyrene-co-divinylbenzene)
26 Poly-L-arginine hydrochloride)	72 Poly(1,6-hexanediol/neopentyl glycol-alt-adipic acid)
27 Poly-D-lysine hydrobromide	73 Poly(acrylonitrile)
28 Poly-L-glutamic acid sodium salt	74 Poly(styrene-co-allyl alcohol)
29 Poly-L-ornithine hydrobromide	75 Poly(N,N'-(1,3-phenylene)-isophthalamide)
30 Poly(2-ethyl-2-oxazoline)	76 Poly(trimellitic anhydride chloride-co-4,4'-methylene-dianiline)
31 Poly(oligoethylene glycol methyl ethyl methacrylate)	77 Poly(Bispenol A carbonate)
32 Poly(butyl methacrylate)	78 Poly(azelaic anhydride)
33 Poly(ethyl methacrylate)	79 Poly(trimethylolpronaie di(propylene glycol)-alt-adipic acid/phtyhalic anhydride)
34 Poly(styrene-co-methacrylic acid)	80 Poly(di(ethylene glycol adipate)
35 Poly-L-arginine hydrochloride	81 Poly(allyamine)
36 Poly(ethylene glycol) methacrylate	82 Poly(diallyl dimethyl ammonium)
37 Poly(styrene-alt-maleic acid)	83 Poly(diallyl methamine hydrochloride)
38 Poly(styrene)	84 Poly(1-glycerol monomethacrylate)
39 Poly(ethylene-alt-maleic anhydride)	85 Poly(3-chloro-2-hydroxypropyl-2-methacroyethydimethylammonium chloride)
40 Poly(4-styrenesulfonic acid-co-maleic acid)	86 Poly(butadienne maleic acid)
41 Poly(methyl vinyl ether-alt-maleic acid)	87 Poly(vinyl pyrrolidone)
42 Poly(methyl vinyl ether)	88 Poly(n-vinylpyrrolidone-vinylacetate)
43 Poly(styrene-co-maleic anhydride)	89 Poly(ethylenimine)
44 Poly(isobutylene-co-maleic acid)	90 Chitosan
45 Poly(maleic anhydride-alt-1-octadecene)	91 Poly(1-glycerol monomethacrylate)
46 Poly(styrene-alt-maleic anhydride), partial methyl ester	

## CHAPTER 6

### FUTURE PROSPECTIVES

#### 6.1 ABSTRACT

We have developed a technology platform, called arrayed cellular microenvironments (ACME), which allows for the real-time simultaneous screening of thousands of biological and synthetic physiochemical parameters on cell attachment, proliferation, differentiation and gene expressions. Although still in its infancy, ACME is a powerful and robust technology that can be used for a wide range of applications and cell types. Here we speculate on the future of this cell microarray technology and its potential use to address fundamental questions in biomedical research.

#### 6.2 CREATING “COMPREHENSIVE” MICROENVIRONMENTS

The ability to mimic stem cell niches/microenvironments in a defined manner will aide in the large production of specialized cells needed for applications in regenerative medicine [15]. Currently, ACME is capable of screening several components of these microenvironments such as glycans, ECMPs, and signaling molecules. However, additional factors such as mechanical force and matrix stiffness play a critical role in the microenvironment and determination of cell fate.

*In vivo*, the complex network of signaling and matrix molecules is subject to mechanical forces (such as pressure, fluid shear stress, and stretch), which play important roles in specifying embryonic polarity [161] and tissue development [162]

Recent studies have shown that application of shear stress to mouse embryonic stem cells (mESCs) induces cell proliferation and endothelial cell (EC) lineage differentiation with the expression of marker genes indicative of ECs and enhanced endothelial functions [163-165]. Application of cyclic stretch may induce differentiation toward smooth muscle lineage[165], and compression induces chondrogenesis [166]. These mechanical forces, such as shear stress, can be incorporated into the ACME technology using methodologies already established in our lab (Figure 6-1).

Substrate compliance is known to influence cell fate decisions. For example, human mesenchymal stem cells (MSCs) showed higher rates of growth on stiffer substrates [167]. Recently, Engler *et al.* demonstrated that lineage specific differentiation of MSCs is induced by matrix stiffness that matches the respective tissue—soft matrices are neurogenic, rigid matrices are osteogenic, and intermediate matrices are myogenic [168]. Substrate rigidity can be easily varied on ACME by varying the acrylamide/bis-acrylamide ratio of the acrylamide hydrogels using previously established protocols [169].

### **6.3 “OFF CHIP” ANALYSIS**

Current analysis procedures are limited to “on chip” methodologies such as staining for DNA and protein. However, harvesting of the cell colonies growing on the microenvironment spots and performing “off chip” analysis such as quantitative PCR (qPCR) and fluorescent activated cell sorting could provide detailed information about cell responses to the various microenvironments. Such a procedure for performing “off chip” analysis is presented in Figure 6-2. Entire slides can be scanned to identify colonies by automated image analysis that meet certain thresholds for phenotype or fluorescence of a reporter gene. Single “hit” colonies could be harvested under



microscopic control utilizing a robotic system for automated isolation of cell colonies [170]. After detachment of the cells from the array, the cells are delivered into a multi-well plate for subsequent analysis.

## **6.4 ARRAY BASED RNA INTERFERENCE TO STUDY GENE FUNCTION**

Elucidation of gene function is a critical aspect of advancing biomedical research. Functional genomics typically involve gain- and loss- of function studies in which reveal the molecular mechanisms of a cellular phenotype are difficult to implement at the genome-wide scale in cultured human cells. Thus, most gene-silencing studies are restricted to knockout strains of model organisms such as yeast, flies, and mice.

Recent advances in RNA interference (RNAi) are aiding the field of functional genomics by allowing for loss-of-function studies in mammalian cells without the need for germline inactivation of the gene being studied [171]. RNAi occurs through the effect of the ribonuclease (RNase) enzyme Dicer on double stranded RNA. Dicer cleaves the dsRNA into double-stranded small interfering RNAs (siRNAs) which can act either through the RNA-induced silencing complex (RISC) to degrade complementary mRNA sequences or through the RNA-induced transcriptional silencing (RITS) complex to repress transcription and modify DNA and histone methylation [172].

RNAi screens have been used to study the effect of genetic control elements on stem cell behavior. For example, Zhang *et al.* used a subtractive library approach to identify multiple genes involved in the regulation of expression of Oct4 and of self-renewal [173]. However, large scale cell-based RNAi screens have been hampered by the demands and inefficiency of traditional HTS. RNAi cell microarrays could offer an efficient platform for carrying out high-throughput loss-of-function studies [174]. Arrays

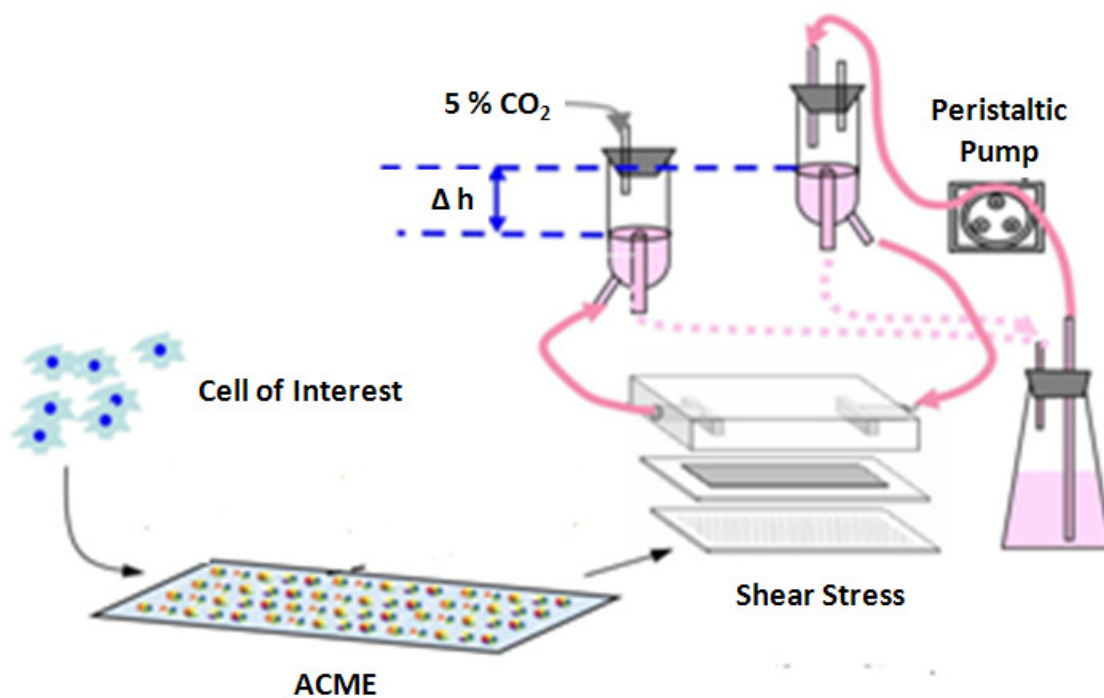
can be fabricated by spotting (1) lentiviruses that express short hairpin (shRNA) that silence gene expression through RNAi [175] or (2) peptide transduction domain – double stranded RNA binding domains (PTD-dRBDs) that carry siRNA across the cell membrane and knockdown gene expression [176, 177]. RNAi arrays will aid in the rapid functional annotation of mammalian genomes and in the identification of genes involved in stem cell self-renewal and differentiation.

## **6.5 CELLULAR MICROARRAYS IN DRUG DISCOVERY**

Cell microarrays could find use in the pharmaceutical industry by aiding two crucial steps in drug development—target identification and lead assessment. The current method of target identification involves the use of 96- or 384-well microtiter plates with monolayer cell cultures [51]. However, the multi-well plate format suffers from several limitations, most notably the cost of the relatively large amounts of reagents and cells needed. Cell microarrays which increase the parallelism and efficiency of screening compound libraries offer an alternative solution. Additionally, cell microarrays could be used to identify potentially toxic compounds earlier in the drug development process. For example, Lee *et al.* developed an array-based high throughput system that can be used to mimic the effects of human liver metabolism and simultaneously evaluate the cytotoxicity of small molecules and their metabolites [178]. Along similar lines, using stem cells and their differentiated progenitors along with cell microarrays could provide more realistic *in vitro* models for predicting the effectiveness and toxicity of drug candidates and chemicals in humans.

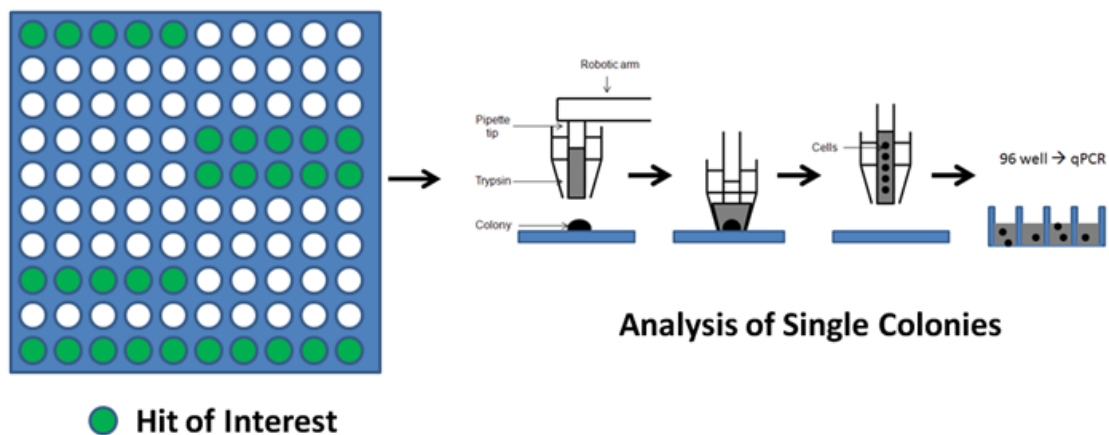
## 6.6 CONCLUSION

Technologies like ACME will have a significant impact of HTS by increasing throughput and reducing the consumption of reagents and cells. Furthermore, by using ACME to create culture systems that better resemble the *in vivo* state, cell-based drug discovery and therapies will be improved and become more reliable. Here we have highlighted some future improvements and uses of the ACME technology that we have developed. It is our hope that such improvements will lead to the wide spread implementation of ACME in all areas of biomedical research.



**Figure 6-1: Diagram of Set-up to Apply Mechanical Stimuli to ACME.**

A circulation flow system can be used to impose shear stress on cultured cells. In brief, a slide containing cells of interest on an ACME slide will be mounted in a rectangular flow channel created by sandwiching a silicon gasket between the glass slide (with cells) and an acrylic plate. The channel has inlet and outlet for perfusing the cultured cells with shear flows generated by the height difference between two reservoirs. During the flow experiments, the system is kept at 37°C in a constant temperature hood, and the circulating medium is equilibrated with humidified 5% CO<sub>2</sub>-95% air. The cells cultured on the ACME slides can be assembled into the flow chamber and subjected to various magnitudes of shear stress (0.5 to 20 dyn/cm<sup>2</sup>) for various time durations.

**Figure 6-2: Design of "Off Chip" Analysis**

Hits of interest are identified by automated microscopy. A robotic arm with a pipette tip filled with trypsin is placed over a hit colony. Trypsin is then delivered into the sealed perfusion chamber that surrounds the colony. After detachment, the cells are aspirated into the pipette tip and delivered to a multi-well plate.

## REFERENCES

1. Jang, J.H. and D.V. Schaffer, *Microarraying the cellular microenvironment*. Mol Syst Biol, 2006. **2**: p. 39.
2. Schaffer, D., *Exploring and Engineering Stem Cells and their Niches*. Curr Opin Chem Biol, 2007. **11**(4): p. 355-356.
3. Kim, S., M. Harris, and J.A. Varner, *Regulation of integrin alpha vbeta 3-mediated endothelial cell migration and angiogenesis by integrin alpha5beta1 and protein kinase A*. J Biol Chem, 2000. **275**(43): p. 33920-8.
4. Fashena, S.J. and S.M. Thomas, *Signalling by adhesion receptors*. Nat Cell Biol, 2000. **2**(12): p. E225-9.
5. Clark, E.A. and J.S. Brugge, *Integrins and signal transduction pathways: the road taken*. Science, 1995. **268**(5208): p. 233-9.
6. Schneller, M., K. Vuori, and E. Ruoslahti, *Alphavbeta3 integrin associates with activated insulin and PDGFbeta receptors and potentiates the biological activity of PDGF*. EMBO J, 1997. **16**(18): p. 5600-7.
7. Pacifici, R., et al., *Collagen-induced release of interleukin 1 from human blood mononuclear cells. Potentiation by fibronectin binding to the alpha 5 beta 1 integrin*. J Clin Invest, 1992. **89**(1): p. 61-7.
8. Fuchs, E., T. Tumber, and G. Guasch, *Socializing with the neighbors: stem cells and their niche*. Cell, 2004. **116**(6): p. 769-78.
9. Morrison, S.J. and A.C. Spradling, *Stem cells and niches: mechanisms that promote stem cell maintenance throughout life*. Cell, 2008. **132**(4): p. 598-611.
10. Moore, K.A. and I.R. Lemischka, *Stem cells and their niches*. Science, 2006. **311**(5769): p. 1880-5.
11. Weissman, I.L., D.J. Anderson, and F. Gage, *Stem and progenitor cells: origins, phenotypes, lineage commitments, and transdifferentiations*. Annu Rev Cell Dev Biol, 2001. **17**: p. 387-403.
12. Li, L. and T. Xie, *Stem cell niche: structure and function*. Annu Rev Cell Dev Biol, 2005. **21**: p. 605-31.
13. Walker, M.R., K.K. Patel, and T.S. Stappenbeck, *The stem cell niche*. J Pathol, 2009. **217**(2): p. 169-80.
14. Walker, M.R. and T.S. Stappenbeck, *Deciphering the 'black box' of the intestinal stem cell niche: taking direction from other systems*. Curr Opin Gastroenterol, 2008. **24**(2): p. 115-20.

15. Dellatore, S.M., A.S. Garcia, and W.M. Miller, *Mimicking stem cell niches to increase stem cell expansion*. *Curr Opin Biotechnol*, 2008. **19**(5): p. 534-40.
16. Hoffman, L.M. and M.K. Carpenter, *Characterization and culture of human embryonic stem cells*. *Nat Biotechnol*, 2005. **23**(6): p. 699-708.
17. Xu, C., et al., *Feeder-free growth of undifferentiated human embryonic stem cells*. *Nat Biotechnol*, 2001. **19**(10): p. 971-4.
18. Skottman, H. and O. Hovatta, *Culture conditions for human embryonic stem cells*. *Reproduction*, 2006. **132**(5): p. 691-8.
19. Martin, M.J., et al., *Human embryonic stem cells express an immunogenic nonhuman sialic acid*. *Nat Med*, 2005. **11**(2): p. 228-32.
20. Xu, C., et al., *Basic fibroblast growth factor supports undifferentiated human embryonic stem cell growth without conditioned medium*. *Stem Cells*, 2005. **23**(3): p. 315-23.
21. Xu, R.H., et al., *Basic FGF and suppression of BMP signaling sustain undifferentiated proliferation of human ES cells*. *Nat Methods*, 2005. **2**(3): p. 185-90.
22. James, D., et al., *TGFbeta/activin/nodal signaling is necessary for the maintenance of pluripotency in human embryonic stem cells*. *Development*, 2005. **132**(6): p. 1273-82.
23. Heins, N., et al., *Derivation, characterization, and differentiation of human embryonic stem cells*. *Stem Cells*, 2004. **22**(3): p. 367-76.
24. Sato, N., et al., *Maintenance of pluripotency in human and mouse embryonic stem cells through activation of Wnt signaling by a pharmacological GSK-3-specific inhibitor*. *Nat Med*, 2004. **10**(1): p. 55-63.
25. Xiao, L., X. Yuan, and S.J. Sharkis, *Activin A maintains self-renewal and regulates fibroblast growth factor, Wnt, and bone morphogenic protein pathways in human embryonic stem cells*. *Stem Cells*, 2006. **24**(6): p. 1476-86.
26. Pebay, A., et al., *Essential roles of sphingosine-1-phosphate and platelet-derived growth factor in the maintenance of human embryonic stem cells*. *Stem Cells*, 2005. **23**(10): p. 1541-8.
27. Wang, G., et al., *Noggin and bFGF cooperate to maintain the pluripotency of human embryonic stem cells in the absence of feeder layers*. *Biochem Biophys Res Commun*, 2005. **330**(3): p. 934-42.
28. Wang, L., et al., *Self-renewal of human embryonic stem cells requires insulin-like growth factor-1 receptor and ERBB2 receptor signaling*. *Blood*, 2007. **110**(12): p. 4111-9.

29. Ludwig, T.E., et al., *Derivation of human embryonic stem cells in defined conditions*. Nat Biotechnol, 2006. **24**(2): p. 185-7.
30. Amit, M., et al., *Feeder layer- and serum-free culture of human embryonic stem cells*. Biol Reprod, 2004. **70**(3): p. 837-45.
31. Noaksson, K., et al., *Monitoring differentiation of human embryonic stem cells using real-time PCR*. Stem Cells, 2005. **23**(10): p. 1460-7.
32. Genbacev, O., et al., *Serum-free derivation of human embryonic stem cell lines on human placental fibroblast feeders*. Fertil Steril, 2005. **83**(5): p. 1517-29.
33. Braam, S.R., et al., *Recombinant vitronectin is a functionally defined substrate that supports human embryonic stem cell self-renewal via alphavbeta5 integrin*. Stem Cells, 2008. **26**(9): p. 2257-65.
34. Beattie, G.M., et al., *Activin A maintains pluripotency of human embryonic stem cells in the absence of feeder layers*. Stem Cells, 2005. **23**(4): p. 489-95.
35. Chen, S.S., et al., *Cell-cell and cell-extracellular matrix interactions regulate embryonic stem cell differentiation*. Stem Cells, 2007. **25**(3): p. 553-61.
36. Campbell, A., M.S. Wicha, and M. Long, *Extracellular matrix promotes the growth and differentiation of murine hematopoietic cells in vitro*. J Clin Invest, 1985. **75**(6): p. 2085-90.
37. Curran, J.M., R. Chen, and J.A. Hunt, *The guidance of human mesenchymal stem cell differentiation in vitro by controlled modifications to the cell substrate*. Biomaterials, 2006. **27**(27): p. 4783-93.
38. Kotobuki, N., et al., *In vivo survival and osteogenic differentiation of allogeneic rat bone marrow mesenchymal stem cells (MSCs)*. Cell Transplant, 2008. **17**(6): p. 705-12.
39. Zhao, F., et al., *Effects of hydroxyapatite in 3-D chitosan-gelatin polymer network on human mesenchymal stem cell construct development*. Biomaterials, 2006. **27**(9): p. 1859-67.
40. Fan, H., et al., *Cartilage regeneration using mesenchymal stem cells and a PLGA-gelatin/chondroitin/hyaluronate hybrid scaffold*. Biomaterials, 2006. **27**(26): p. 4573-80.
41. Richardson, S.M., et al., *Human mesenchymal stem cell differentiation to NP-like cells in chitosan-glycerophosphate hydrogels*. Biomaterials, 2008. **29**(1): p. 85-93.
42. Hayman, M.W., et al., *Growth of human stem cell-derived neurons on solid three-dimensional polymers*. J Biochem Biophys Methods, 2005. **62**(3): p. 231-40.



43. Harrison, J., et al., *Colonization and maintenance of murine embryonic stem cells on poly(alpha-hydroxy esters)*. *Biomaterials*, 2004. **25**(20): p. 4963-70.
44. Chai, C. and K.W. Leong, *Biomaterials approach to expand and direct differentiation of stem cells*. *Mol Ther*, 2007. **15**(3): p. 467-80.
45. Chen, S., et al., *Self-renewal of embryonic stem cells by a small molecule*. *Proc Natl Acad Sci U S A*, 2006. **103**(46): p. 17266-71.
46. Ding, S., et al., *Synthetic small molecules that control stem cell fate*. *Proc Natl Acad Sci U S A*, 2003. **100**(13): p. 7632-7.
47. Wei, Z.L., et al., *Isoxazolyl-serine-based agonists of peroxisome proliferator-activated receptor: design, synthesis, and effects on cardiomyocyte differentiation*. *J Am Chem Soc*, 2004. **126**(51): p. 16714-5.
48. Wu, X., et al., *Small molecules that induce cardiomyogenesis in embryonic stem cells*. *J Am Chem Soc*, 2004. **126**(6): p. 1590-1.
49. Desbordes, S.C., et al., *High-throughput screening assay for the identification of compounds regulating self-renewal and differentiation in human embryonic stem cells*. *Cell Stem Cell*, 2008. **2**(6): p. 602-12.
50. Zhu, S., et al., *A small molecule primes embryonic stem cells for differentiation*. *Cell Stem Cell*, 2009. **4**(5): p. 416-26.
51. Fernandes, T.G., et al., *High-throughput cellular microarray platforms: applications in drug discovery, toxicology and stem cell research*. *Trends Biotechnol*, 2009. **27**(6): p. 342-349.
52. van Noort, D., et al., *Stem cells in microfluidics*. *Biotechnol Prog*, 2009. **25**(1): p. 52-60.
53. Kim, L., et al., *Microfluidic arrays for logarithmically perfused embryonic stem cell culture*. *Lab Chip*, 2006. **6**(3): p. 394-406.
54. Figallo, E., et al., *Micro-bioreactor array for controlling cellular microenvironments*. *Lab Chip*, 2007. **7**(6): p. 710-9.
55. Zhong, J.F., et al., *A microfluidic processor for gene expression profiling of single human embryonic stem cells*. *Lab Chip*, 2008. **8**(1): p. 68-74.
56. Chin, V.I., et al., *Microfabricated platform for studying stem cell fates*. *Biotechnol Bioeng*, 2004. **88**(3): p. 399-415.
57. Buckner, B., et al., *Involving undergraduates in the annotation and analysis of global gene expression studies: creation of a maize shoot apical meristem expression database*. *Genetics*, 2007. **176**(2): p. 741-7.

58. Ashton, R.S., et al., *High-throughput screening of gene function in stem cells using clonal microarrays*. *Stem Cells*, 2007. **25**(11): p. 2928-35.
59. Keller, G.M., *In vitro differentiation of embryonic stem cells*. *Curr Opin Cell Biol*, 1995. **7**(6): p. 862-9.
60. Itskovitz-Eldor, J., et al., *Differentiation of human embryonic stem cells into embryoid bodies compromising the three embryonic germ layers*. *Mol Med*, 2000. **6**(2): p. 88-95.
61. Mohr, J.C., J.J. de Pablo, and S.P. Palecek, *3-D microwell culture of human embryonic stem cells*. *Biomaterials*, 2006. **27**(36): p. 6032-42.
62. Flaim, C.J., S. Chien, and S.N. Bhatia, *An extracellular matrix microarray for probing cellular differentiation*. *Nat Methods*, 2005. **2**(2): p. 119-25.
63. Flaim, C.J., et al., *Combinatorial signaling microenvironments for studying stem cell fate*. *Stem Cells Dev*, 2008. **17**(1): p. 29-39.
64. Soen, Y., et al., *Exploring the regulation of human neural precursor cell differentiation using arrays of signaling microenvironments*. *Mol Syst Biol*, 2006. **2**: p. 37.
65. Anderson, D.G., S. Levenberg, and R. Langer, *Nanoliter-scale synthesis of arrayed biomaterials and application to human embryonic stem cells*. *Nat Biotechnol*, 2004. **22**(7): p. 863-6.
66. Thomson, J.A., et al., *Embryonic stem cell lines derived from human blastocysts*. *Science*, 1998. **282**(5391): p. 1145-7.
67. Schena, M., et al., *Quantitative monitoring of gene expression patterns with a complementary DNA microarray*. *Science*, 1995. **270**(5235): p. 467-70.
68. Liu, S., et al., *Automated parallel DNA sequencing on multiple channel microchips*. *Proc Natl Acad Sci U S A*, 2000. **97**(10): p. 5369-74.
69. Howbrook, D.N., et al., *Developments in microarray technologies*. *Drug Discov Today*, 2003. **8**(14): p. 642-51.
70. Huang, R.P., *Detection of multiple proteins in an antibody-based protein microarray system*. *J Immunol Methods*, 2001. **255**(1-2): p. 1-13.
71. Huang, R.P., *Simultaneous detection of multiple proteins with an array-based enzyme-linked immunosorbent assay (ELISA) and enhanced chemiluminescence (ECL)*. *Clin Chem Lab Med*, 2001. **39**(3): p. 209-14.
72. Huang, R.P., et al., *Simultaneous detection of multiple cytokines from conditioned media and patient's sera by an antibody-based protein array system*. *Anal Biochem*, 2001. **294**(1): p. 55-62.

73. Willert, K., et al., *Wnt proteins are lipid-modified and can act as stem cell growth factors*. Nature, 2003. **423**(6938): p. 448-52.
74. Friedman, S.L., *Molecular regulation of hepatic fibrosis, an integrated cellular response to tissue injury*. J Biol Chem, 2000. **275**(4): p. 2247-50.
75. Friedman, S.L., *Liver fibrosis -- from bench to bedside*. J Hepatol, 2003. **38 Suppl 1**: p. S38-53.
76. Bataller, R. and D.A. Brenner, *Hepatic stellate cells as a target for the treatment of liver fibrosis*. Semin Liver Dis, 2001. **21**(3): p. 437-51.
77. Hautekeete, M.L. and A. Geerts, *The hepatic stellate (Ito) cell: its role in human liver disease*. Virchows Arch, 1997. **430**(3): p. 195-207.
78. Kordes, C., I. Sawitza, and D. Haussinger, *Canonical Wnt signaling maintains the quiescent stage of hepatic stellate cells*. Biochem Biophys Res Commun, 2008. **367**(1): p. 116-23.
79. Cheng, J.H., et al., *Wnt antagonism inhibits hepatic stellate cell activation and liver fibrosis*. Am J Physiol Gastrointest Liver Physiol, 2008. **294**(1): p. G39-49.
80. Myung, S.J., et al., *Wnt signaling enhances the activation and survival of human hepatic stellate cells*. FEBS Lett, 2007. **581**(16): p. 2954-8.
81. Reya, T. and H. Clevers, *Wnt signalling in stem cells and cancer*. Nature, 2005. **434**(7035): p. 843-50.
82. Zhang, D.L., et al., *Effect of Wnt signaling pathway on wound healing*. Biochem Biophys Res Commun, 2009. **378**(2): p. 149-51.
83. Ben-Ze'ev, A., et al., *Cell-cell and cell-matrix interactions differentially regulate the expression of hepatic and cytoskeletal genes in primary cultures of rat hepatocytes*. Proc Natl Acad Sci U S A, 1988. **85**(7): p. 2161-5.
84. Schuetz, E.G., et al., *Regulation of gene expression in adult rat hepatocytes cultured on a basement membrane matrix*. J Cell Physiol, 1988. **134**(3): p. 309-23.
85. Nagaki, M., et al., *Regulation of hepatic genes and liver transcription factors in rat hepatocytes by extracellular matrix*. Biochem Biophys Res Commun, 1995. **210**(1): p. 38-43.
86. Oda, H., et al., *Laminin-rich extracellular matrix maintains high level of hepatocyte nuclear factor 4 in rat hepatocyte culture*. Biochem Biophys Res Commun, 1995. **212**(3): p. 800-5.
87. Sohara, N., et al., *Reversal of activation of human myofibroblast-like cells by culture on a basement membrane-like substrate*. J Hepatol, 2002. **37**(2): p. 214-21.

88. Gressner, A.M. and M. Althaus, *Effects of ethanol, acetaldehyde, and lactate on proteoglycan synthesis and proliferation of cultured rat liver fat-storing cells*. Gastroenterology, 1988. **94**(3): p. 797-807.
89. Mallat, A., et al., *Interferon alfa and gamma inhibit proliferation and collagen synthesis of human Ito cells in culture*. Hepatology, 1995. **21**(4): p. 1003-10.
90. Ogawa, K., et al., *Sequential changes of extracellular matrix and proliferation of Ito cells with enhanced expression of desmin and actin in focal hepatic injury*. Am J Pathol, 1986. **125**(3): p. 611-9.
91. Brafman, D., et al., *Defining long-term maintenance conditions of human embryonic stem cells with arrayed cellular microenvironment technology*. Stem Cells Dev, 2009.
92. La Barge, M.A., et al., *Human mammary progenitor cell fate decisions are products of interactions with combinatorial microenvironments*. Integrative Biology, 2009. **1**(1): p. 70-79.
93. Magness, S.T., et al., *A dual reporter gene transgenic mouse demonstrates heterogeneity in hepatic fibrogenic cell populations*. Hepatology, 2004. **40**(5): p. 1151-9.
94. Siegmund, S.V., et al., *Fatty acid amide hydrolase determines anandamide-induced cell death in the liver*. J Biol Chem, 2006. **281**(15): p. 10431-8.
95. Bataller, R., et al., *NADPH oxidase signal transduces angiotensin II in hepatic stellate cells and is critical in hepatic fibrosis*. J Clin Invest, 2003. **112**(9): p. 1383-94.
96. Eisen, M.B., et al., *Cluster analysis and display of genome-wide expression patterns*. Proc Natl Acad Sci U S A, 1998. **95**(25): p. 14863-8.
97. De Minicis, S., et al., *Gene expression profiles during hepatic stellate cell activation in culture and in vivo*. Gastroenterology, 2007. **132**(5): p. 1937-46.
98. Martinez-Hernandez, A., *The hepatic extracellular matrix. II. Electron immunohistochemical studies in rats with CCl4-induced cirrhosis*. Lab Invest, 1985. **53**(2): p. 166-86.
99. Logan, C.Y. and R. Nusse, *The Wnt signaling pathway in development and disease*. Annu Rev Cell Dev Biol, 2004. **20**: p. 781-810.
100. Surendran, K., S.P. McCaul, and T.C. Simon, *A role for Wnt-4 in renal fibrosis*. Am J Physiol Renal Physiol, 2002. **282**(3): p. F431-41.
101. Cheon, S.S., et al., *beta-Catenin stabilization dysregulates mesenchymal cell proliferation, motility, and invasiveness and causes aggressive fibromatosis and hyperplastic cutaneous wounds*. Proc Natl Acad Sci U S A, 2002. **99**(10): p. 6973-8.

102. Morrisey, E.E., *Wnt signaling and pulmonary fibrosis*. Am J Pathol, 2003. **162**(5): p. 1393-7.
103. Brack, A.S., et al., *Increased Wnt signaling during aging alters muscle stem cell fate and increases fibrosis*. Science, 2007. **317**(5839): p. 807-10.
104. Topol, L., et al., *Wnt-5a inhibits the canonical Wnt pathway by promoting GSK-3-independent beta-catenin degradation*. J Cell Biol, 2003. **162**(5): p. 899-908.
105. Bailey, S.N., D.M. Sabatini, and B.R. Stockwell, *Microarrays of small molecules embedded in biodegradable polymers for use in mammalian cell-based screens*. Proc Natl Acad Sci U S A, 2004. **101**(46): p. 16144-9.
106. Willems, E., L. Leyns, and J. Vandesompele, *Standardization of real-time PCR gene expression data from independent biological replicates*. Anal Biochem, 2008. **379**(1): p. 127-9.
107. Legate, K.R., S.A. Wickstrom, and R. Fassler, *Genetic and cell biological analysis of integrin outside-in signaling*. Genes Dev, 2009. **23**(4): p. 397-418.
108. Luo, B.H., C.V. Carman, and T.A. Springer, *Structural basis of integrin regulation and signaling*. Annu Rev Immunol, 2007. **25**: p. 619-47.
109. Luo, B.H. and T.A. Springer, *Integrin structures and conformational signaling*. Curr Opin Cell Biol, 2006. **18**(5): p. 579-86.
110. Milani, S., et al., *Procollagen expression by nonparenchymal rat liver cells in experimental biliary fibrosis*. Gastroenterology, 1990. **98**(1): p. 175-84.
111. Milani, S., et al., *In situ hybridization for procollagen types I, III and IV mRNA in normal and fibrotic rat liver: evidence for predominant expression in nonparenchymal liver cells*. Hepatology, 1989. **10**(1): p. 84-92.
112. Garamszegi, N., et al., *Extracellular matrix-induced gene expression in human breast cancer cells*. Mol Cancer Res, 2009. **7**(3): p. 319-29.
113. Pacifici, R., et al., *Ligand binding to monocyte alpha 5 beta 1 integrin activates the alpha 2 beta 1 receptor via the alpha 5 subunit cytoplasmic domain and protein kinase C*. J Immunol, 1994. **153**(5): p. 2222-33.
114. Schwartz, M.A. and M.H. Ginsberg, *Networks and crosstalk: integrin signalling spreads*. Nat Cell Biol, 2002. **4**(4): p. E65-8.
115. Runge, D., et al., *Matrix induced re-differentiation of cultured rat hepatocytes and changes of CCAAT/enhancer binding proteins*. Biol Chem, 1997. **378**(8): p. 873-81.
116. Yamada, K.M. and S. Even-Ram, *Integrin regulation of growth factor receptors*. Nat Cell Biol, 2002. **4**(4): p. E75-6.

117. Comoglio, P.M., C. Boccaccio, and L. Trusolino, *Interactions between growth factor receptors and adhesion molecules: breaking the rules*. *Curr Opin Cell Biol*, 2003. **15**(5): p. 565-71.
118. Fischbach, C., et al., *Engineering tumors with 3D scaffolds*. *Nat Methods*, 2007. **4**(10): p. 855-60.
119. Griffith, L.G. and M.A. Swartz, *Capturing complex 3D tissue physiology in vitro*. *Nat Rev Mol Cell Biol*, 2006. **7**(3): p. 211-24.
120. Huang, C.P., et al., *Engineering microscale cellular niches for three-dimensional multicellular co-cultures*. *Lab Chip*, 2009. **9**(12): p. 1740-8.
121. Box, G., Hunter, W., Hunter, J., *Statistics for Experimenters*. 1978, New York: Wiley.
122. Horak, V. and J.E. Flechon, *Immunocytochemical characterisation of rabbit and mouse embryonic fibroblasts*. *Reprod Nutr Dev*, 1998. **38**(6): p. 683-95.
123. Stojkovic, P., et al., *Human-serum matrix supports undifferentiated growth of human embryonic stem cells*. *Stem Cells*, 2005. **23**(7): p. 895-902.
124. Li, Y., et al., *Expansion of human embryonic stem cells in defined serum-free medium devoid of animal-derived products*. *Biotechnol Bioeng*, 2005. **91**(6): p. 688-98.
125. Adewumi, O., et al., *Characterization of human embryonic stem cell lines by the International Stem Cell Initiative*. *Nat Biotechnol*, 2007. **25**(7): p. 803-16.
126. Metallo, C.M., et al., *Retinoic acid and bone morphogenetic protein signaling synergize to efficiently direct epithelial differentiation of human embryonic stem cells*. *Stem Cells*, 2008. **26**(2): p. 372-80.
127. Pyle, A.D., L.F. Lock, and P.J. Donovan, *Neurotrophins mediate human embryonic stem cell survival*. *Nat Biotechnol*, 2006. **24**(3): p. 344-50.
128. Yao, S., et al., *Long-term self-renewal and directed differentiation of human embryonic stem cells in chemically defined conditions*. *Proc Natl Acad Sci U S A*, 2006. **103**(18): p. 6907-12.
129. Gorfinkiel, N., et al., *The Drosophila ortholog of the human Wnt inhibitor factor Shifted controls the diffusion of lipid-modified Hedgehog*. *Dev Cell*, 2005. **8**(2): p. 241-53.
130. Czubayko, F., et al., *Tumor growth and angiogenesis induced by a secreted binding protein for fibroblast growth factors*. *J Biol Chem*, 1994. **269**(45): p. 28243-8.

131. Begum, S., et al., *Immunohistochemical expression of heparin-binding protein 17/fibroblast growth factor-binding protein-1 (HBp17/FGFBP-1) as an angiogenic factor in head and neck tumorigenesis*. *Oncol Rep*, 2007. **17**(3): p. 591-6.
132. Ware, C.B., A.M. Nelson, and C.A. Blau, *A comparison of NIH-approved human ESC lines*. *Stem Cells*, 2006. **24**(12): p. 2677-84.
133. Draghici, S., et al., *Reliability and reproducibility issues in DNA microarray measurements*. *Trends Genet*, 2006. **22**(2): p. 101-9.
134. Bammler, T., et al., *Standardizing global gene expression analysis between laboratories and across platforms*. *Nat Methods*, 2005. **2**(5): p. 351-6.
135. Hubbell, J.A., *Bioactive biomaterials*. *Curr Opin Biotechnol*, 1999. **10**(2): p. 123-9.
136. Bagley, J., et al., *Extended culture of multipotent hematopoietic progenitors without cytokine augmentation in a novel three-dimensional device*. *Exp Hematol*, 1999. **27**(3): p. 496-504.
137. Banu, N., et al., *Cytokine-augmented culture of haematopoietic progenitor cells in a novel three-dimensional cell growth matrix*. *Cytokine*, 2001. **13**(6): p. 349-58.
138. Berrios, V.M., et al., *The molecular basis for the cytokine-induced defect in homing and engraftment of hematopoietic stem cells*. *Exp Hematol*, 2001. **29**(11): p. 1326-35.
139. Ehring, B., et al., *Expansion of HPCs from cord blood in a novel 3D matrix*. *Cytotherapy*, 2003. **5**(6): p. 490-9.
140. Tare, R.S., et al., *A microarray approach to the identification of polyurethanes for the isolation of human skeletal progenitor cells and augmentation of skeletal cell growth*. *Biomaterials*, 2009. **30**(6): p. 1045-55.
141. Tourniaire, G., J.J. Diaz-Mochon, and M. Bradley, *Fingerprinting Polymer Microarray*. *Comb Chem High Throughput Screen*, 2009.
142. Pernagallo, S., J.J. Diaz-Mochon, and M. Bradley, *A cooperative polymer-DNA microarray approach to biomaterial investigation*. *Lab Chip*, 2009. **9**(3): p. 397-403.
143. Diaz-Mochon, J.J., G. Tourniaire, and M. Bradley, *Microarray platforms for enzymatic and cell-based assays*. *Chem Soc Rev*, 2007. **36**(3): p. 449-57.
144. Mant, A., et al., *Polymer microarrays: identification of substrates for phagocytosis assays*. *Biomaterials*, 2006. **27**(30): p. 5299-306.
145. Tourniaire, G., et al., *Polymer microarrays for cellular adhesion*. *Chem Commun (Camb)*, 2006(20): p. 2118-20.

146. Anderson, D.G., et al., *Biomaterial microarrays: rapid, microscale screening of polymer-cell interaction*. *Biomaterials*, 2005. **26**(23): p. 4892-7.
147. Miyoshi, H., et al., *Development of a self-inactivating lentivirus vector*. *J Virol*, 1998. **72**(10): p. 8150-7.
148. Zufferey, R., et al., *Self-inactivating lentivirus vector for safe and efficient in vivo gene delivery*. *J Virol*, 1998. **72**(12): p. 9873-80.
149. Shin, H., S. Jo, and A.G. Mikos, *Biomimetic materials for tissue engineering*. *Biomaterials*, 2003. **24**(24): p. 4353-64.
150. Saltzman, W.M., *Cell Interactions with Polymers*, in *Principles of Tissue Engineering*. 2000, Academic Press: San Diego. p. 221-235.
151. Ma, W., et al., *Cell-extracellular matrix interactions regulate neural differentiation of human embryonic stem cells*. *BMC Dev Biol*, 2008. **8**: p. 90.
152. Gong, J., et al., *Effects of extracellular matrix and neighboring cells on induction of human embryonic stem cells into retinal or retinal pigment epithelial progenitors*. *Exp Eye Res*, 2008. **86**(6): p. 957-65.
153. Toh, W.S., et al., *Differentiation and Enrichment of Expandable Chondrogenic Cells from Human Embryonic Stem Cells in Vitro*. *J Cell Mol Med*, 2009.
154. Gil, J.E., et al., *Vitronectin promotes oligodendrocyte differentiation during neurogenesis of human embryonic stem cells*. *FEBS Lett*, 2009. **583**(3): p. 561-7.
155. Hakala, H., et al., *Comparison of Biomaterials and Extracellular Matrices as a Culture Platform for Multiple, Independently Derived Human Embryonic Stem Cell Lines*. *Tissue Eng Part A*, 2009.
156. Benoit, D.S., et al., *Small functional groups for controlled differentiation of hydrogel-encapsulated human mesenchymal stem cells*. *Nat Mater*, 2008. **7**(10): p. 816-23.
157. Meredith, J.C., et al., *Combinatorial characterization of cell interactions with polymer surfaces*. *J Biomed Mater Res A*, 2003. **66**(3): p. 483-90.
158. Keselowsky, B.G., D.M. Collard, and A.J. Garcia, *Surface chemistry modulates fibronectin conformation and directs integrin binding and specificity to control cell adhesion*. *J Biomed Mater Res A*, 2003. **66**(2): p. 247-59.
159. van Wachem, P.B., et al., *Adhesion of cultured human endothelial cells onto methacrylate polymers with varying surface wettability and charge*. *Biomaterials*, 1987. **8**(5): p. 323-8.
160. Nuttelman, C.R., et al., *The effect of ethylene glycol methacrylate phosphate in PEG hydrogels on mineralization and viability of encapsulated hMSCs*. *Biomaterials*, 2006. **27**(8): p. 1377-86.



161. Keller, R., *Mechanisms of elongation in embryogenesis*. Development, 2006. **133**(12): p. 2291-302.
162. Benjamin, M. and B. Hillen, *Mechanical influences on cells, tissues and organs - 'Mechanical Morphogenesis'*. Eur J Morphol, 2003. **41**(1): p. 3-7.
163. Yamamoto, K., et al., *Fluid shear stress induces differentiation of Flk-1-positive embryonic stem cells into vascular endothelial cells in vitro*. Am J Physiol Heart Circ Physiol, 2005. **288**(4): p. H1915-24.
164. Illi, B., et al., *Epigenetic histone modification and cardiovascular lineage programming in mouse embryonic stem cells exposed to laminar shear stress*. Circ Res, 2005. **96**(5): p. 501-8.
165. Huang, H., et al., *Differentiation from embryonic stem cells to vascular wall cells under in vitro pulsatile flow loading*. J Artif Organs, 2005. **8**(2): p. 110-8.
166. Angele, P., et al., *Cyclic, mechanical compression enhances chondrogenesis of mesenchymal progenitor cells in tissue engineering scaffolds*. Biorheology, 2004. **41**(3-4): p. 335-46.
167. Hsiong, S.X., et al., *Differentiation stage alters matrix control of stem cells*. J Biomed Mater Res A, 2008. **85**(1): p. 145-56.
168. Engler, A.J., et al., *Matrix elasticity directs stem cell lineage specification*. Cell, 2006. **126**(4): p. 677-89.
169. Engler, A., et al., *Substrate compliance versus ligand density in cell on gel responses*. Biophys J, 2004. **86**(1 Pt 1): p. 617-28.
170. Peterbauer, T., et al., *Simple and versatile methods for the fabrication of arrays of live mammalian cells*. Lab Chip, 2006. **6**(7): p. 857-63.
171. Brummelkamp, T.R. and R. Bernards, *New tools for functional mammalian cancer genetics*. Nat Rev Cancer, 2003. **3**(10): p. 781-9.
172. Alberts, B., Johnson, A., Lewis, J., Raff, M., Roberts, K., Walter, P., *Molecular Biology of the Cell*. 5 ed. 2008, New York: Garland Science.
173. Zhang, J.Z., et al., *Screening for genes essential for mouse embryonic stem cell self-renewal using a subtractive RNA interference library*. Stem Cells, 2006. **24**(12): p. 2661-8.
174. Wheeler, D.B., A.E. Carpenter, and D.M. Sabatini, *Cell microarrays and RNA interference chip away at gene function*. Nat Genet, 2005. **37** Suppl: p. S25-30.
175. Bailey, S.N., et al., *Microarrays of lentiviruses for gene function screens in immortalized and primary cells*. Nat Methods, 2006. **3**(2): p. 117-22.

176. Eguchi, A., et al., *Efficient siRNA delivery into primary cells by a peptide transduction domain-dsRNA binding domain fusion protein*. Nat Biotechnol, 2009. **27**(6): p. 567-71.
177. Yoshikawa, T., et al., *Transfection microarray of human mesenchymal stem cells and on-chip siRNA gene knockdown*. J Control Release, 2004. **96**(2): p. 227-32.
178. Lee, M.Y., et al., *Three-dimensional cellular microarray for high-throughput toxicology assays*. Proc Natl Acad Sci U S A, 2008. **105**(1): p. 59-63.